SIMULINK model of a quarter-vehicle with an Anti-lock Braking System

Eindhoven University of Technology
Stan Ackerman Institute
Mechatronic Design

SIMULINK Model of a Quarter-Vehicle with an Anti-lock Braking System

Kiril Z. Rangelov

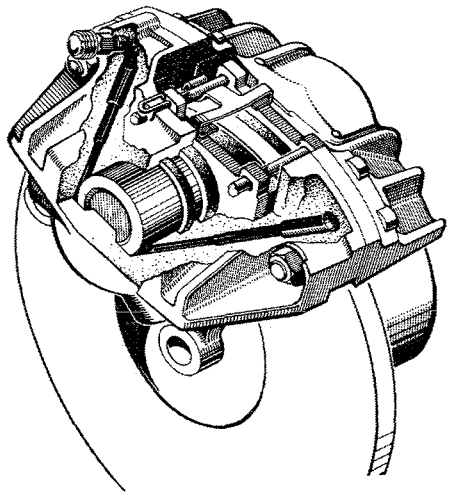

Eindhoven, March 2004

CIP-DATA STAN ACKERMANS INSTITUUT

Rangelov, Kiril Z.

SIMULINK model of a quarter-vehicle with an anti-lock braking system / by Kiril Z. Rangelov. - Eindhoven : Stan Ackermans Instituut, 2004. - Eindverslagen Stan Ackermans Instituut ; 2004/028.
ISBN 90-444-0377-X
NUR 951
Keywords: Automotive braking systems / Anti-lock braking systems (ABS); ABS modeling / Quarter-vehicle modeling

Eindhoven University of Technology
Stan Ackerman Institute
Mechatronic Design

SIMULINK Model of a Quarter-Vehicle with an Anti-lock Braking System

ir. Kiril Z. Rangelov

Exam Committee

1. prof.dr.ir. M. Steinbuch
2. dr.ir. F.E. Veldpaus
3. dr.ir. I.J.M. Besselink

Mentors:

TU/e:	prof.dr.ir. M. Steinbuch
TU/e:	dr.ir. F.E. Veldpaus
TNO&TU/e:	dr.ir. I.J.M. Besselink

Exam Date:

25 May 2004

DCT 2004/052

ISBN: 90-444-0377-X

SUMMARY

Essential to the understanding of the technology associated with modern automotive vehicle braking is knowledge of the tire-to-road interface, vehicle dynamics during braking and the components of a brake system.

In this thesis a model of the quarter vehicle is developed and used to study the braking performance of a straight-line braking test vehicle on both flat and uneven roads in Matlab-Simulink software environment. The vehicle model includes suspension model, tire (SWIFT) model and model of an Anti-lock braking system.

The developed suspension model consists of a horizontal suspension modeled by linear spring stiffness and viscous damping, and a wheel hub compliance model in fore-aft direction also modeled by linear spring stiffness and viscous damping. Only in-plain motions are considered. It is assumed that motion in vertical direction is decoupled from the motion in longitudinal direction.
The tire-to-road interaction and tire modeling are represented by a SWIFT model. The implemented tire model is a ready software product developed by TNO-Automotive and Delft University. The SWIFT model is in form of Matlab-Simulink block. External elements are added to the tire model to simulate correctly the locked wheel angular acceleration and torque generated by the brake in the test vehicle.
The developed Anti-lock braking system model includes models of the brake pressure modulator unit and central processor unit. The model of the central processor unit is subdivided in signal processing block model and logic controller block model.

Various wheel lock criteria are used during braking performance study. Comparison of the braking distances on flat and uneven roads is made when those criteria are employed.
Additional control strategy is tested. The strategy is based on the assumption that information of the tire load and torque transmitted from the tire to the road are available.

Simulation results are used to evaluate the different wheel lock criteria and their contribution to the stopping distance. On flat road, a solution where the tire torque was used to control the brake torque has found to be with the best performance. The next criterion in the performance list has found to be the ratio between the wheel angular acceleration and the wheel angular velocity.

Acknowledgements

This thesis presents the results of my work performed at the Eindhoven University of Technology for period of six months. When I start working on this project, I mainly considered it as a challenge. And a challenge it has been. Although the limited project duration it was a valuable experience for me. I was very fortunate of the ability to use knowledge and experience of the automotive group in the Dynamical System Design Division at the Eindhoven University of Technology.
In that respect I would like to thank my supervisors Igo Besellink and Frants Veldpaus, who played a critical role in this project. Their knowledge, experience and organization skills were from great importance. They provided a valuable feedback that helped to improve the final thesis version. Thank you very much.

I owe a special thanks to Professor M. Steinbuch. It was a privilege to be under the coaching of the professor Steinbuch. His support during these years of study and especially in the second year was unique.
In addition, I would like to thank dr. Piet Mulders coordinator of the Mechatronic Design for his restless and continues support during these two years of study.

I want to thank my student colleagues in the Mechatronic education: Diego Garcia, Christos Kadoglou, Raymond Tinsel, Paola Jimenes, Iciar Font and Christos Vottis.

Special thanks to my friends Sotir, Georgi J., Sasho, Veronica and Hans, Emi and Ivan, Nadya, Eli and Georgi, Kiti, Sneja and Mitko, Petio, Mircho, Chrisi and Alex, Valeri, Maria and Kamen, Mladen, Gabi and Alain, Athon, Eva, Apostol, Erikjan, Kiril and Ani, Samoil, Fifi, Vili, Denka, Lizzy, Corrie and Piet. We shared together nice and unforgettable moments.

Last but definitely not least, I want to thank my parents Vania and Zhivko and my brother Bojan for their love and unconditional support through the years. Thank you!

Eindhoven, March 2004

Kiril Rangelov

Table of contents

1. Introduction

An Antilock Braking System is an important component of modern cars. The first ABS systems were developed for the aircraft industry. On cars an ABS system was implemented in 1972 in England. The Jensen Interceptor automobile became the first production car to offer a Maxaret-based ABS, the main objective of the control system being prevention of wheel lock. Most of the ABS controllers available on the market today are table and relay-feedback based, making use of hydraulic actuators to deliver the braking force. Nowadays, the control objective shifts to maintain a specified tire slip rather then just preventing wheel locks. The setpoint slip is supposed to be provided by a higher level in the hierarchy (e.g. an ESP system), and can be used for stabilizing the steering dynamics of the car while braking. This might imply different slip setpoints for each wheel.

It turns out that the slip control task is not trivial, one of the main reasons being the high amount of uncertainty involved. Most uncertainty arises from the friction between the tires and the road surface. In addition, the tire-road characteristic is highly nonlinear. A special problem arises due to fast changes in surface conditions while braking (e.g. a wet spot on a dry surface). Another problem is posed by disturbances of the wheel angular velocity due to road irregularities. Misinterpretation of those disturbances by the ABS system can cause a decrease in the braking performance of the vehicle on uneven roads.

The scope of this report includes three stages. In the first stage a description of the model of a quarter-vehicle and an ABS in MATLAB–SIMULINK is given. The second stage comprises a simulation study of the straight-line braking performance of the test vehicle. And, finally, the third stage explores the opportunities of the braking performance improvement, if extra information on the tire's load and the transferred tire moment is provided by "smart" tires and bearings. The ABS-controller exploits the principles of the early Bosch algorithm. The controller controls a two-valve hydraulic pressure-modulator unit. Four modes of the torque (pressure) control are possible: build-up, hold, decrease, and slow build-up.

The ABS will be implemented on a one-wheel quarter-vehicle model and evaluated for an emergency straight-line braking maneuver on a high-friction surface. Here, a one-wheel vehicle is used to run away from the yaw moment control problem during braking of a four-wheel vehicle. To model the tire characteristics and the dynamic behavior on a flat as well as an uneven road, the SWIFT-tire model is employed. This Short Wave Intermediate Frequency Tire model offers an accurate description of the tire behavior up to 60 Hz disturbance excitations.

2. The Basics of Anti-Lock Braking system (ABS)

Anti-lock brake systems prevent brakes from locking during braking. Under normal braking conditions the driver controls the brakes. However, on slippery roadways or during severe braking, when the driver causes the wheels to approach lockup, the antilock system takes over. ABS modulates the brake line pressure independent of the pedal force, to bring the wheel speed back to the slip level range that is necessary for optimal braking performance. An antilock system consists of a hydraulic modulator, wheel speed sensors, and an electronic control unit. The ABS is a feedback control system that modulates the brake pressure in response to wheel deceleration and wheel angular velocity to prevent the controlled wheel from locking. The system shuts down when the vehicle speed is below a pre-set threshold.

2.1. Objectives of the ABS

The objectives of antilock systems are threefold: to reduce stopping distances, to improve stability, and to improve steerability during braking.

- ***Stopping Distance.*** The distance to stop is a function of the initial velocity, the mass of the vehicle, and the braking force. By maximizing the braking force the stopping distance will be minimized if all other factors remain constant. However, on all types of surfaces, to a greater or lesser extent, there exists a peak in friction coefficient. It follows that by keeping all of the wheels of a vehicle near the peak, an antilock system can attain maximum frictional force and, therefore, minimum stopping distance. This objective of antilock systems however, is tempered by the need for vehicle stability and steerability.

- ***Stability.*** Although decelerating and stopping vehicles constitutes a fundamental purpose of braking systems, maximum friction force may not be desirable in all cases, for example not if the vehicle is on a so-called μ-split surface (asphalt and ice, for example), such that significantly more braking force is obtainable on one side of the vehicle than on the other side. Applying maximum braking force on both sides will result in a yaw moment that will tend to pull the vehicle to the high friction side and contribute to vehicle instability, and forces the operator to make excessive steering corrections to counteract the yaw moment. If an antilock system can maintain the slip of both rear wheels at the level where the lower of the two friction coefficients peaks (*select low* see section 7.3), then lateral force is reasonably high, though not maximized. This contributes to stability and is an objective of antilock systems.

- ***Steerability.*** Good peak frictional force control is necessary in order to achieve satisfactory lateral forces and, therefore, satisfactory steerability. Steerability while braking is important not only for minor course corrections but also for the possibility of steering around an obstacle.

2.2. Tire Characteristics

Tire characteristics play an important role in the braking and steering response of a vehicle. For ABS-equipped vehicles the tire performance is of critical significance. All braking and steering forces must be generated within the small tire contact zone between the vehicle and the road. Tire traction forces as well as side forces can only be produced when a difference exists between the speed of the tire circumference and the speed of the vehicle relative to the road surface. This difference is denote as slip. It is common to relate the tire braking force to the

tire braking slip. After the peak value has been reached, increased tire slip causes reduction of tire-road friction coefficient. ABS has to limit the slip to values below the peak value to prevent wheel from locking. Tires with a high peak friction point achieve maximum friction at 10 to 20% slip. The optimum slip value decreases as tire-road friction decreases

2.3. Historical Overview

Development of ABS brakes, one of the truly outstanding safety features, resulted in the Dunlop "Maxaret" for aircrafts in 1952. In 1972 in England, the Jensen Interceptor automobile became the first production car to offer a Maxaret-based ABS using a propeller shaft speed sensor and viscous coupling. In the U.S., vehicle manufacturers worked with various brake manufacturers to develop ABS systems. In 1969, a rear-wheel-only ABS, developed by Ford and Kelsey Hayes, was offered on the Thunderbird. Chrysler and Bendix produced a four-wheel ABS for the '71 Imperial. General Motors likewise offered ABS brakes on some of their luxury models by the mid-'70s. For example, ABS were available on the GM Eldorado, Toronado, Cadillac Deville and Fleetwood between 1976 and 1982.

All ABS manufacturers in the early '70s used state-of-the-art components, including vacuum as energy source, and analog electronics. Development of high-pressure energy sources including accumulators was underway in Europe. The basic shortcomings of the early ABS brakes were the low reliability of system electronics and to some extent also the low cycles rates due to limitations associated with the vacuum source. These reasons, and probably low public awareness and additional cost to the buyer, led to their quiet withdrawal from the market in the mid-'70s.

In the early '70s the National Highway and Traffic Safety Administration (NHTSA) of the U.S. Department of Transportation issued a regulation (FMVSS 121) which indirectly required the installation of ABS brakes on airbrake-equipped trucks and trailers by 1975. Early reliability and electronic controller problems caused the government to amend the standard, effectively removing the no-wheels lock requirement of the standard. NHTSA research showed the following causes of breakdown of ABS: 41% sensors, 16% valves, 8% computers, 3% incorrect installation, 1% electrical connections, 30% electromagnetic wave interference.

In Europe during the early and mid-'70s, brake and electronics suppliers had developed digital electronics changing from analog components to microprocessors. This resulted in the introduction of the first Bosch ABS on Mercedes passenger vehicles in 1978. This four-wheel add-on system was installed in the existing vacuum or hydraulic boost brake system. BMW and others followed shortly. Japanese brake and vehicle manufacturers introduced ABS brakes based on the Bosch system as well as their own designs by the mid-' 80s. The Bosch ABS was used in the '86 Corvette and Cadillac Allante. In 1984 an integrated ABS produced by ITT-Teves was introduced on the Lincoln Mark VII in the U.S. and, in 1985, as standard equipment on the Ford Scorpio in Germany. The Teves integrated system combines the ABS actuator, hydraulic booster and master cylinder into one unit. The Teves ABS system was likewise available on luxury GM cars in the '86 model year.

3. A Quarter-Vehicle Model

A quarter-vehicle model (QVT) will be used to analyze a vehicle-braking maneuver during straight line driving. The QVT includes a model of the suspension in vertical direction, a fore-aft axle compliance model, and a tire (SWIFT) model (see Figure 3.1).

It is assumed that the vertical (along the z-axis) displacement of the axle with respect to the vehicle body is within the nominal range of the suspension. The suspension, modeled as a linear spring with stiffness k_z and a linear viscous damper with damping c_z, connects the quarter of the vehicle body with mass m_2 and the axle with mass m_1, where m_1 is the sum of the masses of all components rigidly connected to the unspring mass, such as axle hub, brake disk, brake's clipper, rim, mass of the spring and the damper, and all of the moving parts connected to the axle hub.

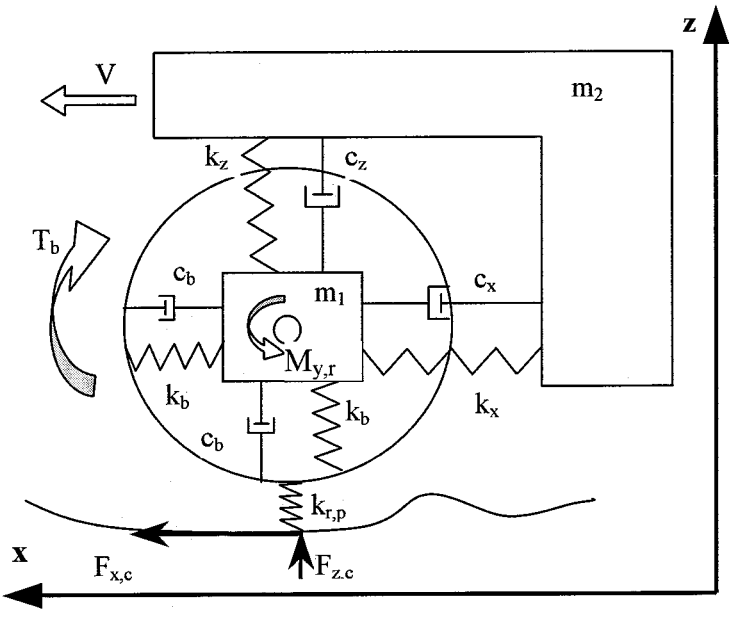

Figure 3.1: *Quarter vehicle, suspension and tire representation in X and Z directions*

The adopted model for the tire dynamics and the tire-road interaction is the Short Wave Intermediate Frequency Tire (SWIFT) model. The SWIFT model combines a Magic Formula slip force description with a rigid ring model. The tire belt is modeled as a rigid ring suspended to the rim by a vertical and longitudinal sidewall stiffness k_b and damping c_b. Rotational sidewall stiffness and damping are also included in the model. The contact model uses the spring stiffness $k_{r,p}$ to model the vertical force at the contact point (see Figure 3.2).

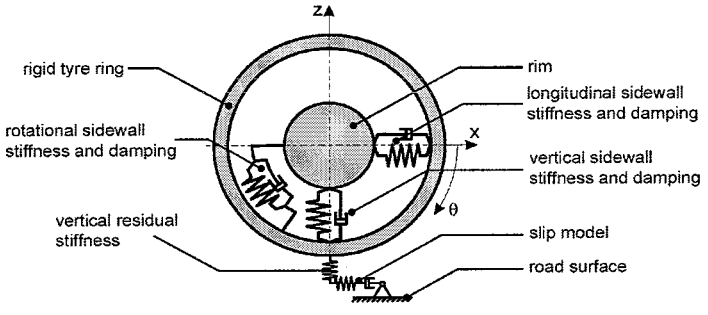

Figure 3.2: *Side view of the rigid-ring representation of the tire. In-plain characteristics.*

The Fore-aft axle suspension is modeled with a stiffness k_x and a damping c_x. The motion of the axle along the x-axis is decoupled from the motion along the z-axis see Figure 3.1. For clarity we will analyze the decoupled model with displacement along one axis only. The SWIFT model delivers amongst others the forces exerted on the tire at the ground contact point (denoted with subscript ***c*** in Figure 3.1) As output of the SWIFT model we have the forces acting on the rim (axle) denoted with subscript *r* (**Appendix-A** and **Appendix -B**). Those forces will be used as input in the QVT model.

In this study only braking of the test vehicle is considered. That is why during all simulations the driving torque from the engine is zero. The torques applied on the tire are:

- Tire torque $M_{y,r}$, positive as denoted in Figure 3.1.
- Brake torque T_b, positive as denoted in Figure 3.1. The maximum torque that can be generated by the brakes depends amongst others, on the pressure in the wheel hydraulic cylinder. The brake line pressure depends on the force, exerted by the driver on the brake pedal, respectively on the master cylinder.

4. Suspension Model

4.1. Suspension Model in Vertical Direction (z-axis)

By considering all forces acting along the z-axis (see Figure 4.1) we can write the following differential equations of motion:

$$\ddot{z}_1 \cdot m_1 = -k_z \cdot (z_1 - z_2) - c_z \cdot (\dot{z}_1 - \dot{z}_2) - m_1 \cdot g + F_{z,r} \quad (4.1)$$

$$\ddot{z}_2 \cdot m_2 = -k_z \cdot (z_2 - z_1) - c_z \cdot (\dot{z}_2 - \dot{z}_1) - m_2 \cdot g \quad (4.2)$$

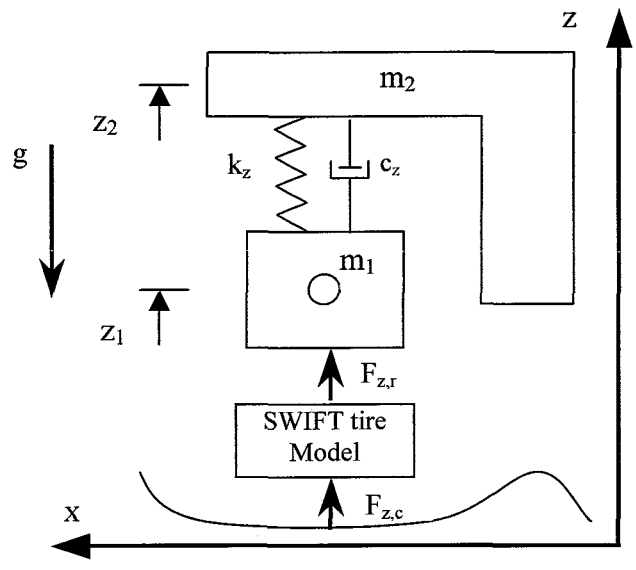

Figure 4.1: *Decoupled model representation of the forces acting along z-axis.*

Here $F_{z,r}$ is the vertical force of the tire on the rim. It is the z-component of the tire-road interaction forces. $F_{z,r}$ is determined in the SWIFT model, using the road profile and the axle vertical position z_1 and velocity $\dot{z}$. At steady state the magnitude of the force equals sum of the masses (m_1 and m_2) times the gravity constant.

Initially the system is at rest. The steady state position z_{10} of the axle and displacement z_{20} of the vehicle body are introduced as initial conditions in the integrators respectively. These steady state values follow from:

$$z_{10} = r_0 - g \cdot (m_1 + m_2 + m_{belt}) / k_{z,tire} \quad (4.3)$$

$$z_{20} = z_{10} + l_{z0} - g \cdot m_2 / k_z \quad (4.4)$$

where:

r_0 - unloaded tire radius

$k_{z,tire}$ - vertical tire stiffness as specified in the SWIFT model.

l_{x0} - unloaded spring length

This part of the suspension model is implemented in SIMULINK, see Figure 4.2. The values of the parameters in this model are given in Table 4.1.

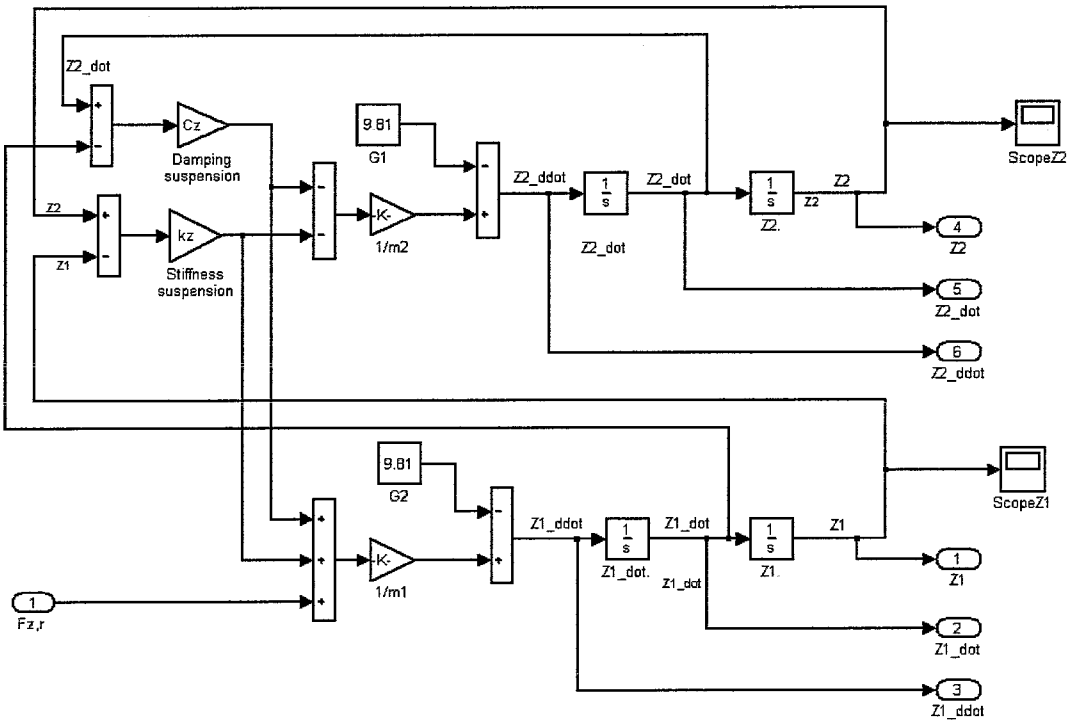

Figure 4.2: *SIMULINK layout representing the QVT suspension in vertical direction.*

The calculation of z_{10} and z_{20} is part of the initial calculation section in the mask of the SIMULINK QVT model.

Table 4.1: *Data used for the z-axis QVT model.*[6,13,18]

Parameter		Value	Dimension
Quarter of the vehicle mass	m_2	300	kg
Mass of the axle and components	m_1	35	kg
Mass of the belt	m_{belt}	7	kg
Unloaded tire radius	r_o	0.3135	m
Suspension spring stiffness	k_z	20000	N/m
Suspension damper damping	c_z	2000	Ns/m
Gravitational constant	g	9.81	m/s^2
Axle initial position equals the loaded tire radius r_{load}.	z_{10}	0.2967	m
Vertical tire stiffness	$k_{z,tire}$	200000	N/m
Vehicle body displacement	z_{20}	-0.1636	m

4.2. Suspension Deflection Model Along the x-axis

By considering all forces acting along the x-axis (see Figure 4.3) we can write the following differential equations of motion:

$$\ddot{x}_1 \cdot m_1 = -k_x \cdot (x_1 - x_2) - c_x \cdot (\dot{x}_1 - \dot{x}_2) + F_{x,r} \tag{4.5}$$

$$\ddot{x}_2 \cdot m_2 = -k_x \cdot (x_2 - x_1) - c_x \cdot (\dot{x}_2 - \dot{x}_1) \tag{4.6}$$

The SIMULINK layout of the model for the longitudinal suspension is given in Figure 4.4. The value of the initial position of the tire contact point is set to zero ($x_{10} = 0$). Value of the vehicle body displacement in its initial position is set to zero ($x_{20} = 0$). For the relative difference in the positions between the axle and the vehicle body the length (0.1 m) of the unloaded spring is used.
For both the axle and the vehicle the initial horizontal velocity is introduced in the model by initial conditions in the respective integrators.

The horizontal component *Fx,r* of the tire reaction force is determine by the SWIFT model based on the horizontal position x_1 and velocity $\dot{x}_1$.

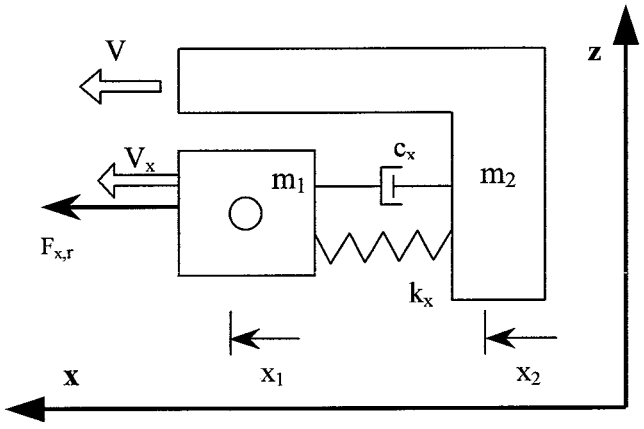

***Figure 4.3**: Decoupled model representation of the forces acting along x-axis.*

The values of the data used in this model are given in Table 4.2. The initial horizontal positions and velocities are implemented in the mask of the SIMULINK QVT model. It is assumed that the vehicle is already speeded up and is cruising with constant speed V_{in}. No other forces or moments are acting on the vehicle, i.e. the assumption is that the external forces and/or moments on the vehicle are significantly small and can be neglected.

The combination of the *STOP* block and the *Relation operator* block is used to stop the simulation when the vehicle speed is lower than or equal to the predefined value *Vstop* of the *zero velocity* block. To calculate the stopping distance an additional integrator is used. It starts to integrate the vehicle velocity when the brakes are applied (*Start to Brake* signal is set to "1"). It is also possible to calculate the stopping distance by the difference between the stopped position and the position at which the brakes are applied. This requires a memory element to store the initial position. The implemented stopping distance calculation is simpler. The output signal (*X1–X2*) represents the suspension deflection, i.e. the axle fore–aft displacement relative to the vehicle body.

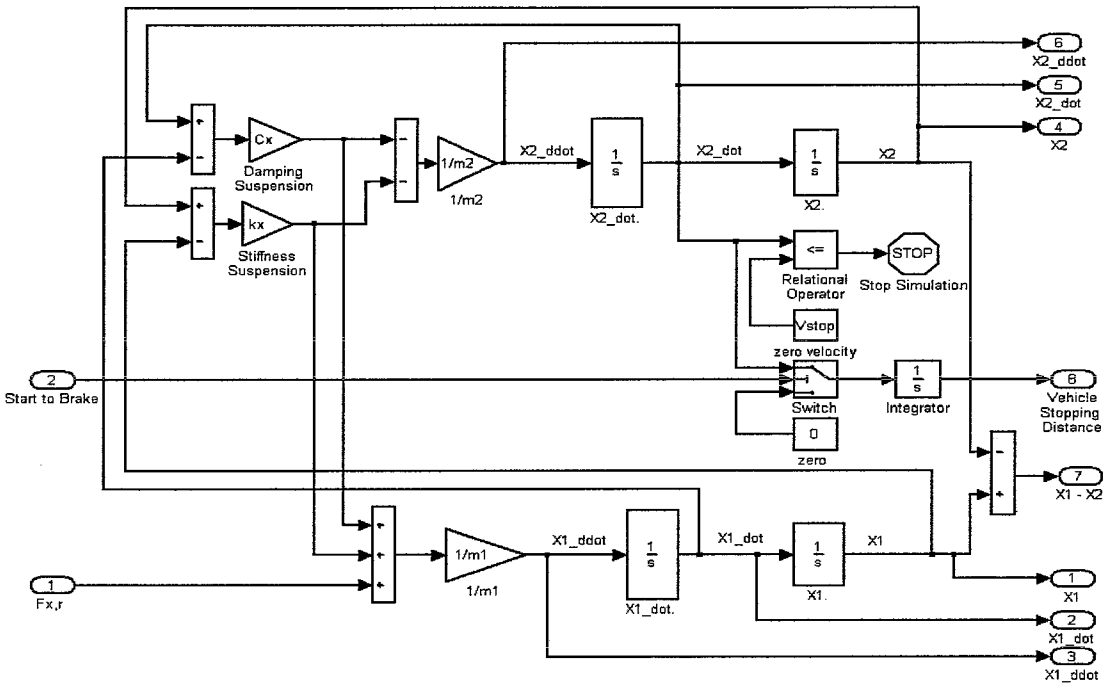

Figure 4.4: *SIMULINK layout representing the QVT suspension model in vertical direction.*

Table 4.2: *Data used for the x-axis QVT model.* [6,13,18]

Parameter		Value	Dimension
Quarter of the vehicle mass	m_2	300	kg
Mass of the axle and components	m_1	35	kg
Suspension compliance stiffness	k_x	100000	N/m
Suspension compliance damping	c_x	2000	Ns/m
Vehicle velocity before braking	V_{in}	Variable	m/s
Velocity value at which the vehicle is considered stopped	V_{stop}	1	m/s

5. Tire Model and Torques Around the y-axis

5.1. The Pneumatic Tire

The pneumatic tire forms a vital component of a road vehicle as it interacts with the road in order to produce the forces necessary for support and movement of the vehicle. An accurate description of the behavior of the tire is essential of the analysis of the dynamics of vehicles. Due to the interaction between wheel and road, the tire deflects and as result generates forces and moments. In the longitudinal direction force variations, due to road irregularities, are transmitted to the wheel axle and through the wheel suspension to the car body. Fluctuations in the wheel angular speed due to braking will also generate longitudinal force variations. The vertical oscillations induced by road and tire irregularities are transmitted to the axle and further to the vehicle. The variations in normal load of the tire have an important effect on the longitudinal force generation.

5.1.1. Construction of a radial-ply tire

A pneumatic tire is a very complex construction. It can be seen as a visco-elastic torus composed of high-tensile-strength cords and rubber. Figure 5.1 shows the construction of a radial-ply tire, which is used in most of today's automobile tires. The radial-ply tire, or just radial tire, is characterized by parallel cords running directly across the tire from one bead to the other. These cords are referred to as the carcass plies. Directional stability of the tire is supplied by the enclosed pressurized air acting on the sidewalls of the carcass and by a stiff belt of fabric or steel that runs around the circumference of the tire. The direction of the parallel belt plies is relatively close to the circumferential: typically 20°.

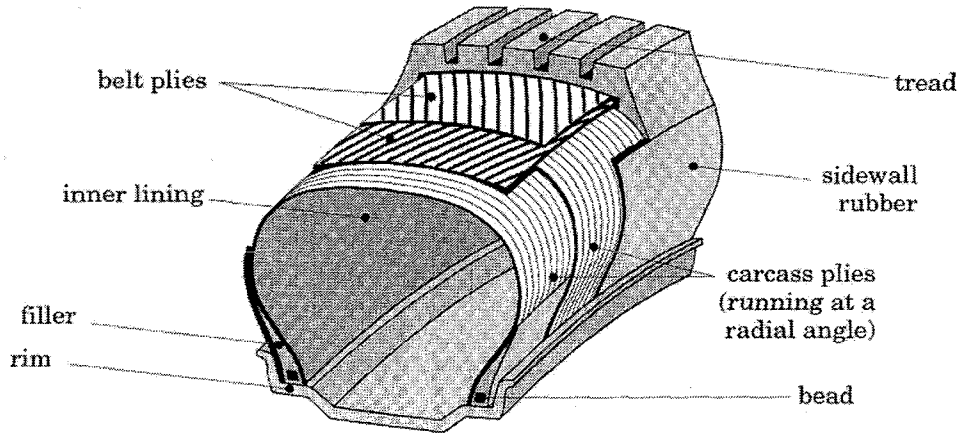

Figure 5.1: *Construction of a radial-ply tire.*

The relatively soft carcass of the radial tire results in a soft ride. On the other hand a stiff belt provides the radial tire with good cornering properties by keeping the tread flat on the road despite of horizontal deflections of the tire. The function of the tread is to establish and maintain contact between the tire and the road. The key factor for the generation of horizontal forces in the contact zone is the adhesion between tread and road. The remaining components of the tire are the steel-cable beads which firmly anchor the assembly to the rim.

5.1.2. Tire modeling for vehicle dynamic analysis

Understanding of tire properties is essential of a proper design of vehicle components such as wheel suspensions and steering and braking systems. To understand the force generation of the tire, it is useful to introduce the concept of slip of a rolling tire. This concept is related to the difference between the actual wheel velocity and the wheel velocity at free rolling. Free rolling is the situation in which the tire is neither braked nor driven (no torque transmitted). The relationship between the generated horizontal force and the slip in steady-state conditions is called the steady-state slip characteristic or the stationary slip characteristic. At small values of slip, the horizontal force depend mainly on the elastic deformation of tire and is more or less proportional to the slip. The ratio is called the slip stiffness. At higher levels of slip the horizontal forces are limited by the friction between the tire and the road. [1,5,10,17]. The influences of the inertia forces become more important at higher velocities [18,10].

The dynamic properties of tires play an important role in the design of control algorithms like Anti-lock Brake Systems (ABS) or Vehicle Dynamics Control systems (VDC). For instance, the rapid brake pressure variations during ABS operation cause oscillations of the tire-wheel system. Adequate dynamic tire models are needed to design and evaluate the control systems [7], and also to analyze the performance of ABS on uneven roads [6, 17].

5.1.3. The tire used in the model

The model developed in this thesis is considered to be a general model for the in-plane tire behavior. The tire used in this model is a standard passenger car tire of type ***205/60R15***, where (see Figure 5.2):

205 = section width of the tire in millimeters.
60 = aspect ratio: the ratio between the section height and section width in %.
R = construction of the tire: radial tire.
15 = diameter of the rim in inches.

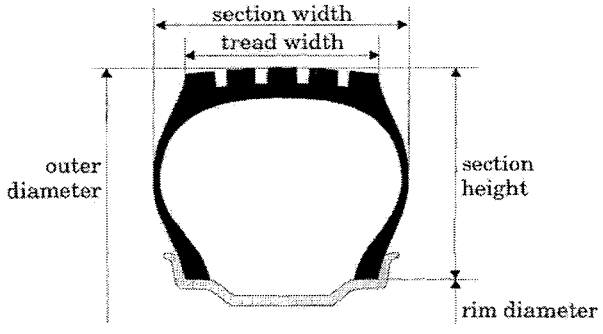

Figure 5.2: *The tire cross-section*

5.1.4. Inertia properties of the tire

The dynamic properties of the tire are mostly determined by the inertia and stiffness properties of the tire. In the SWIFT model the tire tread-band is represented by a rigid ring suspended on springs representing the tire sidewalls and pressurized air.

Consequently, the mass and moment of inertia of the tire has to be subdivided into a part that moves together with the rigid ring and a part that moves together with the rim. To enable this, the tire is divided into five components: two beads, two sidewalls and one tread-band, see Figure 5.3. The two beads move together with the rim, and the tread-band moves together with the rigid ring. The sidewall connects the tread-band with the beads. The sidewall is divided into two pieces: the inner half of the sidewall is assumed to move together with the rim while the outer half of the sidewall is assumed to move together with the rigid ring.[18]

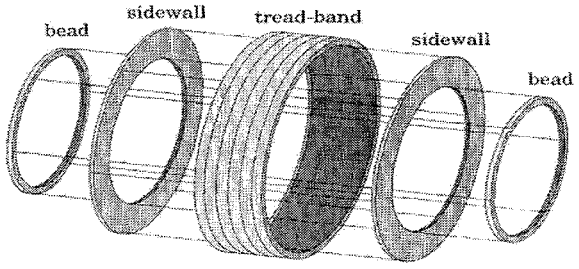

Figure 5.3: *Decomposition of the tire into five components.*

5.2. Torques Around y-axis

Tire characteristics play an important role in braking. For ABS-equipped vehicles the tire performance is of critical significance. All braking and steering forces must be generated within the small tire contact (tread patch) between the vehicle and the road. Tire longitudinal braking forces as well as side forces can only be produced when a difference exists between the speed of the tire circumference and the speed of the vehicle relative to the road surface.

Under straight-line braking, as well as during acceleration the level of force transfer depends upon the longitudinal tire slip κ. The relationship between κ and the tire-road interface friction coefficient μ_x is basically the same for accelerating or braking.

The wheel is attached to an axle and can rotate around it. The y-axis coincides with the axle center and is perpendicular to the plane of the drawing (see Figure 5.4). The torque exerted by the tire $M_{y,r}$ acts on the rim in positive (counterclockwise) direction. The brake torque Tb as commanded by the brakes also acts on the rim but opposite to $M_{y,r}$.

In the SWIFT model the tire belt is represented by a rigid ring suspended on springs with stiffness k_b and dampers with damping c_b representing the tire sidewalls and pressurized air. The tire model uses a spring with stiffness $k_{r,p}$ to generate the normal force $F_{z,c}$ in the tire-road contact zone(see Figure 5.4).

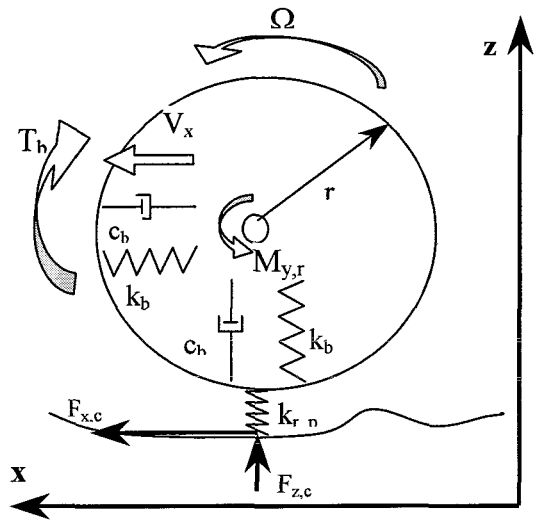

Figure 5.4: *Forces in the contact point and torques on the rim.*

5.2.1. Effective tire rolling radius and longitudinal slip

The loaded tire radius r_{load} is the distance of the center of the wheel to the contact point c between the tire and the road (see Figure 5.5). This radius is related to the unloaded radius r_0 by $r_{load} = r_0 - \rho$ where ρ is the vertical tire deflection. Assuming a constant vertical tire stiffness $k_{z,tire}$, ρ is follows from:

$$\rho = \frac{F_{z,c}}{k_{z,tire}} \tag{5.1}$$

The tire longitudinal slip κ is negative during braking and positive when accelerating. This slip is defined by:

$$\kappa = -\frac{V_{sx}}{V_x} \tag{5.2}$$

where V_x is the linear velocity of the wheel center in x-direction whereas the longitudinal slip speed V_{sx} is defined by:

$$V_{sx} = V_x - \Omega \cdot r_{eff} \tag{5.3}$$

where:

r_{eff} - effective rolling radius.

V_x - longitudinal wheel center forward velocity.

Ω - angular velocity of the rim.

The –yet undefined – quantity in this relation is the so-called effective rolling radius r_{eff}. In the SWIFT model a Magic Formula – like approach to determine r_{eff}:

$$r_{eff} = r_0 - \left(D \cdot \arctan\left(B \cdot \rho^{\text{dim.}}\right) + F \cdot \rho^{\text{dim.}}\right) \cdot \frac{F_{z,c}}{k_{z,tire}} \qquad (5.4)$$

where:

r_0 - unloaded radius

F_{z0} - nominal force used to in the experiments to estimate the coefficients

B,D,F - constant coefficients of the Magic Formula Equation

$\rho^{dim.}$ - dimensionless radial tire deflection

$$\rho^{\text{dim.}} = \frac{\rho}{\rho_{F_{z,nom}}}$$

where:

$\rho_{Fz,nom}$ - radial tire deflection at nominal tire load.

The longitudinal slip κ describes the normalized difference between the wheel axle speed V_x and the speed $\Omega.r_{eff}$ of the wheel perimeter. The slip $\kappa = 0$ characterizes free rolling of the wheel (no friction force $F_{x,c}$). In fact due to the rolling resistance, there is a small contribution to the friction force. If the slip $\kappa = -1$, then the wheel is locked ($\Omega = 0$).

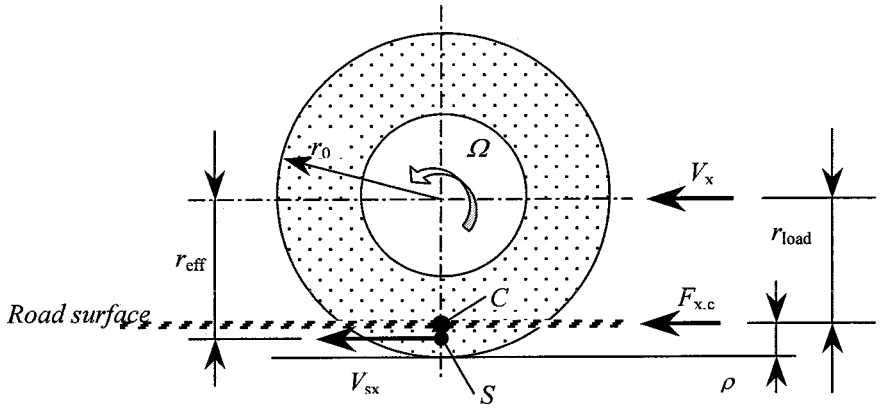

Figure 5.5: *Effective rolling radius and Longitudinal slip speed.*

5.2.2. Forces/moments in the tire-road interface during braking.

The friction coefficient μ_x in longitudinal direction is a nonlinear function of the slip κ. For a dry asphalt road the peak value of μ_x is reached for κ in the range of 10 to 20 %. The relation between the longitudinal force $F_{x,c}$, the normal force $F_{z,c}$, and the friction coefficient μ_x reads:

$$F_{x,c} = \mu_x \cdot F_{z,c} \qquad \mu_x = f\left(F_{z,c}, \kappa\right) \qquad (5.5)$$

The friction coefficient μ_x depends on the type of the road surface, the weather conditions and the type of the tire. See Table 5.1.

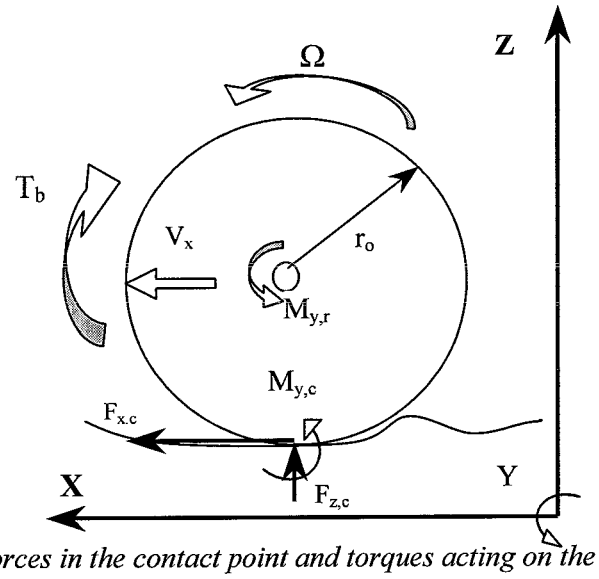

Figure 5.6: *Forces in the contact point and torques acting on the tire rim around y-axis.*

Figure 5.7 gives a curve of $F_{x,c}$ versus κ for negative values of κ, i.e. in braking. Parameters of the vehicle and employed tire type are given in Table 5.2

Table 5.1: *Peak value of the tire/road friction coefficient.*[1,17,15,]

Surface	Weather conditions	Friction coefficient peak value
Asphalt and concrete	dry	0.8-0.9
Concrete	wet	0.8
Asphalt	wet	0.5-0.6
Earth road	dry	0.7
Earth road	wet	0.5-0.6
Snow	hard packed	0.3
Ice		0.1

Figure 5.8 shows that, for small values of $|\kappa|$ an increase in slip $|\kappa|$ will result in increase in μ_x. The friction coefficient reaches its maximum value of 1.207 for $|\kappa|$ = 15% slip.

For $|\kappa|$>15% (see Figure 5.8), the friction coefficient enters the unstable region. Any further increase in slip within this region will lead to a decrease in μ_x until the coefficient reaches the value of sliding friction.

5.3. Wheel Dynamics

The relation between torques around the y-axis, the wheel angular acceleration $\dot{\Omega}$ and the wheel polar moment of inertia I_p can be described by the following differential equation:

$$I_p \cdot \dot{\Omega} = M_{y,r} - T_b \cdot sign(\Omega) \quad \text{if} \quad \Omega \neq 0 \tag{5.6}$$

where

$$I_{belt} \cdot \dot{\Omega} = r_{load} \cdot F_{x,c} - M_{y,r} \tag{5.7}$$

Equation (5.6) holds only for a rotating wheel (angular velocity $\Omega \neq 0$). For $\Omega = 0$ and $V_x > 0$ (wheel locked, longitudinal slip $\kappa = -1$) the brake torque T_b equals the available tire torque $M_{y,r}$ for a sliding tire.

Table 5.2: *Data used for the tire and quarter vehicle model.*

Parameter			Value	Dimension
Vehicle	Quarter of the vehicle mass	m_2	300	kg
	Mass of the axle and components	m_1	35	kg
	Wheel angular velocity before braking	Ω_0	Variable	rad/s
	Wheel-tire assemble polar moment of inertia	I_p	1.04	kg.m^2
Tire	Type – 205/60 R15			
	Tire belt mass	m_{belt}	7.10	kg
	Tire belt polar moment of inertia	I_{belt}	0.695	kg.m^2
	Unloaded tire radius	r_o	0.3135	m
	Loaded tire radius	r_{load}	0.2968	m
	Effective rolling radius (the tire loaded is $m_1 + m_2 + m_{belt}$)	r_{eff}	0.3067	m
Road	surface		Asphalt	
	condition		Dry	
	profile		Smoot	
Brake	Rate of the brake torque increase	R1	19000	N.m/s
	Rate of the brake torque decrease	R2	19000	N.m/s

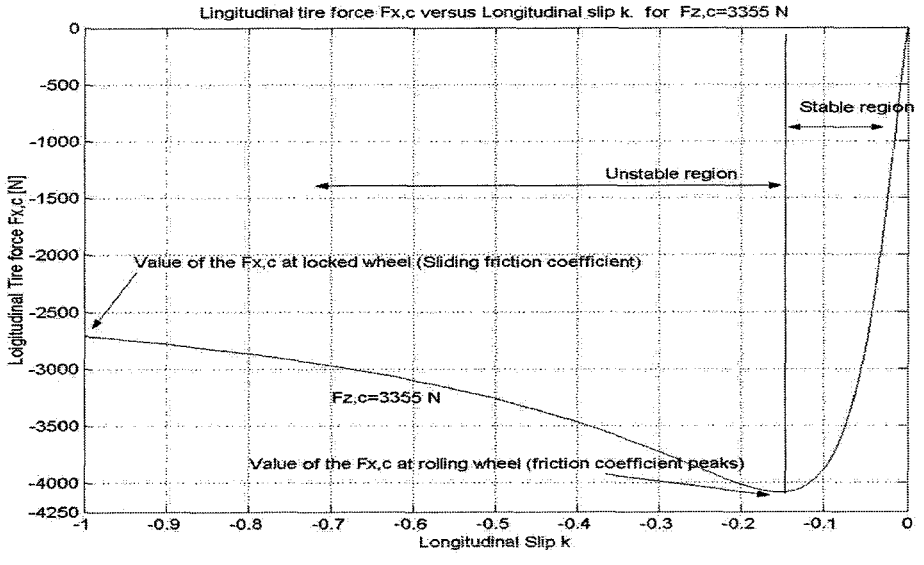

Figure 5.7: *Profile of the longitudinal braking force $F_{x,c}$ exerted at the tire-road contact point. The brake force is function of both slip dependent friction coefficient μ_x and the normal force $F_{z,c}$ the plot is generated for the $F_{z,c}$ =3355 N (342kg.9,81m/s^2)*

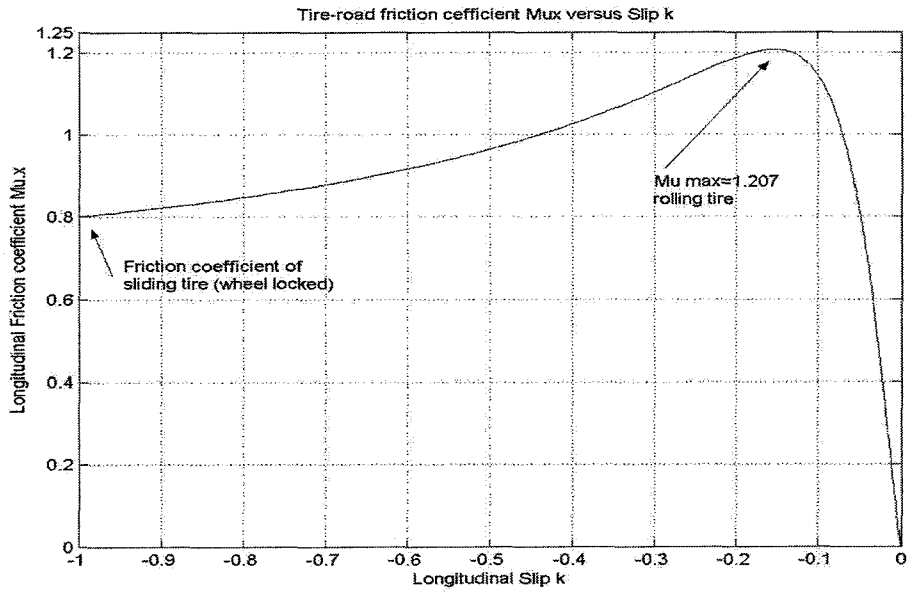

Figure 5.8: *Slip dependent friction coefficient μ_x, simulation results. For the model parameters see Table 5.2.*

5.3.1. SWIFT model

The SWIFT model describes the forces and moments generated at the tire-road interface. Combining the SWIFT model and Equation. (5.6), SIMULINK model is developed (see Figure 5.8). A detailed explanation of the SWIFT model interface is given in **Appendix-B, Appendix –A** and **Appendix –D.**

The SWIFT model requires the following input signals:

- **road** – settings for the road profile. In SWIFT-Tyre, the road profile must be given as an ASCII file when the check box 'Effective inputs' is selected. In the road property file the road height is specified as a function of the traveled distance. SWIFT uses a zero-order sample and hold when evaluating the road profile.
- **dist** – a vector with the x, y and z-coordinate of the wheel axis in the global coordinate system.
- **tramat** – a vector with nine components to specify the transformation from the coordinate system, fixed to the wheel carrier, to the global coordinate system. For the current model this is a 3x3 unit matrix.
- **vel** – a vector with the three components of the global velocity of the wheel center expressed in the wheel carrier local frame.
- **omegar** – relative angular velocity of the wheel with respect to the wheel carrier about the wheel spin axis. In the current application equal to Ω.
- **angtwc** – rotation angle φ of the wheel with respect to the wheel carrier about the wheel spin axis, so $\dot{\varphi} = \Omega$ in the current application.

- **omega** – a vector with the three components of the global angular velocity of the wheel center expressed in the wheel carrier local frame. Zero in our case.

From the input signals, the SWIFT model calculates the following output signals:

- **forces** – components of the force, applied by the tire on the rim at the center of the wheel, expressed in the carrier frame.
- **torque** – components of the torque, applied by the tire on the rim at the center of the wheel, expressed in the carrier axis system.
- **varinf** – array containing the value of 40 extra output variables on the tire behavior

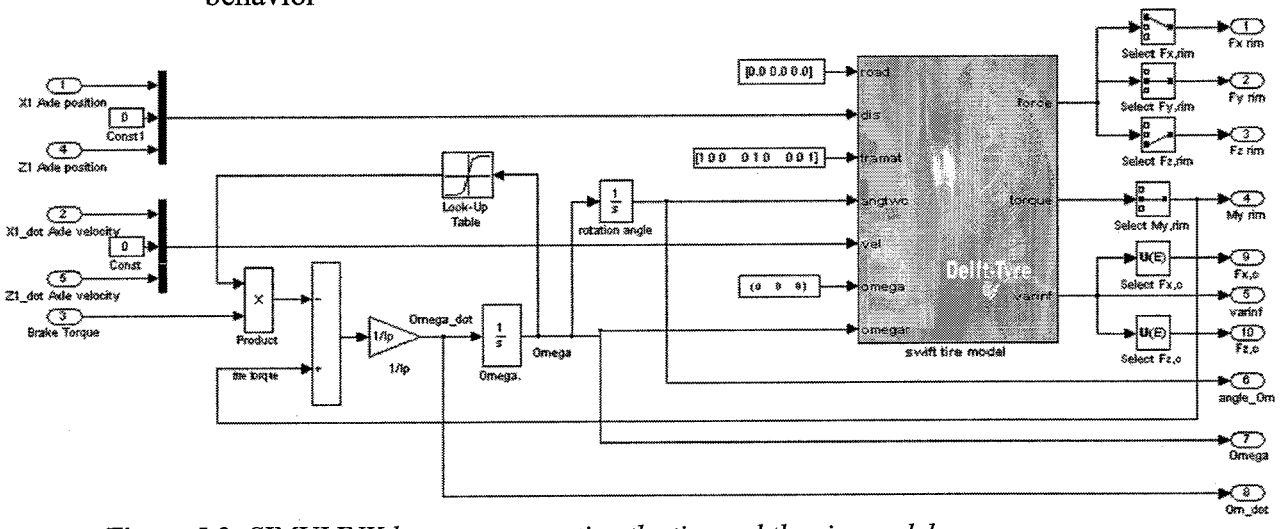

Figure 5.8: SIMULINK layout representing the tire and the rim model.

5.3.2. The tire torque $M_{y,r}$ components

The term r_{load}. $F_{x,c}$ of Equation (5.7) originates from the tangential friction force $F_{x,c}$ times its effective arm r_{load}. The maximum of that force is limited by the product of the normal force $F_{z,c}$ and the value of the tire-road friction coefficient μ_x in longitudinal direction.

The inertial term I_{belt} . $\dot{\Omega}$ of Equation (5.7) is related to the polar moment of inertia of the tire belt. During braking the rate of brake torque increase representative for the wheel deceleration $\dot{\Omega}$ and here for the contribution of the inertial term to the moment generated by the tire. High increase rates of T_b cause a rapid change of $\dot{\Omega}$ and as a consequence a contribution to the tire torque. This contribution can be significant, especially for high levels of slip after the maximum of μ_x, as will be shown in Section 6.

To arrived at the tire torque generated only due to the longitudinal friction force we have to correct the $M_{y,r}$ for the inertial term. This correction reads:

$$M_{y,r\_corr.} = M_{y,r} + I_{belt} \cdot \dot{\Omega} = r_{load} \cdot F_{x,c} \qquad (5.8)$$

For given normal force $F_{z,c}$ and tire type, corrected tire torque $M_{y,r\ corr}$ provides information for the value of the friction coefficient and its utilization, taking into account

that $\mu_x(F_{z,c},\kappa)$. In terms of tire parameters, normal load and friction coefficient Equation (5.8) can be rewritten as:

$$M_{y,r\_corr.} = \mu_x \cdot F_{z,c} \cdot \left(r_0 - \frac{F_{z,c}}{k_{z,tire}} \right) \tag{5.9}$$

5.3.3. The Brake torque correction

If the magnitude of maximum brake torque T_b, that can be generated by the brakes[1] exceeds the available tire torque $M_{y,r}$ the resultant torque and consequently the angular wheel acceleration are negative. This is only a numerical, not a "real world" problem. In the reality this situation can never occur. The problem is that the actual brake torque $M_{y,r}=T_b+I_p.\dot{\Omega}$ *as long as* $\Omega > 0$. Then $T_b > M_{y,r}$ and T_b is determined by the hydraulic brake line pressure. If $\Omega = 0$ and $\dot{\Omega}$ then $T_b = M_{y,r}$ brake torque determined by friction between tire and road $T_b < T_{b,max}$ where the $T_{b,max}$ is determined by the brake pressure. During the integration of the negative $\dot{\Omega}$ the angular wheel velocity decreases and finally reaches zero, and the wheel locks up. Equation of motion in a given form no longer valid! This is unacceptable.

To solve this problem the following two solutions were investigated:

Solution I: The first approach employs a integrator for $\dot{\Omega}$ with limited output. The lower output value of the *Omega* integrator was limited to zero.

The result: This solved the problem with the wheel angular velocity, but the angular acceleration continues to be negative after the wheel locks up. This will cause problems if this acceleration is used for control purposes.

Solution II: The second solution is dealing not with the consequences but with the reason of the problem. To prevent the resultant torque to become negative after the wheel is locked the *look –up table* in combination with the *Product* block are implemented in the model. The input vector x values reads- [-10:0.01:10]; the output vector y values reads- tanh*(1/2* x).[1]

The result: This implementation offers the opportunity to change the sign of the torque when the zero wheel angular velocity is reached, and to maintain the resultant torque at zero. This solution will bring the wheel angular acceleration also to zero when the wheel happens to lock. Now the acceleration from the model agrees with the real acceleration and will not cause problems if used for control applications.

It can be concluded that the brake torque T_b needs correction only when the wheel angular velocity approaches zero - the wheel is about to lock. Solution II is implemented in the

[1] The maximum torque, that can be generated by the brakes depends amongst others, on the pressure in the wheel hydraulic cylinder. The brake line pressure depends on the force, exerted by the driver on the brake pedal, respectively on the master cylinder.

model and the correction of T_b is applied if Ω <10 rad/s. The resulting correction of the brake torque is discussed in more details in Section 6.
The initial angular velocity of the free rolling tire (no drive or brake torque, free cursing vehicle) is loaded as an initial condition in the *Omega* integrator.

6. Building the Complete Quarter-Vehicle and Tire model.

The models of the quarter-vehicle and the tire model are described in what precedes. The next step is to establish their interconnections. This will result in a Quarter-Vehicle and Tire (QVT) model.

Each of the three models is implemented as a subsystem block with its ones inputs and outputs. Nearly all input and output signals of the subsystems are exported to the MATLAB workspace for post processing and visualization. The layout of the QVT subsystem interconnections is shown in Figure 6.1.

On the QVT model the operation of subsystem generation was performed and the model block was created. After that, the QVT model has one input *Brake Torque* and eight outputs (see Figure 6.2)

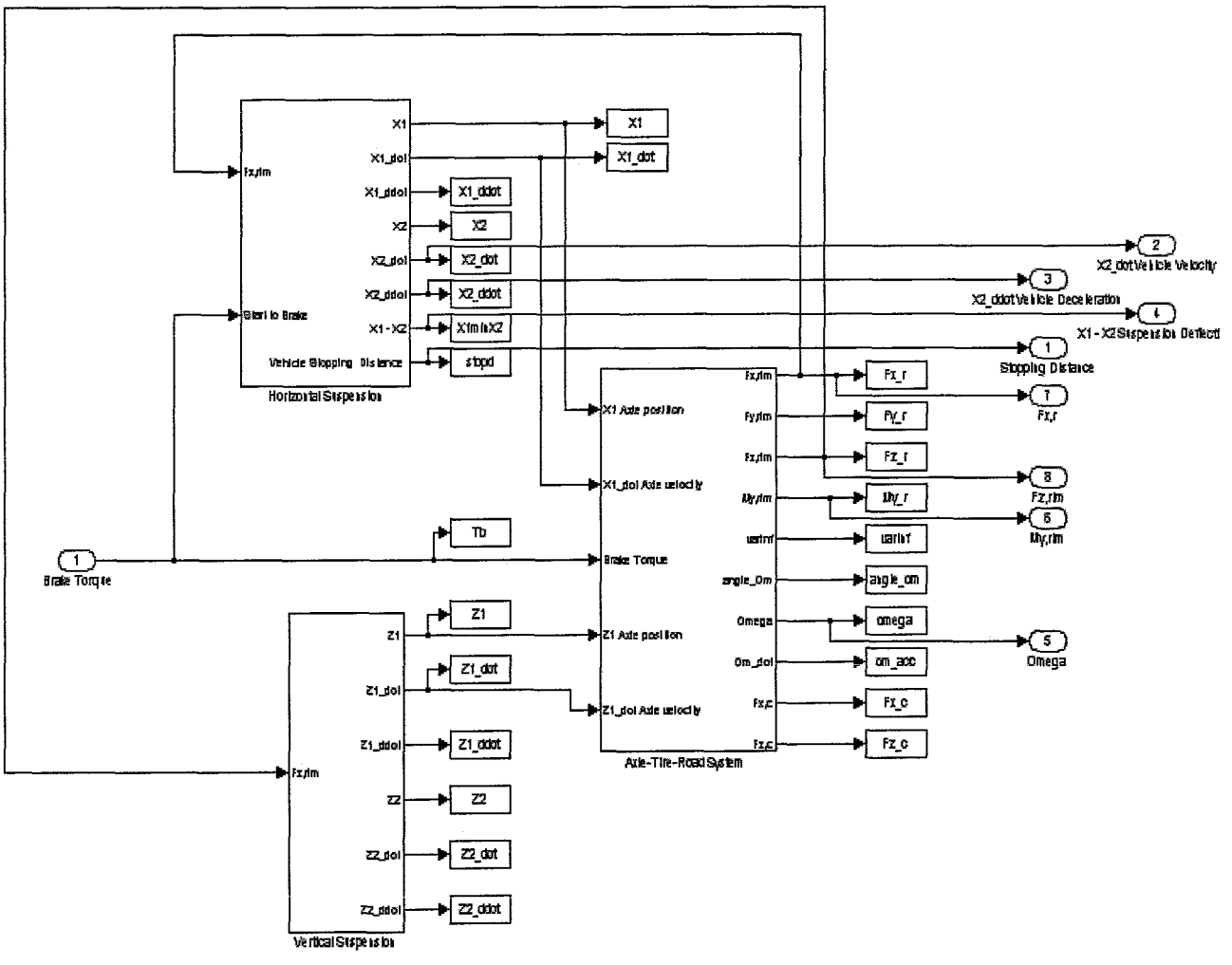

Figure 6.1: *SIMULINK layout representing the interconnections between the QVT model subsystems.*

For clarity, convenience and automation the QVT model was masked. The mask of the model offers the opportunity to specify the values of most of the important model parameters. See Figure 6.2. An alternative approach to specify the model parameters and

to generate plots of some of the simulation results is by the use of a script file. The printout of a possible script file is given in **Appendix -C**.

Through the mask of the SWIFT–standard tire interface the following tire-road model parameters are accessible:

- *Tyre property file* - the file name of the tire property file
- *Road* - enables you to choose road input via file (Data file (effective inputs)) or as flat road (external inputs (smooth road)).
- *Road data file*

The path to reach the mask of the SWIFT interface is:[*Quarter-Vehicle and Tire model* block / *look under mask* / *Axle-Tire-road System* block / *swift_sti.*]

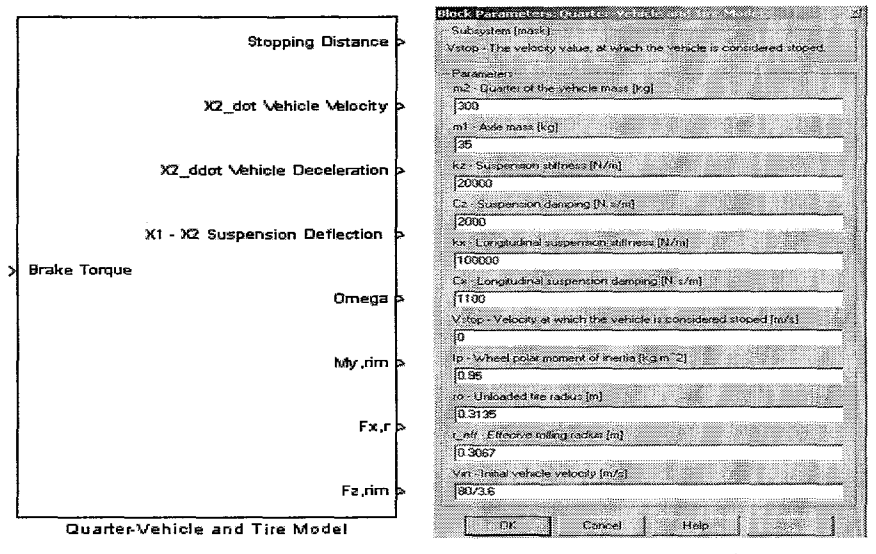

Figure 6.2: *View of the SIMULINK QVT model block and its mask.*

6.1. Validation of the Quarter-Vehicle -Tire model

To validate the QVT model a simulation of an emergency straight-line braking maneuver on a high friction, flat road was performed. Data of the simulation conditions and the QVT model settings are presented in Tables 5.2 and 6.1. Part of the output variables, considered as significant for the model validation, is shown in Figure 6.3 and Figure 6.4. The definitions of some of the variables are repeated here.

- Corrected brake torque $T_{b,corr} = M_{y,r}$ if $\Omega = 0$
- Tire moment on the rim $M_{y,r} = r_{load.} \cdot F_{x,c} - I_{belt} \cdot \dot{\Omega}$
- Corrected tire moment on the rim $M_{y,r\,corr} = M_{y,r} + I_{belt} \cdot \dot{\Omega}$
- Tire belt moment on the rim $M_{belt} = I_{belt} \cdot \dot{\Omega}$
- Wheel peripheral speed $\Omega_{per} = \Omega \cdot r_{eff}$
- Wheel peripheral acceleration $\dot{\Omega}_{per} = \dot{\Omega} \cdot r_{eff}$
- Vehicle speed $\dot{x}_2$
- Vehicle acceleration $\ddot{x}_2$

Table 6.1: *The QVT model parameters accessible through the model mask. Numerical values of the QVT model parameters.*

Parameter		Value	Dimension
Quarter of the vehicle mass	m_2	300	kg
Mass of the axle and components	m_1	35	kg
Suspension spring stiffness	k_z	20000	N/m
Suspension damper damping	c_z	2000	Ns/m
Suspension compliance stiffness	k_x	100000	N/m
Suspension compliance damping	c_x	2000	Ns/m
Velocity at which the vehicle is considered stopped	V_{stop}	1.0	m/s
Wheel-tire assemble polar moment of inertia	I_p	1.0400	$kg.m^2$
Unloaded tire radius	r_o	0.3135	m
Effective rolling radius	r_{eff}	0.3067	m
Vehicle initial velocity	V_{in}	60/3.6	m/s
Maximum value of the brake torque	$T_{b,max}$	2500	Nm

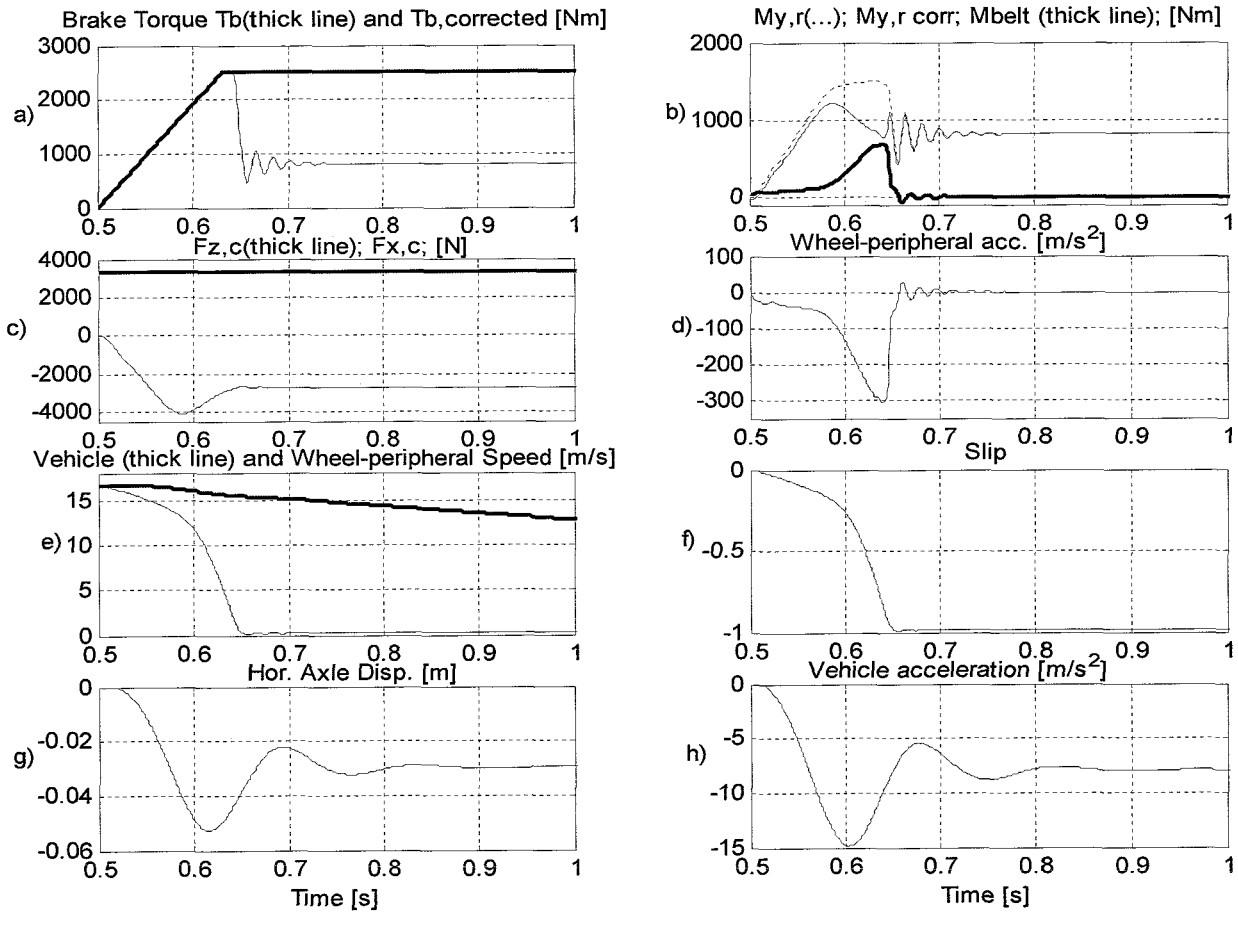

Figure 6.3: *Flat road. Emergency braking without ABS control, V_{in}=60 km/h, day asphalt, tire type 205/60 R15, R1=19000 Nm/s. $T_b$max = 2500 Nm. The instant of the brake maneuver initiation is t_0=0.5*

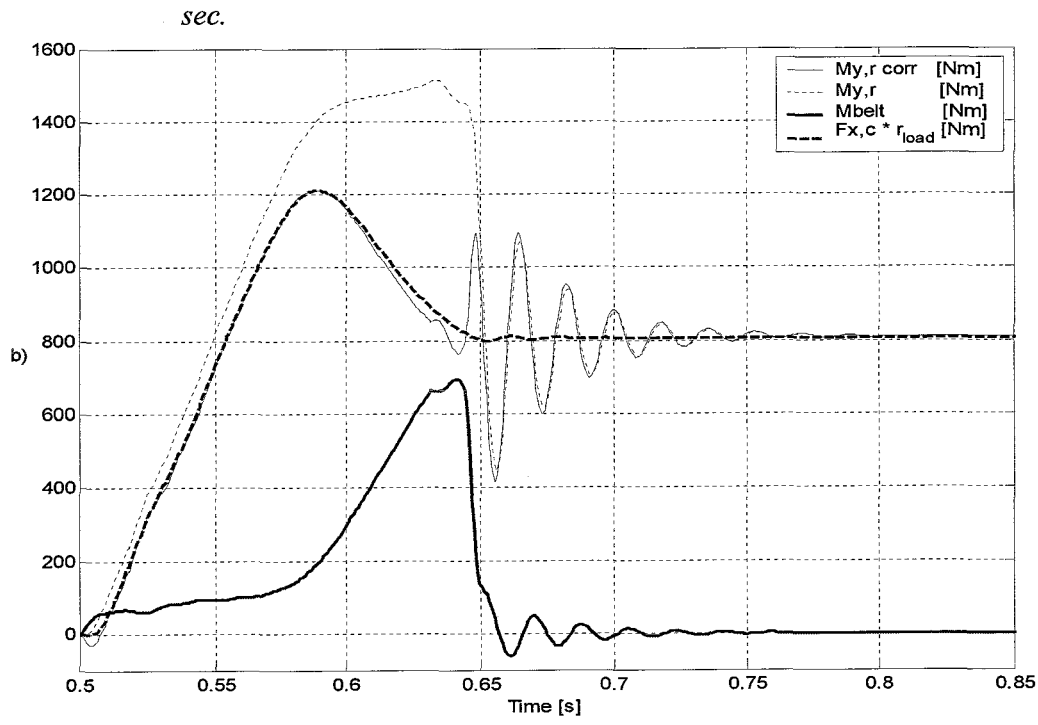

Figure 6.4: *Flat road. Emergency braking without ABS control. Zoom in of Figure 6.3b in the time window 0.5 – 0.85 sec. V_{in}=60 km/h, day asphalt, tire type – 205/60 R15, R1=19000 Nm/s, T_b max = 2500 Nm. The instant of the brake maneuver initiation is t_0=0.5 sec.*

Table 6.2: *Comparison of the stopping distance between the simulation and the theoretical results. The theoretical distance is calculated with Equation (10.15, first with constant vehicle deceleration, and second, with constant longitudinal force. V_{in}=60 km/h, dry asphalt, tire type – 205/60 R15, brake torque rate of increase R1=19000 Nm/s.*

		No ABS			
		Locked Wheel braking		**Theoretical stopping distance with const.**	
Parameter	**Dimension**	Mean value	Standard deviation	Vehicle accel. a_x	Braking force $F_{x,tot}$
Vehicle accel.	**m/s²**	**-8.25**	1.3431	**-8.25**	
Slip	**%**	92.18	16.1356		
$M_{y,r}$ corr	**Nm**	0830.6	0.0764		
$F_{x,c}$	**N**	**-2791.9**	0.2433		**2791.9**
$F_{z,c}$	**N**	3356.0	0.0003		
Stopping distance from 60 km/h to 3.6 km/h **[m]**		**17.54**		**16.77**	**16.95**

6.2. Conclusion on model validation

From simulation results presented in Figures 6.3 and 6.4, and Table 6.2 it can be concluded, that the developed QVT model generates reliable results and is suitable for brake performance study.

7. ABS Design Concepts

7.1. Basic Performance Requirements

The design of an ABS begins with understanding of the tire-road friction characteristics. The braking process would be optimal in terms of minimum stopping distance if the slip of the braked tire could always be kept at the value corresponding to the peak friction level. Ideally then, a sensor would detect the magnitude of the coefficient of friction at the tire-road interface, and the rest of the brake system would use this signal to modulate the brake torque in such a manner that the friction coefficient is maximal throughout the braking process. In practice, it is not feasible to detect the tire-road friction coefficient directly since this would require a fifth wheel as employed in road friction measuring equipment.

In general, the following methods have been suggested as modulating variables for the automatic control of the brake torque:

1. Angular velocity of the wheel.
2. Slip of the tire.
3. Velocity difference V_{sx} between tire and vehicle.
4. Peripheral velocity difference between a tire and the other tires of the vehicle.

Currently used ABS sensors measure the wheel angular velocity Ω from which the wheel deceleration is determined by differentiation. The tire slip is estimated by comparing this measured wheel velocity with a memory of the wheel velocity before initiation of braking. The memory may consist of a flywheel in the case of purely mechanical ABS systems, a capacitor in the case of the earlier analog systems, or a microcomputer memory. In some ABS systems, the longitudinal vehicle deceleration is measured to provide additional data for brake line pressure modulation. In some rare cases, lateral acceleration is measured to improve pressure modulation.[10]

The function of the ABS system is to maintain optimum braking performance of all wheels under all foreseeable operating conditions. Two basic criteria are used to sense wheel lockup, namely circumferential or rotational wheel speed deceleration, and relative wheel slip.

For constant effective rolling radius r_{eff} peripheral deceleration/acceleration of the wheel $\dot{\Omega}_{per}$ [m/s^2] is introduced as:

$$\dot{\Omega}_{per} = \dot{\Omega} \cdot r_{eff} \tag{7.1}$$

Fairly the r_{eff} is not a constant, it vary with the angular velocity, tire pressure, tire load and the tire type. Variation of the r_{eff} due to the angular speed, for given tire pressure, load, and tire type is neglected. We will assume a fixed value.

7.2. ABS Control Loop

In general the ABS feedback control loop (see Figure 7.2) consists of:

- *Controlled system* - Vehicle with wheel brakes, wheels and friction between tires and road surface.

- *Disturbance factors* - Road-surface conditions and profile, brake condition, vehicle load and tires (e.g., low tire pressures, inadequate tread depth).
- *Controller* - Wheel-speed sensors and ABS control unit.
- *Controlled variables* - Wheel-speed, the peripheral wheel deceleration/acceleration and slip.
- *Reference input variable* - Pressure applied to brake pedal (driver's brake-pressure input); Value for the desire slip.
- *Manipulated variable* - Brake pressure.

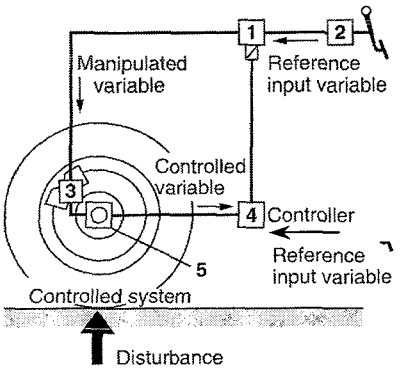

Figure 7.1: *ABS control loop components:1-Hydraulic modulator with solenoid valves, 2-Brake master cylinder, 3-Wheel-brake cylinder, 4-ECU, 5-Wheel-speed sensor. (Bosch)*

7.3. ABS Control Concepts for two axle vehicles

The ABS control can be accomplished in several ways.

In ***single-wheel control*** the wheel speed sensor of a wheel controls the adjustments made to the brake line pressure of that wheel, independent of any other wheels. This control method results in maximum braking on that wheel and, hence, maximum overall vehicle deceleration. On split-coefficient of friction surfaces the different braking forces left and right cause a yaw moment attempting to rotate the vehicle toward the higher traction side. Single-wheel control is generally used on the front wheels of motor vehicles.

In ***select-low control*** the wheel with the lower traction controls the brake line pressure for both brakes on that axle. The traction force on the higher friction surface is not fully utilized resulting in a lower brake torque and, hence, longer stopping distance. The advantages are a higher side force potential and the absence of a yaw moment. Select-low control is typically used on the rear wheels of motor vehicles.

In ***select-high control*** the wheel with the higher traction controls the brake line pressure of both brakes on that axle. The results are a higher braking force, unbalanced brake forces left and right which causes a yaw moment, and locking of the wheel on the low-friction surface. Honda has used select-high on the front and select-low control on the rear axle. Consequently, one front wheel can lock up on a low-friction surface while the ABS system operates as designed.

Vehicles having a front-to-rear dual hydraulic split system generally use single-or independent-wheel control on the front and select-low on the rear, with the rear wheel speed sensor located at the differential. Since both rear brakes are controlled as one unit, only one hydraulic control valve is required for the modulation of the rear brake line pressure.

Diagonal hydraulic split systems require four wheel-speed sensors, one for each wheel, and two hydraulic control valves for the rear brakes. Although four sensor and hydraulic channels are involved, the system in fact is a three-channel system. The select-low control of the rear axle, provides identical brake line pressure modulation to both rear brakes.

8. Components of the ABS

The ABS system consists of the following major subsystems:

8.1. Wheel-Speed Sensors

Electro-magnetic or Hall-effect pulse pickups with toothed wheels mounted directly on the rotating components of the drivetrain or wheel hubs. As the wheel turns the toothed wheel (pulse ring) generates an AC voltage at the wheel-speed sensor (see Figure 8.1). The voltage frequency is directly proportional to the wheel's rotational speed.

8.2. Electronic Control Unit (ECU)

The electronic control unit receives, amplifies and filters the sensor signals for calculating the wheel rotational speed and acceleration. This unit also uses the speeds of two diagonally opposed wheels to calculate an estimate for the speed of the vehicle. The slip at each wheel is derived by comparing this reference speed with the speeds of the individual wheels. The "wheel acceleration" and "wheel slip" signals serve to alert the ECU to any locking tendency. The microcomputers respond to such an alert by sending a signal to trigger the pressure-control valve solenoids of the pressure modulator to modulate the brake pressure in the individual wheel-brake cylinders.

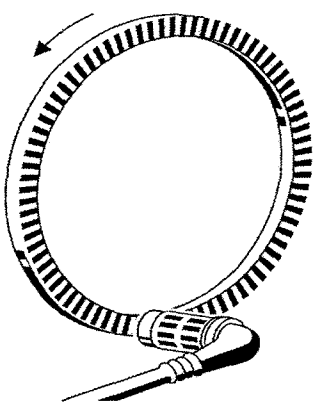

***Figure 8.1**: Wheel-speed sensor with pulse ring. (Bosch)*

The ECU also incorporates a number of features for error recognition for the entire ABS system (wheel-speed sensors, the ECU itself, pressure-control valves, wiring harness). The ECU reacts to a recognized defect or error by switching off the malfunctioning part of the system or shutting down the entire ABS.

8.3. Hydraulic Pressure Modulator

The hydraulic pressure modulator is an electro-hydraulic device for reducing, holding, and restoring the pressure of the wheel brakes by manipulating the solenoid valves in the hydraulic brake system. It forms the hydraulic link between the brake master cylinder and the wheel-brake cylinders (see Figure 8.4). The hydraulic modulator is mounted in the engine compartment to minimize the length of the lines to the brake master cylinder and to

the wheel-brake cylinders. Depending on the design, this device may include a pump/motor assembly, accumulator and reservoir.

8.4. Brakes

8.4.1. Disk brakes

Figure 8.2 shows a schematic diagram of a disc brake. In this type of brake, a force is applied to both sides of a rotor and braking action is achieved through the frictional action of inboard and outboard brake pads against the rotor. The pads are contained within a caliper (not shown), as is the wheel cylinder. Although not a high-gain type of brake, disk brakes have the advantage of providing relatively linear braking with lower susceptibility to fading than drum brakes.

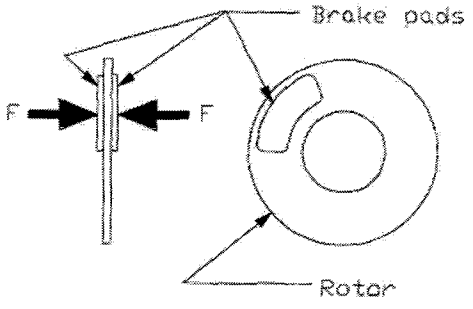

Figure 8.2: *Disk brake schematic.*

The force applied to the rotor by the pads is a function of hydraulic pressure in the brake system and of the area of the wheel cylinder (or cylinders, as the design dictates). The static brake torque can be calculated using the following equation [8]:

$$T_{b,\max} = P \cdot A \cdot E \cdot R \tag{8.1}$$

where:

P = application pressure[Pa]
A = wheel cylinder area [m^2]
E = effectiveness factor
R = brake radius [m]

We will assume that the brake torque is T_b is proportional to the brake line pressure p_{line} with the coefficient of proportionality a constant c_b i.e.

$$T_{b,\max} = c_b \cdot p_{line} \tag{8.2}$$

8.4.2. Drum brakes

Figure (8.3) depicts a schematic diagram of a drum brake. In drum brakes, a force is applied to a pair of brake shoes. A variety of configurations exists, including leading/trailing shoe (simplex), duo-duplex, and duo-servo. Drum brakes feature high gains compared to disk brakes, but some configurations tend to be more nonlinear and sensitive to fading.

The static brake torque equation previously presented for disk brakes, Equation (8.1), is equally applicable to drum brakes with design-specific changes for drum brake radius and effectiveness factor. By design, the brake radius for a drum brake is one-half the drum diameter. The effectiveness factor represents the major functional difference between drum and disk brakes; the geometry of drum brakes may allow a moment to be produced by the friction force on the shoe in such a manner as to rotate it against the drum and increase the friction force developed. This action can yield a mechanical advantage that significantly increases the gain of the brake and the effectiveness factor as compared with disk brakes. The dynamic brake force calculation for drum and disk brakes is more complex since the brake lining coefficient of friction is a function of temperature; as the lining heats during a braking maneuver, the effective coefficient of friction increases (for moderate temperatures) and less pressure is needed to maintain a constant brake torque.

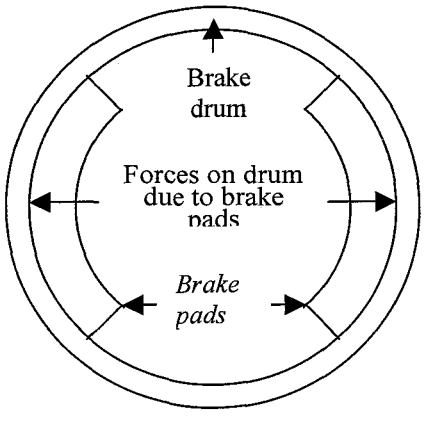

Figure 8.3: *Drum brake schematic*

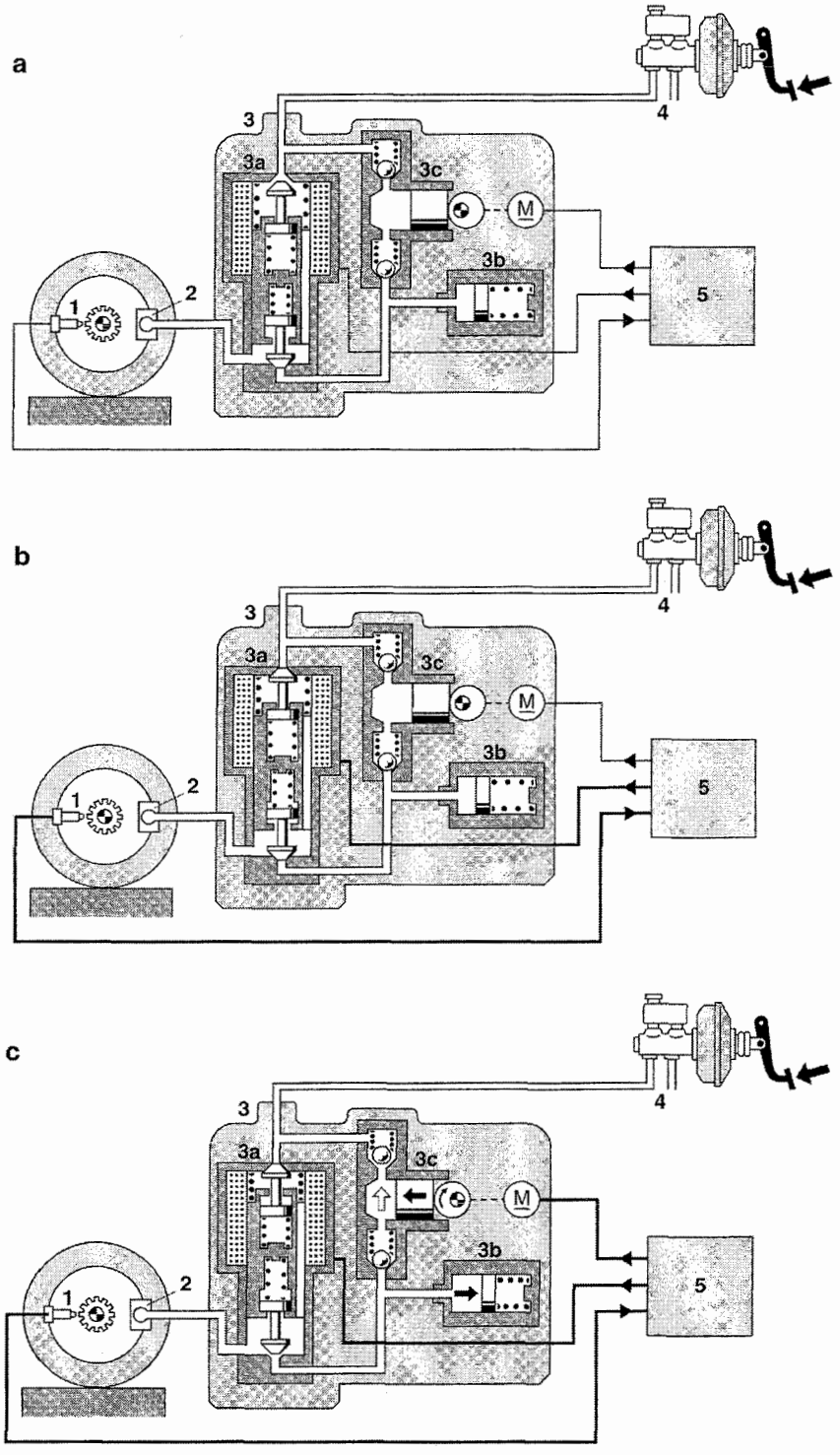

Figure 8.4: *Brake-pressure modulation.* ***a****)Pressure buildup,* ***b****)Hold pressure,* ***c****)Reduce pressure. 1-Wheel-speed sensor, 2-Wheel-brake cylinder, 3-Hydraulic pressure modulator, 3a-Solenoid valve, 3b-Accumulator, 3c-Return pump, 4-Brake master cylinder, 5-ECU, (Bosch)*[15]

9. Description of an Early Bosch ABS Algorithm

9.1. Controlled Variables

A suitable selection of the controlled variables is of major importance for the efficiency of ABS control. The basis is provided by the signals from the wheel-speed sensors. From these signals and assuming constant effective rolling radius the ECU calculates the wheel's peripheral acceleration $\dot{\Omega}_{per}$, slip, reference speed, and vehicle deceleration. On their own, neither the peripheral wheel acceleration nor the slip is suitable for use as a controlled variable.

However, these variables can give satisfactory results when used in a scheme with well defined logical relationships. The slip cannot be measured directly. The ECU therefore calculates a representative slip curve. This is based on the reference speed v_{Ref} that corresponds to the characteristic velocity for optimal braking conditions (optimum brake slip during entire braking maneuver).
The slip curve λ_1 is velocity curve drawn apart from v_{Ref} curve at distance significant to the value of the desired slip. The reference speed can differ from the actual vehicle speed v_F (see Figure 9.1). The ECU determines v_{Ref} based on the constant flow of wheel-speed signals received from the wheel-speed sensors. It selects "diagonal" wheels (for instance, right front and left rear wheel) and uses this as the basis for a reference speed. Under moderate braking, the reference speed will usually be based on the speed of the fastest of the two diagonal wheels. During panic stops with active ABS control, the wheel speeds diverge from vehicle speed, and unless a correction factor is used, they are unsuitable for calculating the reference speed.
During the control phase, the ECU generates this speed based on a ramp-shaped extrapolation of the speed at the start of the cycle. The unit processes logical signals and evaluates relationships to calculate the precise slope angle of the ramp.

To increase the accuracy of the v_{Ref}, estimate of the optimal wheel peripheral speed based on the vehicle speed V, a data for vehicle the deceleration obtained from an onboard accelerometer is employed. This concept has been implemented in the Bosch antilock braking system (ABS).

9.2. Controlled Variables for Non-driven Wheels

The peripheral wheel acceleration can serve as controlled variable for non-driven wheels. The reason for this has to do with the opposed response patterns of the controlled system in the stable and instable region of the braking-force coefficient/ slip curve (see Figure 5.8):

- In the instable range, a minimal increase in pedal pressure will immediately result in wheel lock. This phenomenon can often be employed in using the wheel's peripheral deceleration and its rate to determine the slip, corresponding to optimal braking.

- Any fixed threshold defining the peripheral deceleration beyond which ABS has to become active should not exceed the maximum potential vehicle deceleration by any substantial amount. If, no additional down forces are exerted on the vehicle and only the vehicle weight is present, the maximum potential vehicle deceleration equals the

gravity constant times the peak value of the friction coefficient. To keep this is especially important when light initial brake-pedal applications are followed by emergency braking. An excessively high threshold would allow the wheels to shift well into the instable range on the friction-coefficient versus slip curve before ABS would respond to the incipient instability.

- When a wheel for the first time reaches the fixed threshold for peripheral deceleration during a panic brake, the system should not respond by automatically reducing the brake pressure at this wheel. If modern tires are being used (with improved value of the peak friction coefficient 1,2 - 1,5) on a high-traction surface, this could lead to an unacceptable increase in valuable stopping distance. This factor is of particular importance in braking initiated at high speeds.

9.3. Typical Control Cycles

9.3.1. Closed-loop braking control

When ABS closed-loop control of the braking process is triggered on a high friction surface, in order to avoid suspension and drivetrain resonances, the subsequent pressure rise must be decreased by a factor of 5 ÷ 10, compared to the initial braking phase [10,15] (the period of time after the brake is applied but before the ABS becomes active.

The wheel's peripheral deceleration $\dot{\Omega}_{per}$ moves beyond the defined threshold ($-a$) at the end of Phase 1 (see Figure 9.1), and the solenoid valve shifts to its "maintain pressure" position. It is still too early to start reducing the brake pressure, as the threshold ($-a$)could be exceeded within the stable range of the friction coefficient versus slip curve, and valuable braking distance would be "sacrificed." The reference speed v_{Ref} (setpoint for the wheel peripheral speed) is reduced at the same time in accordance with a defined ramp. The reference speed serves as the basis for determining the slip switching threshold λ_1.

At the end of Phase 2, the wheel's peripheral velocity v_R drops below the λ_1 threshold. The solenoid valve reacts by shifting to its "pressure release" position. The brake pressure then continues to drop until the wheel's peripheral deceleration exceeds the threshold ($-a$) again.

At the end of the 3rd phase $\dot{\Omega}_{per} > -a$, this is followed by a pressure-holding phase of defined duration. During this phase, the wheel's peripheral acceleration has increased enough to exceed the threshold ($+a$). The pressure remains constant.
At the end of Phase 4 the wheel's peripheral acceleration exceeds the relatively pronounced threshold $+A$. The brake pressure then continues to increase for as long as the acceleration remains above the threshold $\dot{\Omega}_{per} > +A$.
In Phase 6 constant pressure is maintained in response to the fact that the threshold $+a$ has been exceeded. This state indicates that the wheel has entered the stable range on the braking-coefficient/slip curve, and is slightly underbraked (angular velocity of the wheel at the point where $\dot{\Omega}_{per}$ is about to cross zero after it passed through a positive maximum, indicates nearly maximal velocity).

The brake pressure is now built up in stages (Phase 7) in a process that continues until the wheel's peripheral deceleration again exceeds the threshold (*-a*) (end of Phase 7). For the rest of the braking maneuver due to the reduced angular wheel velocity the brake pressure is reduced immediately, no need to wait until the λ_1 threshold is crossed. It is assumed that after the first brake control cycle, the wheel slip value is near the values where the friction coefficient peaks. [15]

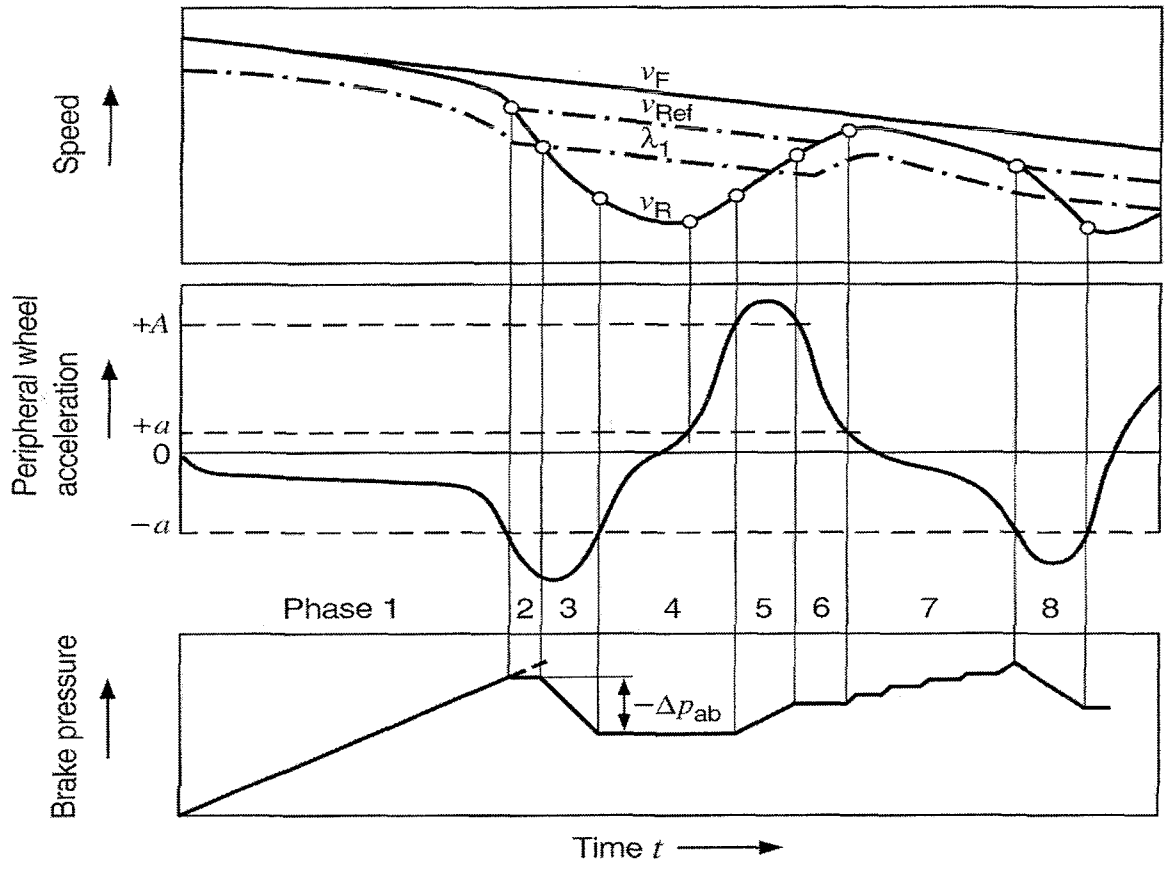

Figure 9.1: *Braking control for high braking-force coefficients* $v_F \equiv V_X$ *Vehicle speed;* v_{Ref} *Reference speed, it could be referred as the wheel peripheral setpoint;* $v_R \equiv \Omega^* r_{eff}$ *Peripheral wheel speed;* $\lambda_1 \equiv \kappa$ *Slip switching threshold;* $+A, +a$ *Thresholds of peripheral wheel acceleration;* $-a$ *Threshold of peripheral wheel deceleration, this threshold value differs from the* $+a$ *value not only by the sign, it is a different threshold;* $-\Delta P_{ab}$ *Brake-pressure decrease(Bosch).*

10. Vehicle Dynamics During Braking

With the forces on the vehicle as shown in Figure (10.1) the Equation of motion becomes:

$$-F_{x1} - F_{x2} + D_a + F_{roll.res.} = -m \cdot a \qquad (10.1)$$

where :

m = mass of the vehicle
a_x = linear acceleration
$-F_{x1}$ = front axle longitudinal braking force
$-F_{x2}$ = rear axle longitudinal braking force
D_a = aerodynamic drag
$F_{roll.res.}$ = force due to the rolling resistance

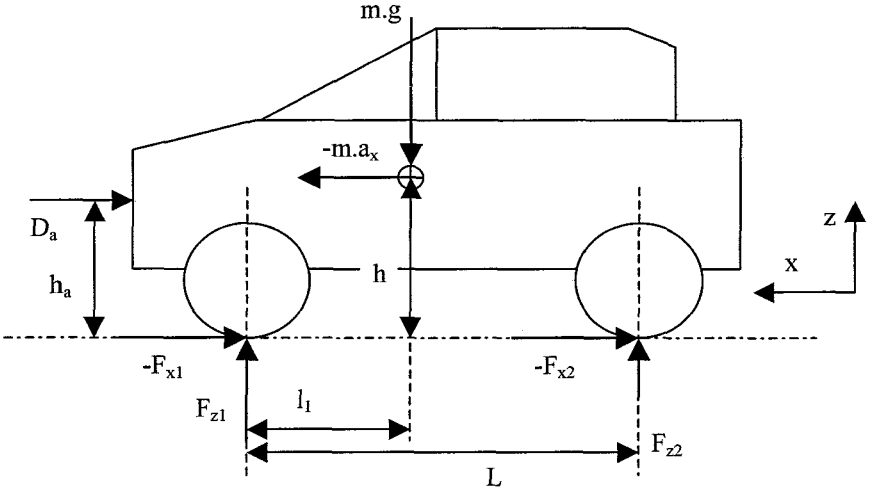

Figure (10.1): *Forces acting on a straight-line braking vehicle.*

10.1. Static Load Distribution

Static normal forces on the front and rear axles for a level road are given by (see Figure 10.1):

$$F'_{z1} = m \cdot g \cdot \frac{L - l_1}{L} \; ; \qquad F'_{z2} = m \cdot g - F'_{z1} = m \cdot g \cdot \frac{l_1}{L}. \qquad (10.2)$$

10.2. Dynamic Load Transfer During Braking

During braking, the dynamic load transfer is a function of the height of the center of gravity, the mass of the vehicle, the wheelbase, and the acceleration a_x. Aerodynamic drag force has also an influence to the dynamic load transfer. Referring to the Figure 10.1 it is seen that

$$F_{z1} = F'_{z1} + \Delta F_z \; ; \qquad F_{z2} = F'_{z2} - \Delta F_z \qquad (10.3)$$

where ΔF_z is given by

$$\Delta F_z = -\frac{h}{L} \cdot m \cdot a_x - \frac{h_a}{L} \cdot D_a \tag{10.4}$$

In the sequel, the drag will be neglected.

10.3. Longitudinal Braking Forces

Assuming friction coefficients μ_1 and μ_2 at the front and rear axles respectively, the longitudinal braking forces are

$$F_{x1} = F_{z1} \cdot \mu_1; \qquad F_{x2} = F_{z2} \cdot \mu_2 \tag{10.5}$$

Neglecting the drag force and the rolling resistance it is seen that their sum is the decelerating force on the vehicle mass.

$$F_{x1} + F_{x2} = m \cdot a_x \tag{10.6}$$

When braking, the friction coefficients μ_1 and μ_2 are negative. If equal grip utilization at both axes is adopted ($\mu_1 = \mu_2$), the Equations (10.3) and (10.5) lead to $\mu_1 = \mu_2 = a_x/g$ ($a_x<0$), and the 'ideal' braking-force distribution is

$$F_{x1} = m \cdot a_x [g \cdot (L - l_1) - h \cdot a_x] / (g \cdot L) \tag{10.7}$$

$$F_{x2} = m \cdot a_x [g \cdot l_1 + h \cdot a_x] / (g \cdot L) \tag{10.8}$$

Each loading state of the vehicle of course requires its own ideal braking-force distribution. Equations (10.7) and (10.8) can be rewritten in the following way:

$$F_{x1} = \mu \cdot \left(F_{z1} - m \cdot a_x \cdot \frac{h}{L} \right) \tag{10.9}$$

$$F_{x2} = \mu \cdot \left(F_{z2} + m \cdot a_x \cdot \frac{h}{L} \right) \tag{10.10}$$

10.4. The Stopping Distance

If the deceleration $-a_x$ is held constant the time for a vehicle velocity change Equation. (10.11), and the distance traveled s during a velocity change Equation. (10.12) are expressed as:

$$V_{(t)} = V_{(t_0)} + (t - t_0) \cdot a_x \tag{10.11}$$

$$s_{(t)} = s_{(t_0)} + (t - t_0) \cdot V_{(t_0)} + \frac{1}{2} \cdot (t - t_0)^2 \cdot a_x \tag{10.12}$$

If we substitute $V_{(t_0)} = V_{in}$ in Equations (10.11) and (10.12) for stop at time t_s the expressions yields:

$$V_{(t_s)} = 0 \Rightarrow t_s = t_0 - \frac{V_{in}}{a_x} \tag{10.13}$$

$$s_{(t_s)} = s_{(t_0)} - \frac{V_{in}^2}{a_x} + \frac{1}{2} \cdot \frac{V_{in}^2}{a_x} = s_{(t_0)} - \frac{1}{2} \cdot \frac{V_{in}^2}{a_x} \tag{10.14}$$

However, the stopping distance can be computed with Equation (10.13), in which the longitudinal deceleration force, vehicle mass, and the friction coefficient are linked. In case $V_f = 0$ the stopping distance yields:

$$s = \frac{m}{F_{x,tot}} \left(\frac{V_{in}^2 - V_f^2}{2} \right) = \frac{m}{\mu \cdot m \cdot g} \left(\frac{V_{in}^2}{2} \right) = \frac{V_{in}^2}{2 \cdot \mu \cdot g} = \frac{V_{in}^2}{2 \cdot a_x} \tag{10.15}$$

where:

s = stopping distance
$F_{x,tot}$ = total of all longitudinal deceleration forces on the vehicle
V_{in} = initial velocity
Vf = final velocity

The presented equations indicate, that the time to stop is proportional to vehicle velocity and the stopping distance is proportional to the square of the vehicle velocity if the deceleration is constant.

11. Modeling of an Antilock Braking System

An ABS is a highly complex system. Detailed modeling of each of its components requires development of sophisticated models. To simplify the model it is necessary to impose some restrictions and assumptions for the model to be made.

11.1. Assumptions and Restrictions

- Only straight-line emergency braking until stop or till a pre-set velocity threshold is crossed, is considered
- The ABS is not operational for velocities below 1 m/s.
- The braking is performed on a dry road surface and road conditions do not change.
- A linear relation between the brake pressure and maximum deliverable brake torque $T_{b,max}$.
- The $T_{b,max}$ is input of the overall model. It is a manipulated variable.
- Rates of the brake pressure increase and decrease are fixed.
- At each time t the wheel angular velocity Ω and the vehicle longitudinal velocity V are available from measurements and/or reconstruction.

11.2. Components of the ABS Model

The model of the ABS contains the following three blocks:

Signal Processing Block - Computes the wheel deceleration $-\dot{\Omega}$, wheel slip $\kappa = -1 + \frac{\Omega \cdot r_{eff}}{V_x}$ and the ratio $-\dot{\Omega}/\Omega$. The block compares the respective signals with their thresholds and generates output signals when a certain threshold is exceeded.

Logic Control Block - The controller uses a predefined sequence of actions to modulate the brake torque via brake torque modulator (BTM) to prevent wheel locking and to maintain the wheel slip below a preset level.
Four signals can be employed in the wheel lock criteria, namely:

- the wheel peripheral deceleration $-\dot{\Omega}$
- the wheel slip $\kappa = -1 + \frac{\Omega \cdot r_{eff}}{V_x}$
- the combination between the wheel deceleration and slip
- the ratio $-\dot{\Omega}/\Omega$

The logical structure of the controller and sequence of actions is the same regardless the signal used for the wheel lock criteria. Four flow charts (Figures 11.21 to 11.24) are used to explain the sequence of the actions for each criterion.

Brake Torque Modulator (BTM) Block - Modulates the brake torque values as outputted by the Controller.

11.3. Brake Torque Modulator Block

11.3.1. Requirements for the brake-pressure/ brake-torque modulator model

The maximal deliverable brake torque $T_{b,max}$ is assumed to be proportional to the brake pressure, so modulating the brake pressure is equivalent to modulating the brake torque. From now on the term brake torque modulator (BTM) will be employed. A model of a two valve BTM is developed. The BTM has one inlet and one outlet valve. If there is no danger of wheel-locking the BTM is in its Initial position - no actuated valve, see Figure 8.4 – *Pressure buildup cycle.* When the inlet valve is actuated the wheel-brake cylinder is disconnected from the master-cylinder – *Hold pressure cycle.* In case both valves are actuated, the wheel-brake cylinder is connected to an accumulator – *Reduce pressure cycle.* The BTM model requirements are given in Table 11.1.

11.3.2. Syntheses of the brake-torque modulator

To fulfill the requirements for the brake-torque modulator stated in Table 11.1 the following approach is used.

For unit activation a conditional dependant switch *Switch* 2 is employed. To initiate the braking event, a Boolean signal[2] "1" is applied at the *Brake Applic* input (see Figure 11.1). Then *Switch 2* connects the *Rate of increase* constant to the *Integrator*. The result is an increase of the torque $T_{b,max}$ with a rate R_1, i.e. $\dot{T}_{b,max} = R_1$ with $R_1 > 0$. This continues until the maximum of the $T_{b,max}$ is reached of until inlet valve is activated ("1" at the *Inlet valve* input).

Table 11.1: *The brake-torque modulator requirements.*

Requirements description	Cycle		
	Pressure buildup cycle	*Hold pressure cycle*	*Reduce pressure cycle*
	1. To increase the brake torque with a constant rate R_1. 2. Adjustable increasing rate R_1. 3. Adjustable value of the maximum of $T_{b,max}$.	1. To maintain the realized brake torque level.	1. To decrease the brake torque with a constant rate R_2. 2. Adjustable R_2.
Actuated valves	-	Inlet valve	Inlet valve
	-	-	Outlet valve

If the inlet valve is activated the *Switch* connects the *Integrator* via sum block and *Switch2* to the zero value of *Constant 2*. The result is a pressure hold.

The pressure reduce cycle is obtained if, the *Outlet valve* is actuated ("1" at the *Outlet valve* input) during the pressure hold cycle. Then *Switch1* connects the *Rate of decrease* block to the *Integrator*. This will cause the brake torque to decrease with a constant rate *R2*.

[2] To explain the principle of operation of various simulation blocks, signals with logical levels are used. Signals significant to the high logical levels, logical 1 (Boolean 1), will be designated by "1"or "one" and low level logical signals (Boolean 0) will be designated respectively by "0"or "zero".

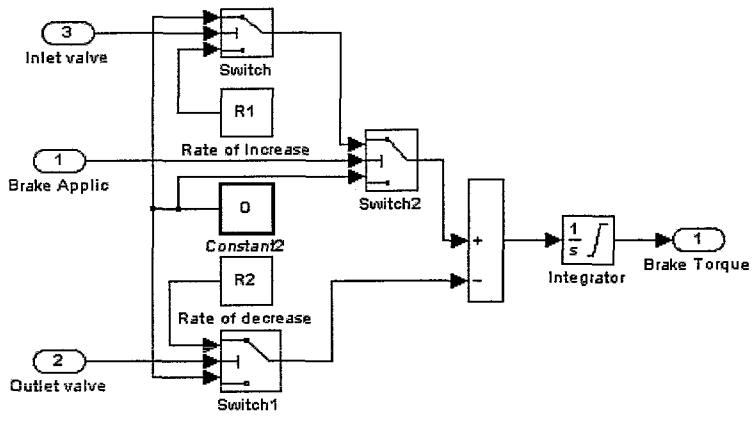

Figure 11.1: Brake-torque modulator layout.

The output value of the *Integrator* is limited by two saturation levels. The lower saturation level is zero – the minimum value of the brake-torque. The upper saturation level is set to the maximum brake-torque that can be realized by the brake system. The SIMULINK - subsystem block of the BTM unit and its mask are shown in Figure 11.2

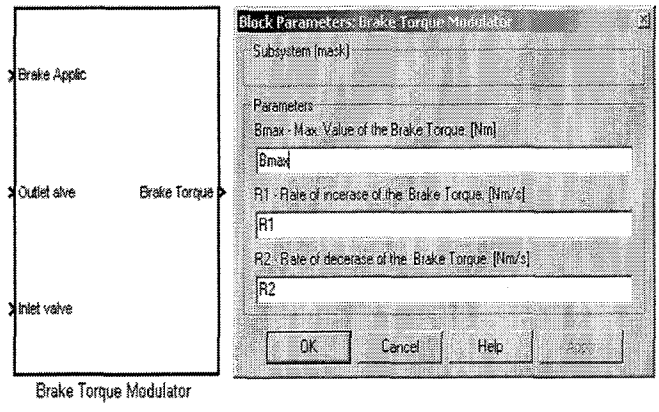

Figure 11.2: SIMULINK block of the BTM modulator unit and its mask.

11.4. Development of the ABS Controller Model

The ABS includes the *Logic Controller Block* and the *Signal Processing Block.* A basic function of the ABS controller is to prevent wheel lock-up and to control the wheel slip during emergency braking maneuvers. To meet those requirements the ABS monitors the wheel peripheral velocity, the wheel deceleration/acceleration, and the vehicle velocity. The control commands (to hold, decrease or increase the brake torque) depend on the actual values of the monitored parameters and, whether or not certain threshold levels have been exceeded.
The control algorithm to be implemented exploits the previously described Bosch algorithm. The implementation in the ABS model is explained in Section 11.4.2.

11.4.1. Signal processing unit

The *Signal Processing* block incorporates signal processing and various other operations on the input variables to generate estimates for, amongst others, the wheel peripheral acceleration, and the wheel slip, threshold levels of the monitored parameters, and outputs of the threshold-comparators.

11.4.1.1. Slip computation block

The *Slip computation* block (see Figure 11.3) calculates the slip κ. The negative sign of the slip during braking is omitted to avoid mistakes when comparing the signal value with the threshold value. The *Slip Comparator* compares the computed slip with the threshold value of the *Slip setpoint* block. The comparator outputs "1" when the computed slip exceeds the threshold.

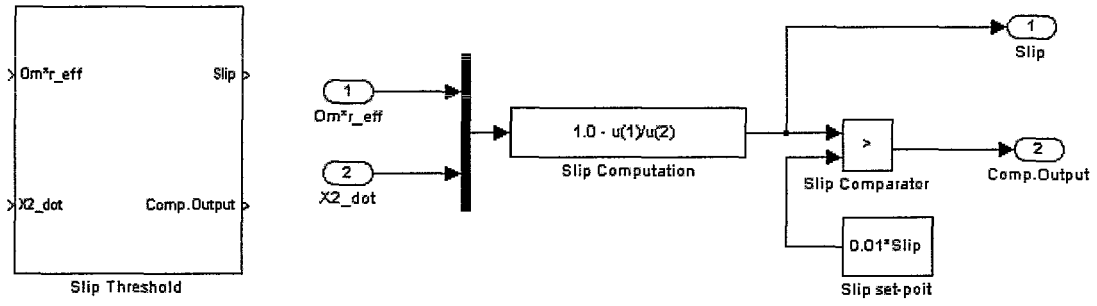

Figure 11.3: *The Slip Threshold block and its layout.*

11.4.1.2. Slope detector block

Two additional blocks are connected to the comparator's output, i.e. the positive and negative slope detectors. The positive slope detector (see Figure 13) detects a positive stepwise change in the monitored output. The detector generates a narrow impulse when a positive slope is detected. The negative slope indicator reacts in the same way on a negative stepwise change in the output of the comparator. A description of the *Slope detector* principle of operation is given in **Appendix –E.3.**

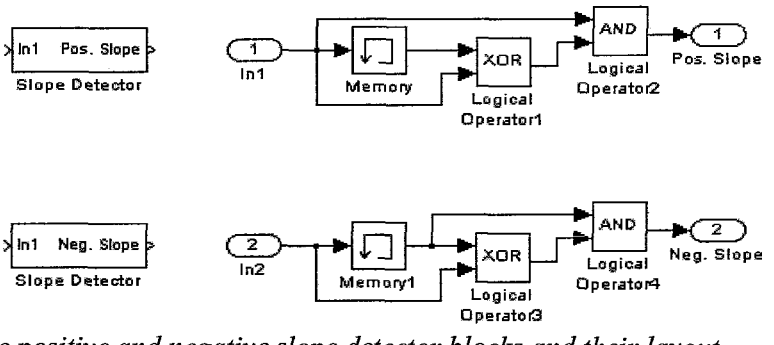

Figure 11.4: *The positive and negative slope detector blocks and their layout.*

11.4.1.3. Acceleration/deceleration computation

Estimates of the wheel angular velocity Ω and of the wheel effective rolling radius r_{eff} are used in the calculation of the wheel-peripheral acceleration $\dot{\Omega}_{per}$.

From a mathematical point of view there is no difference between the way of processing of Figure 11.5 and the following transfer function form Ω to $\dot{\Omega}_{per}$:

$$\frac{1.15 \cdot s}{0.0105 \cdot s + 1} \qquad (11.1)$$

The implemented solution offers a higher simulation speed.

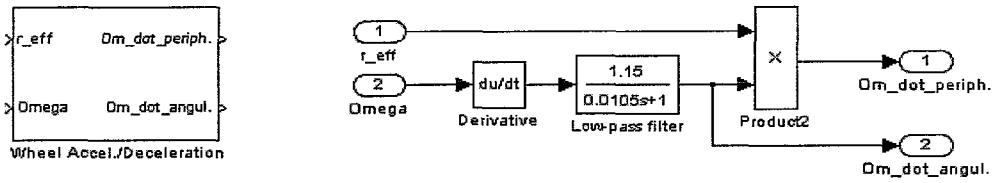

Figure 11.5: *Wheel angular and peripheral acceleration/deceleration computation block and its layout.*

The filter has cut-off frequency of 95,2 rad/s (15,15 Hz) [4,8]. Figure 11.6 illustrates the difference between the original and filtered signals. Filtering of the acceleration signal is necessary because ripples can cause faulty threshold-crossing detection.

To arrive at the peripheral acceleration the wheel angular acceleration is multiplied by the effective rolling radius of the wheel. Three acceleration comparators monitor the wheel-peripheral acceleration namely: *Threshold –a, Threshold +A* and *Threshold +a.*

To generate a signal significant to the wheel acceleration the wheel angular velocity is differentiated by the *Derivative* block. A low-pass filter filters the acceleration signal.

11.4.1.4. Deceleration threshold (*-a*)

Threshold –a compares the peripheral deceleration during a torque buildup cycle with the threshold value *–a* (see Figure 11.7). Until the signal exceeds the threshold value, the comparator output value is "1". The *Gain 1* multiplies negative deceleration value by –1 to produce a positive value.

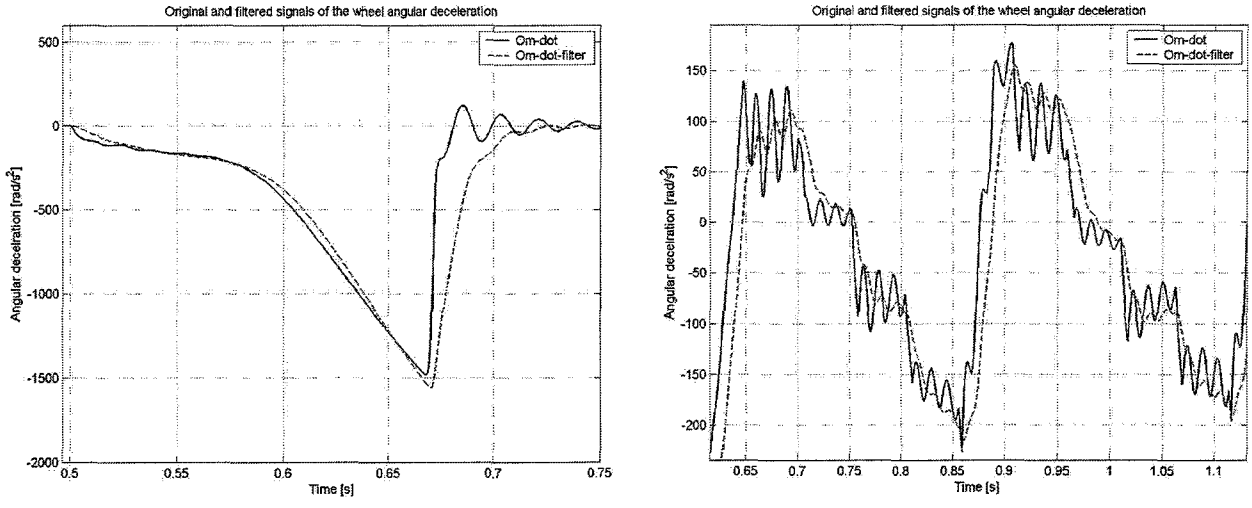

Figure 11.6: *Original and filtered signals of the wheel angular deceleration. Left graph - smooth increase of the brake-torque (R1=19000 Nm/s) till wheel-lock; Right graph - step increase of the brake torque. The rate of the brake torque increase is R1=2533 Nm/s.*

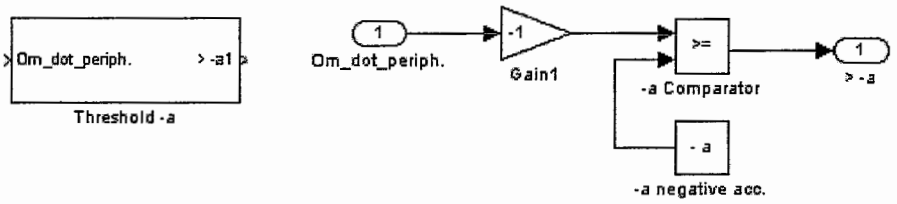

Figure 11.7: *Comparator block of the –a deceleration threshold and its layout.*

11.4.1.5. Acceleration thresholds (+*a*) and (*A*)

Threshold (+a) compares the peripheral acceleration during torque-hold or reduce-torque cycles with the threshold value +*a* (see Figure 11.8). The comparator output equals "1" until the acceleration exceeds the threshold value.
Threshold +A compares the peripheral acceleration during torque-hold or buildup-torque cycles with the threshold value +*A* (see Figure 11.8). The comparator output equals "1" until the acceleration exceeds the threshold value.
The last two comparators are combined in one block. To mark the instant of threshold crossing with narrow pulse, a couples of negative and positive slope detectors are connected to the output of all comparators (see Figure 11.20).
An additional signal for wheel-lock prediction is computed in the signal-processing block, see Figure 11.8. The estimate for $\dot{\Omega}$ is divided by the estimate for Ω. A comparator compares the result with a preset threshold. The comparator outputs "1" until the monitored signal exceeds the threshold value.

The outputs of the signal-processing block are available only when the brake is applied ("1 "at *Brake Appl* input). This is realized by logical
AND gates placed on each output of the signal-processing block (see Figure 11.20). The *AND* gate allows further propagation of the active signal ("1") only if the brake is applied.

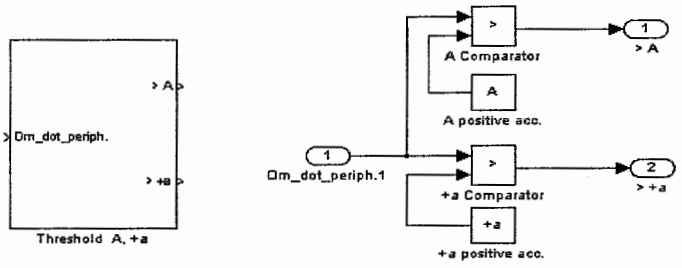

Figure 11.8: *The block of the A and +a acceleration thresholds and its layout.*

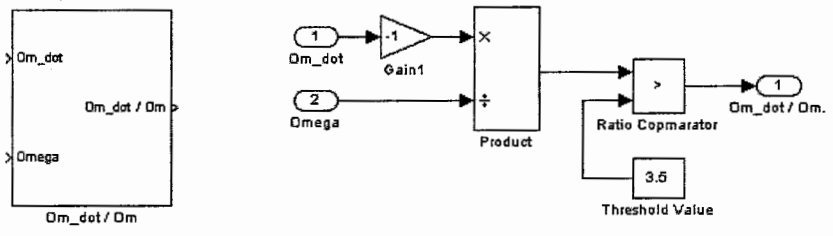

Figure 11.19: *Block view and computational layout of the wheel-angular deceleration to the wheel-angular velocity ratio.*

11.4.2. The Logic controller block

The criteria to decide to hold, decrease or increase, the brake torque depend on momentary values of the wheel angular velocity Ω, vehicle velocity $\dot{x}_2$ and peripheral wheel acceleration $\dot{\Omega}_{per}$.

The employed logic to control the two valves in general does not differ from the one used in the Bosch controller described earlier (see Section 9.3).

The objectives of the controller are to prevent wheel to lock by maintaining the slip κ around the preset value in the range of -10% to -20%: for optimal straight-line braking (shortest stopping distance) the longitudinal-peripheral velocity of the braked wheel is 10 to 20 percent lower than the longitudinal velocity of the vehicle.

The controller has to control the torque generated by the brake pads and brake disk, in order to decelerate the braked wheel to maintain the slip around the set value. The friction coefficient changes its slope from positive to negative after its peak value.
Due to the negative slope any further increase of the slip in that region will result in change of the wheel deceleration rate (steeper slope of the wheel deceleration see Figure 6.3d).

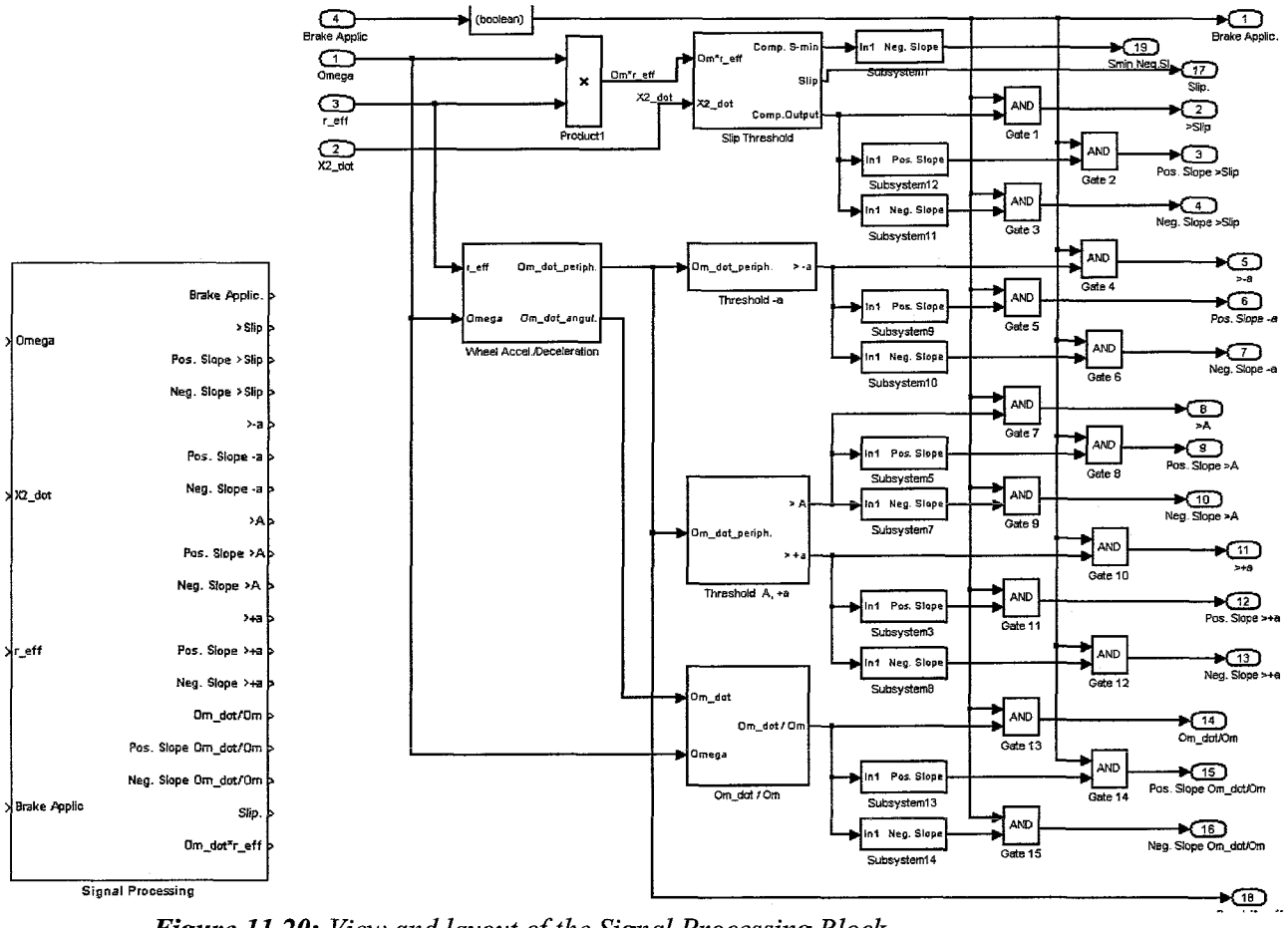

Figure 11.20: *View and layout of the Signal Processing Block*

The brake can generate very high torques, but the tire ability of transmitting a torque is limited! The tire torque $M_{y,r\ corr.}$ attains its maximum at slip values where the μ_x peaks.

Further increase of the brake torque will cause the wheel to lock without improvement of the brake performance, it will even deteriorate it.

11.4.2.1. Control algorithm

Regardless which of the four optional criterions will be used to warn (trigger) the controller for the impending danger of wheel lock, the action of the controller is basically the same. The controller starts to decrease the brake torque by first closing the inlet valve (torque hold cycle) and compares the wheel slip with the slip threshold. If the threshold is exceeded, after one sample time the controller opens the outlet valve (decrease torque cycle).
When the peripheral wheel deceleration is used as the wheel lock criterion the controller closes the inlet valve and waits until the slip threshold is exceeded, then commands decrease torque cycle. A detailed description of that case and a chart flow diagram of the operations sequence (see Figure 11.21) are provided in the next section.

11.4.2.2. Wheel peripheral deceleration as wheel lock criterion

The control logic monitors the peripheral wheel deceleration during braking. When the threshold $-a$ is exceeded the controller commands the inlet valve to close (torque hold cycle).

The wheel continues to decelerate till the slip threshold is exceeded. The controller then commands the outlet valve to open (decrease brake torque cycle). The rate of torque decrease is a fixed value R_2=19000 Nm/s. The wheel starts to accelerate. The decrease of the brake torque continues until the $+a$ threshold is reached. Then the outlet valve is closed where as the inlet valve is still closed (torque hold cycle).

The threshold $+a$ is positive and close to zero. Its meaning is to assure that the brake torque is reduced enough so that the wheel attains a positive acceleration and will not lock. The wheel continues to accelerate until it reaches the A threshold. Now the controller commands the valve to open (torque increase cycle). The value of the threshold A is selected to insure reliable recovery of the wheel-velocity from lock danger. To prevent controller malfunction when this threshold A is not crossed due to insufficient wheel acceleration the negative slope of the $+a$ threshold is also used to trigger the torque increase cycle.

The subsequent increase of the brake torque will appear in steps with lower increase rate R_1=2533 Nm/s compared with the rate R_1= 19000 Nm/s in the very first increase cycle. This is done in order to avoid suspension and drivetrain resonances. The device generating the pulses to modulate the brake torque is the *Generator* block described in **Appendix-E.1.** It generates square pulses with adjustable duty cycle. By choosing proper time values for the inlet valve close time *TC* and open time *TO* various increase torque rates are possible.

The wheel deceleration develops until the $-a$ threshold is exceeded again, but now the controller skips the hold torque cycle and commands directly a decrease brake torque cycle. This change in the algorithm pattern is based on the assumption that the wheel is slowed down enough during the previous cycle and that now the crossing of the $-a$ threshold will occur at a slip value equal or higher than the preset one. The torque decrease stops when the $+a$ threshold is reached and now the torque hold cycle is maintained. The algorithm

follows the previously described patterns until the vehicle reaches the velocity at which the ABS shuts down. After that the braking system continue to operates as a conventional one.

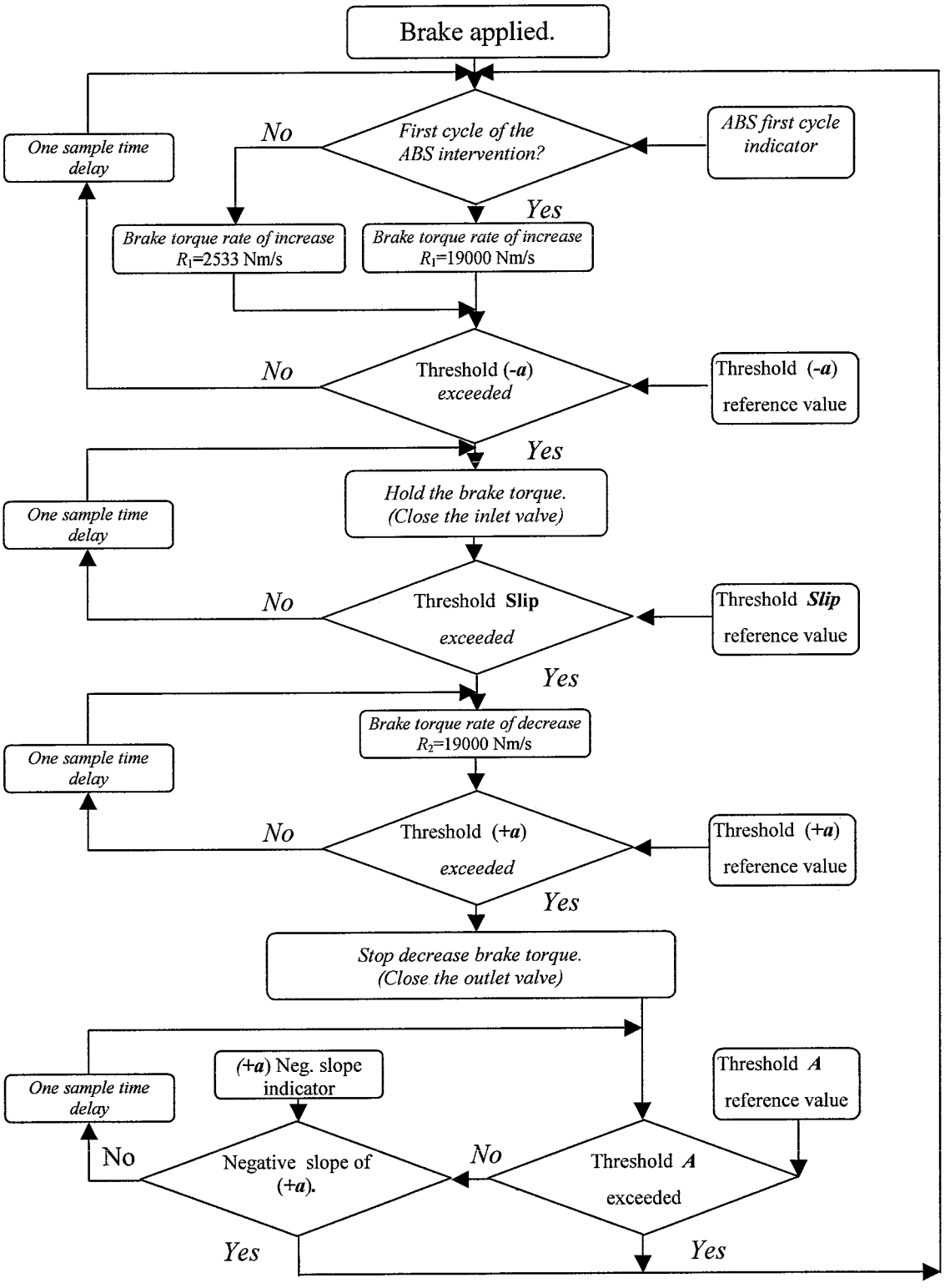

Figure 11.21: *Block diagram of the acceleration threshold used as wheel lock criterion to trigger the brake torque Hold Command of the Logic Controller Block.*

11.4.2.3. Wheel slip as wheel lock criterion

The control logic monitors wheel slip during braking. When the threshold *Slip* is exceeded the controller commands the inlet valve to close (torque hold cycle).

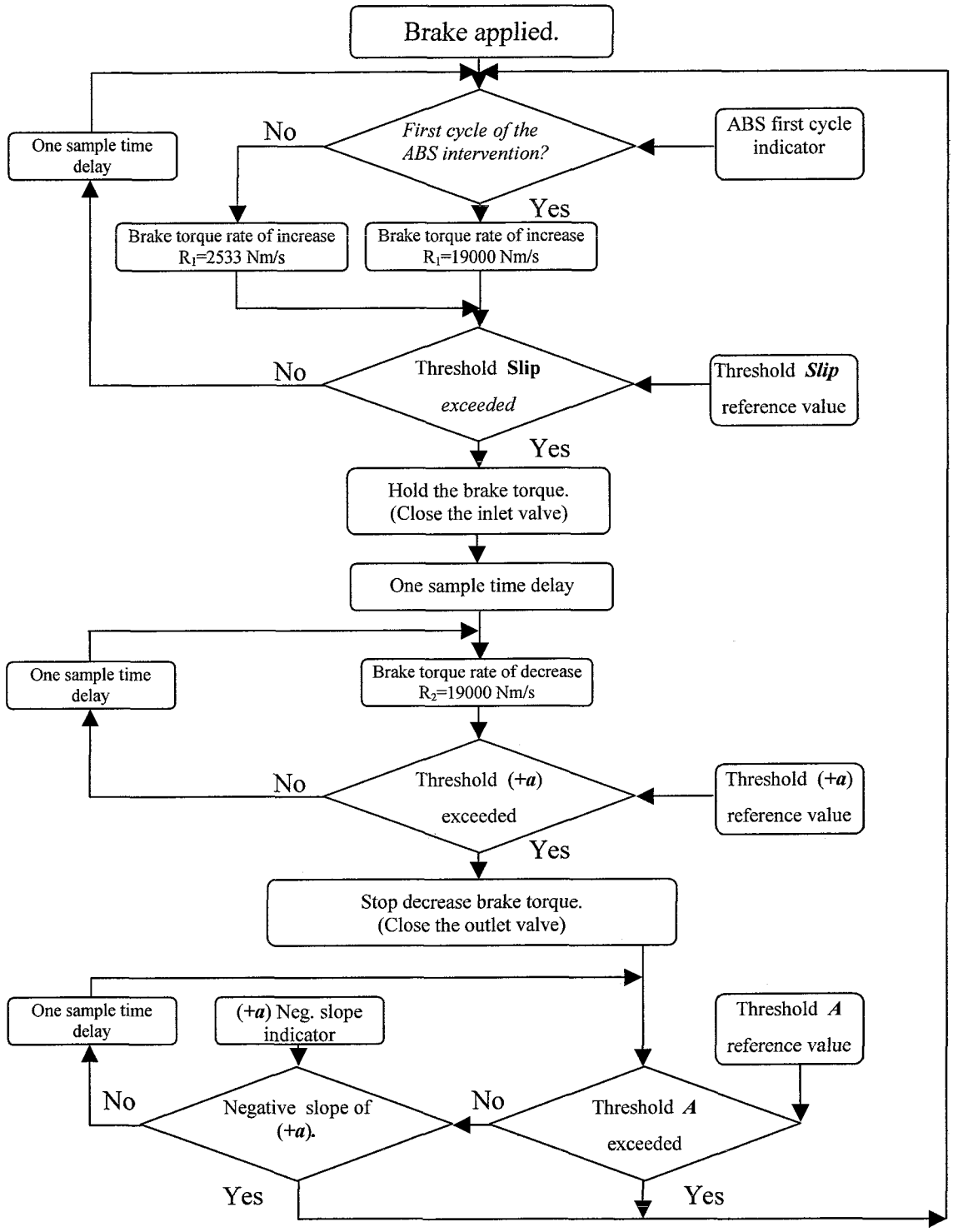

Figure 11.22: *Block diagram of the Slip threshold used as wheel lock criterion to trigger the brake torque Hold Command of the Logic Controller Block.*

11.4.2.4. Combined wheel slip and wheel peripheral deceleration as wheel lock criteria

The control logic monitors wheel slip and peripheral acceleration during braking. When one of the two thresholds is exceeded the controller commands the inlet valve to close (torque hold cycle).

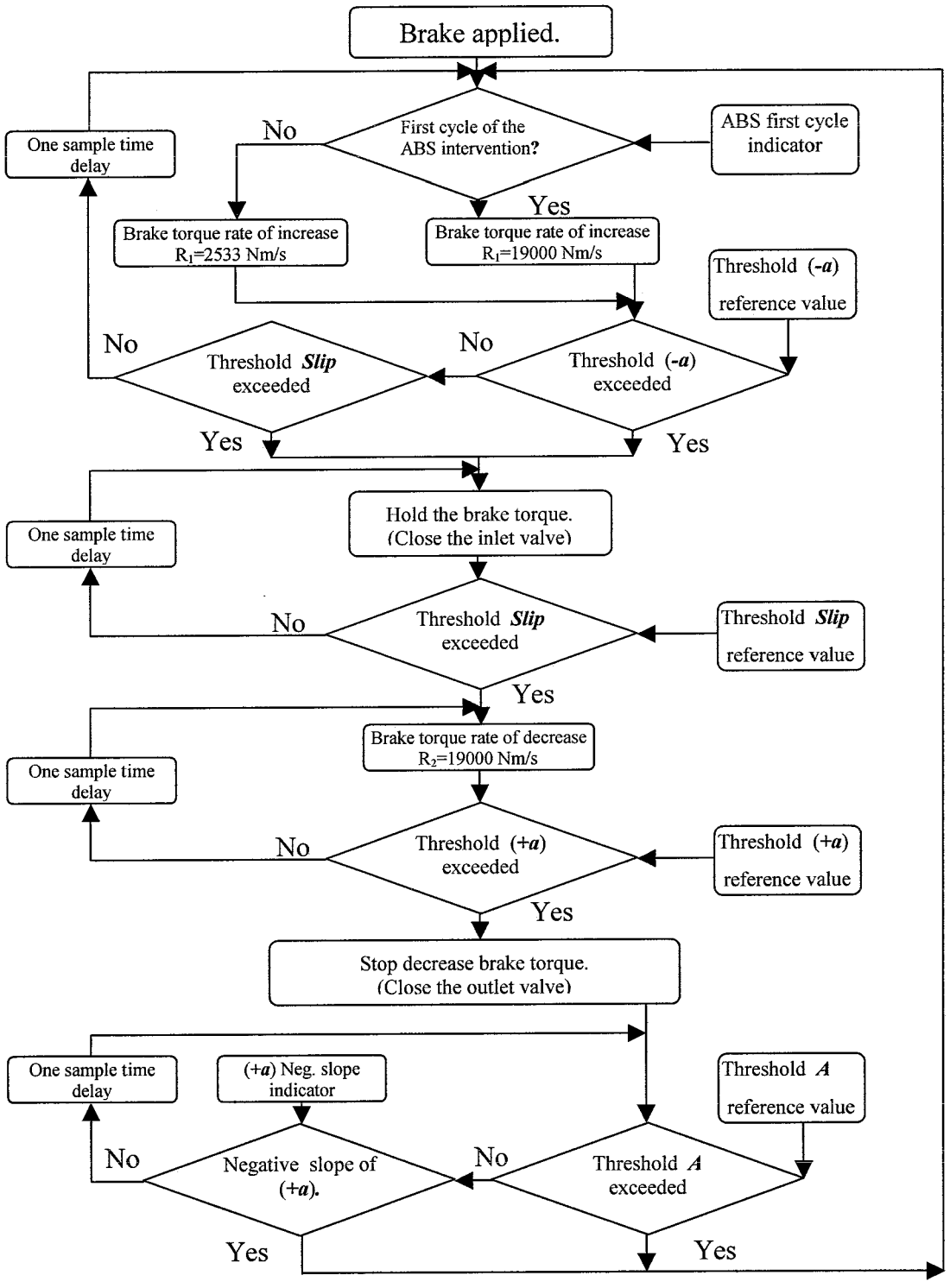

Figure 11.23: *Block diagram of the combined Slip or acc. threshold used as wheel lock criterion to trigger the brake torque Hold Command of the Logic Controller Block*

11.4.2.5. The ratio $-\dot{\Omega}/\Omega$ as wheel lock criterion

The control logic monitors the ratio $-\dot{\Omega}/\Omega$ during braking. When the ratio threshold is exceeded the controller commands the inlet valve to close (torque hold cycle).

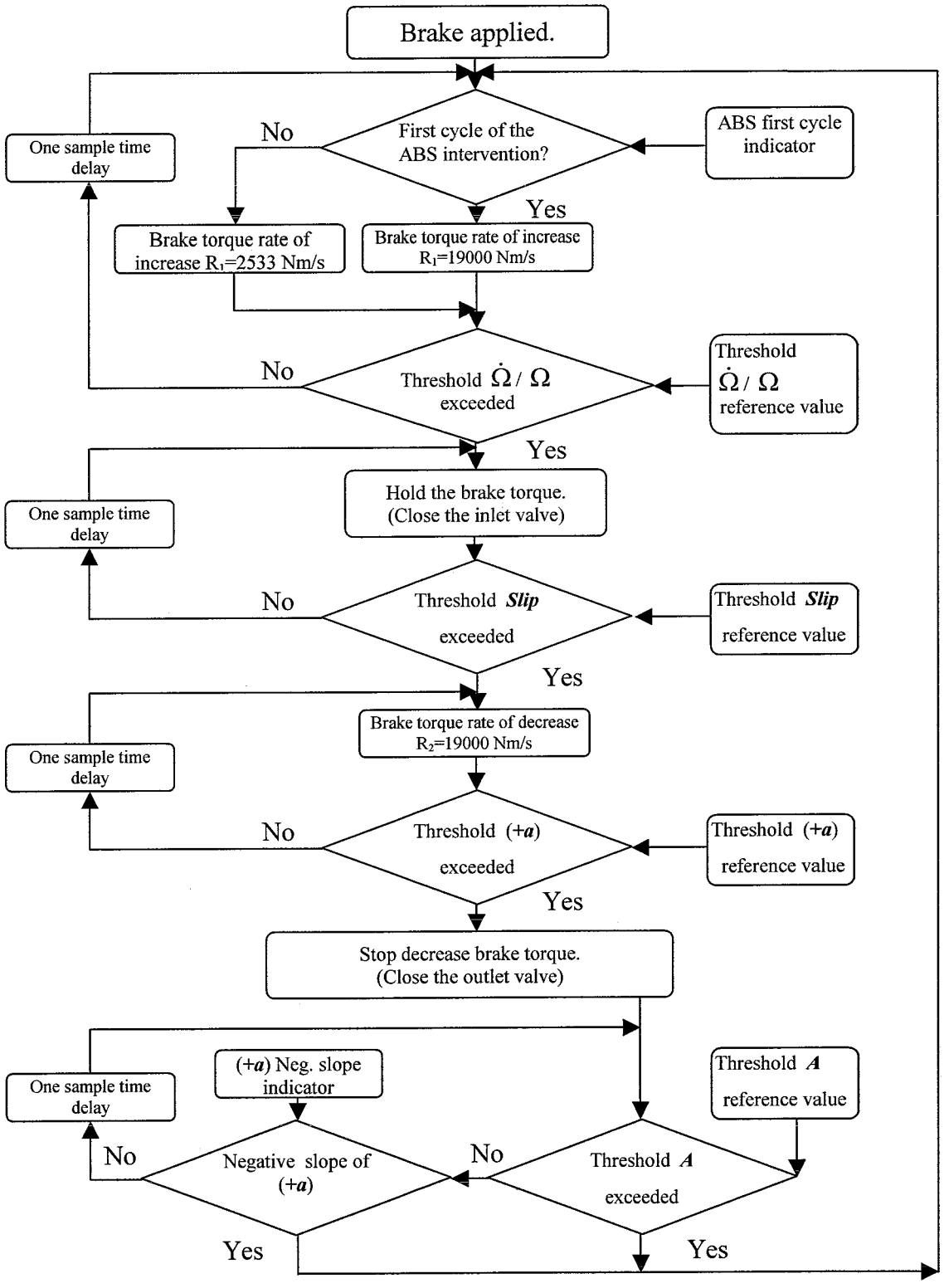

Figure 11.24: *Block diagram of the ratio-signal ($\dot{\Omega}/\Omega$) threshold used as wheel lock criterion to trigger the brake torque Hold Command of the Logic Controller Block*

11.4.2.6. Logic Controller block description

The logic controller block and its layout are shown in Figure 11.25. Each of the two valves is controlled by a flip-flop.

11.4.2.6.1. The Outlet valve control

The *Outlet Valve Control* flip-flop controls the outlet valve. When the flip-flop is *Set* ("1" applied to the *S* input) the valve is open and when the flip-flop is *Reset* ("1" applied to the *R* input) the valve is closed. The initial state of the flip-flop is reset.

The logic control of operation allowed the outlet valve to open only after the inlet valve is closed. To guarantee this sequence an *AND* gate is connected to the *Set* input of the flip-flop.
The valve can close separately or it has to be closed when the inlet valve opens. The closing operation sequence is achieved by an *OR* gate connected to the Reset input of the *Outlet Valve Control* flip-flop.

11.4.2.6.2. The Inlet valve control

The *Inlet Valve Control* flip-flop controls the inlet valve. When the flip-flop is *Set* ("1" applied to the *S* input) the valve is closed and when the flip-flop is *Reset* ("1" applied to the *R* input) the valve is opened. The initial state of the flip-flop is reset.
Additional units are implemented in the inlet valve control to account for the different algorithms to control the torque increase of the first brake cycle and in the consequent brake cycles.

After the wheel peripheral deceleration crosses the $-a$ threshold the hold command is generated. The active signal ("1") is applied to the *Set* input of the *Inlet Valve Control* flip-flop. The flip-flop output Q is activated and through the *Switch* the active signal applies to the *Inlet valve* input of the *Brake Torque Modulator* block and closes the valve. The Q signal is input to the *One Cycle Indicator* block input, this indicator maintain "1" at its output after an active signal is applied on its input. The cycle indicator indicates that the first cycle is past.

When the wheel peripheral acceleration crosses the A threshold the command to increase the brake torque is applied (active signal to the *Reset* input of the flip-flop). The inlet valve opens. The $\overline{Q}$ output of the valve control block is activated. Active signals are applied at both inputs of the *Logical Operator 4* (*AND* gate). The gate transmits the "1" to the inputs of the *Switch* and of the *Generator*. The *Switch* connects the *Generator's* output to the input of the inlet valve. Now the generator has an active signal on its input and starts to generate. The pulses command the inlet valve to open and close. As a result the rate of brake torque increase depends on the duty cycle. Detailed description of the developed *Generator* block is given in **Appendix-E1.**

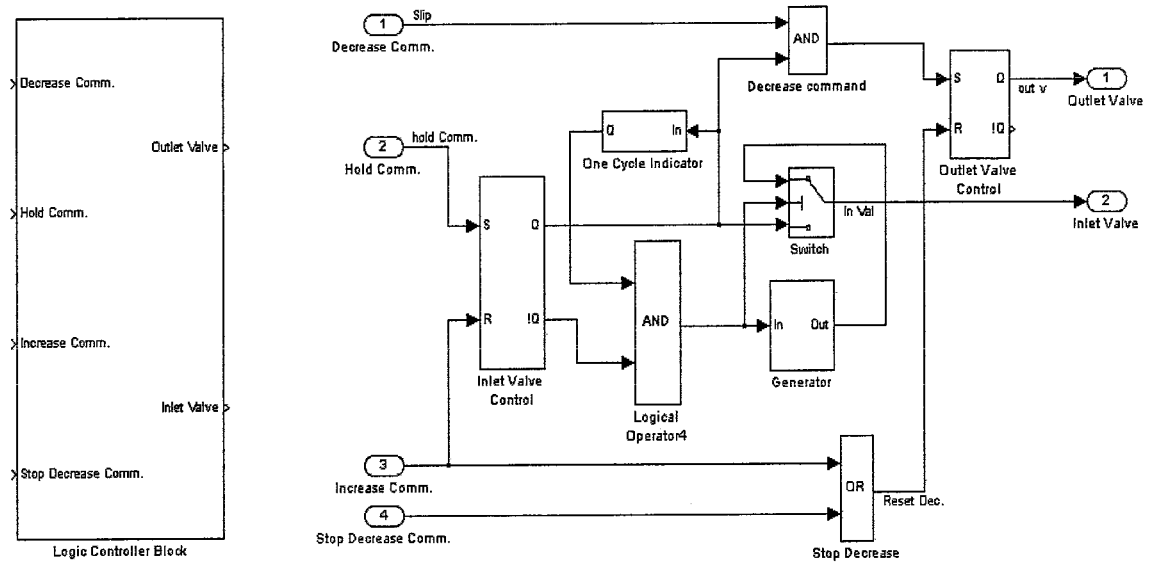

Figure 11.25: *Logic Controller Block view and its layout.*

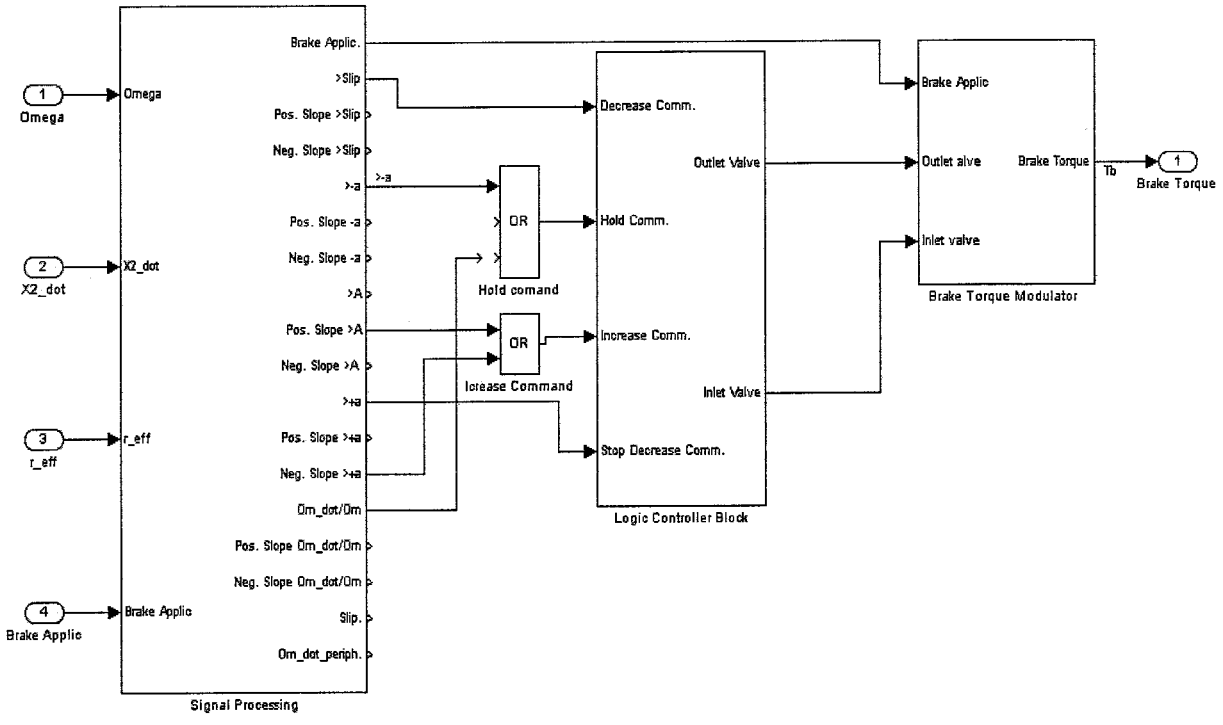

Figure 11.26: *The three main blocks of the ABS system model: the Signal Processing block, the Logic Controller block and the Brake Torque Modulator block.*

11.5. Complete ABS System Model

The model of the ABS connects the following three blocks: the *Signal Processing* block, *Logic Controller* block and the *Brake Torque Modulator* block (See Figure 11.26). In case that more than one comparator signal is used to trigger a command from the Logic Controller a proper logical operator (such as AND, OR, NOT) can solve the problem.
For convenience the three block of the ABS system are combined in a new subsystem block named the ABS block. The main parameters of the three blocks subject to settings are posed on the mask of the ABS block. The view of the ABS block and its mask are shown in Figure 11.27.

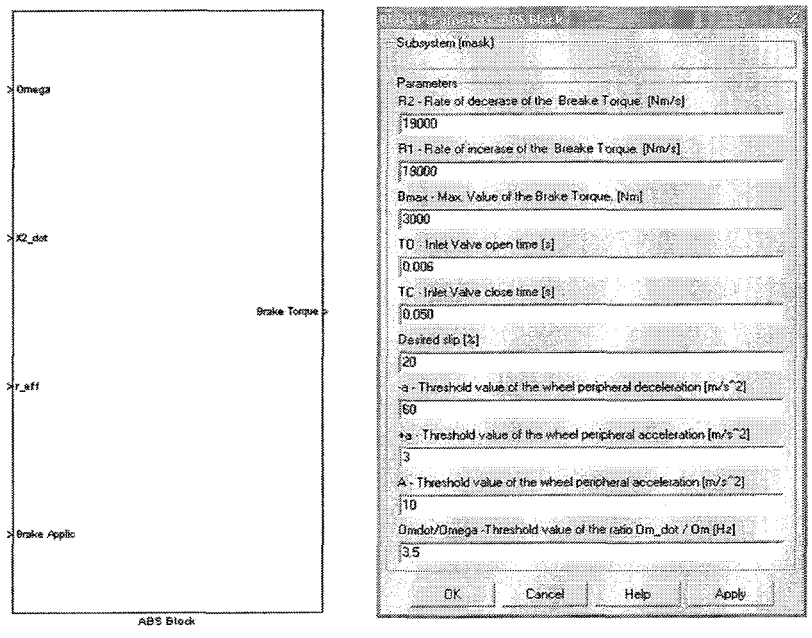

Figure 11.27: *View of the ABS Block and its mask. The three main blocks of the ABS system model are united in ABS Block.*

12. Test Vehicle Model

Now the ABS system model can be connected with the Quarter-vehicle-Tire model. The resulting test vehicle model includes the following components:

- Suspension model.
- Wheel hub fore-aft compliance model.
- SWIFT tire model.
- ABS system model.

This model will be used to perform an ABS system brake performance study. Most of the important quarter-vehicle parameters can be set through the masks of the quarter-vehicle-tire model and ABS model.

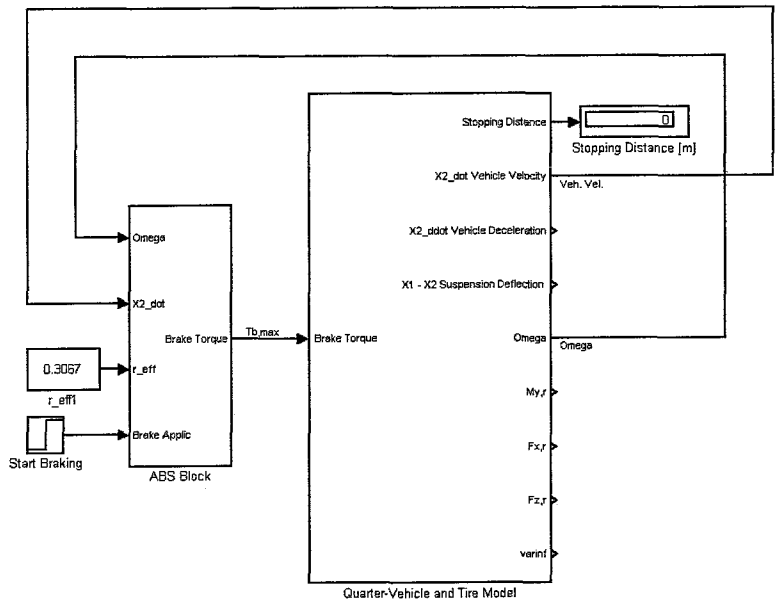

Figure 12.1: *The ABS system model and the Quarter-vehicle-Tire model connected together. Few additional blocks are used to input data to the model. The Start Braking block defines the instant of brake application. The r_eff constant block is used to input the value of the effective rolling radius of the tire. The Stopping Distance display shows the vehicle stopping distance at the end of the simulation.*

13. Assessment of Peripheral Deceleration Threshold Values

A preliminary simulation study of the braking process revealed that for a given tire-rim combination, the value of the (–*a*) slip level depends on:

- rate of brake torque increase R_1
- initial velocity

To acquire information of the braking process and to study the dependence of (-a) on the rate of the brake torque increase and on the initial velocity, the following three experiments were conducted.

13.1. Influence of the Rate of Brake Torque Increase on Wheel Deceleration

13.1.1. Experiment 1

The initial velocity is kept at a fixed value. For three values of R_1, the peripheral wheel deceleration $\dot{\Omega}_{per.}$ and wheel slip κ are determined. The rest of the model parameters (see Table 6.1) is kept fixed during the experiment. The experiment conditions are shown in Table 13.1. Figure 13.1 shows plots of $\dot{\Omega}$ and κ as a function of time.

13.1.2. Analysis of the results from Experiment 1

After observation of the Figure 13.1, we can conclude that for equal other conditions and model parameters, except for R_1, the higher the rates of brake torque increase, larger the values that the wheel-deceleration reaches before the preset slip value is exceeded.

It is evident that there is similarity in the behavior pattern (the ramp changes in the initial phase) in the curves of the peripheral deceleration and the respective longitudinal slip. In both type curves the rapid change in the ramp is observed. This rapid ramp change can be explained whit the decreases of the friction coefficient μ_x after its peak.

13.2. Influence of the Initial Braking Velocity on Wheel Deceleration

13.2.1. Experiment 2

To study the dependence of (-*a*) on the initial velocity V_{in}, the rate of brake torque increase is kept at a fixed value. For three values of V_{in}, the peripheral wheel deceleration $\dot{\Omega}_{per.}$ and wheel slip κ are obtained. The rest of the model parameters (see Table 6.1) is kept fixed during the experiment. The experiment conditions are shown in Table 13.2. Figure 13.2 shows plots of $\dot{\Omega}$ and κ. for this experiment.

13.2.2. Analysis of the results from Experiment 2

From the examination of Figure 13.2 one can conclude that for equal other conditions and fixed model parameters, except for V_{in}, the higher the initial braking velocity, larger the value that the wheel deceleration reaches before the preset slip value is exceeded.

Table 13.1: *Conditions of Experiment 1.*

Straight-line braking until the wheel is locked	
Initial velocity V_{in}	80 [km/h]
Road surface	Asphalt
Road profile	Flat
ABS	OFF
Range of the T_b rate of increase variations	2000, 5000, 19000 [Nm/s]

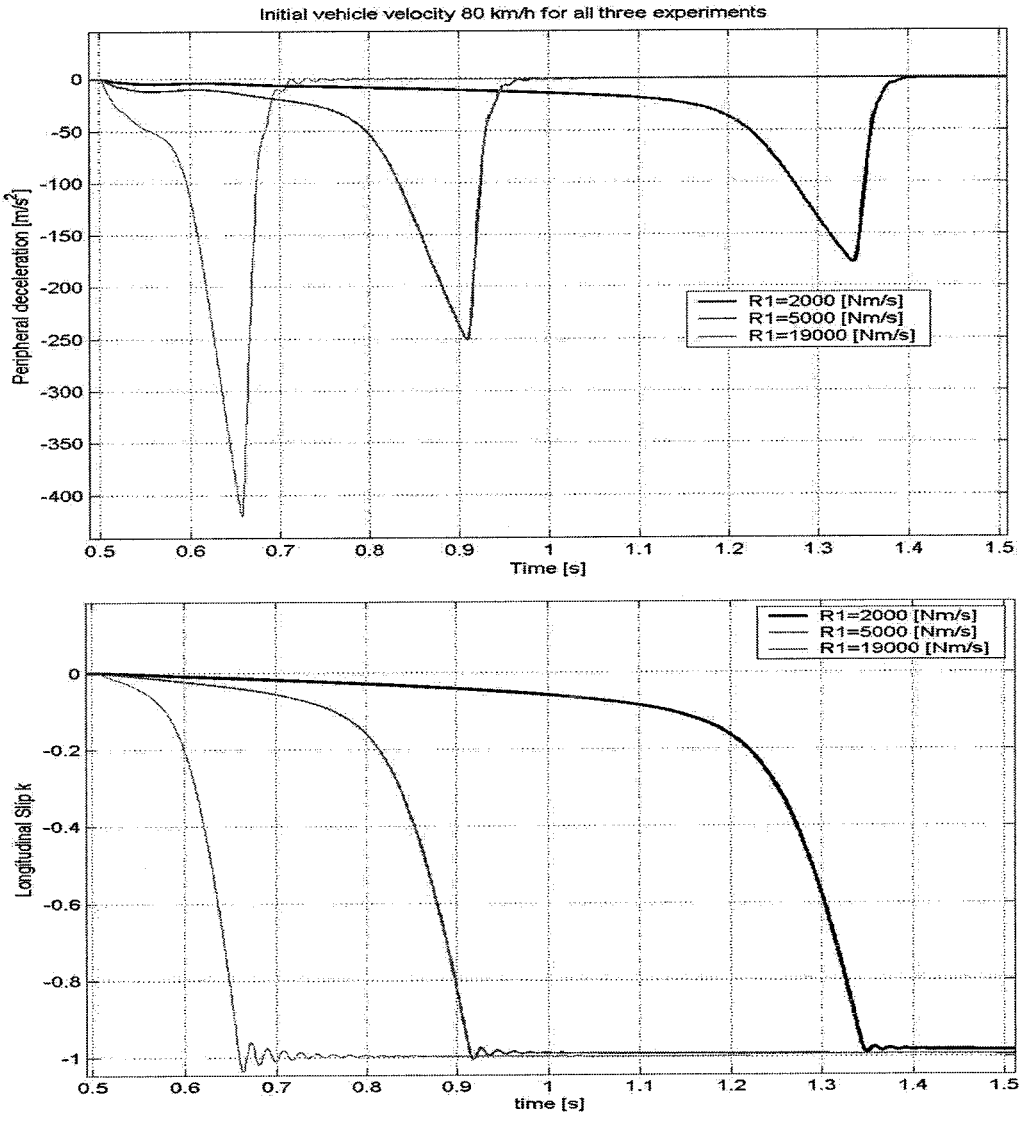

Figure 13.1: *Experiment 1. Wheel-peripheral deceleration $\dot{\Omega}_{per}$ and longitudinal slip κ curves for different rates of brake torque increase. All other model parameters are fixed. For –20% slip the wheel-peripheral deceleration reaches higher values at high torque rates.*

Table 13.2: *Conditions of Experiment 2.*

Straight-line braking	
Rate of T_b of increase variations	19000 [Nm/s]
Road surface	Asphalt
Road profile	Flat
ABS	OFF
Range of the initial velocity V_{in} variations	40, 80, 120 [km/h]

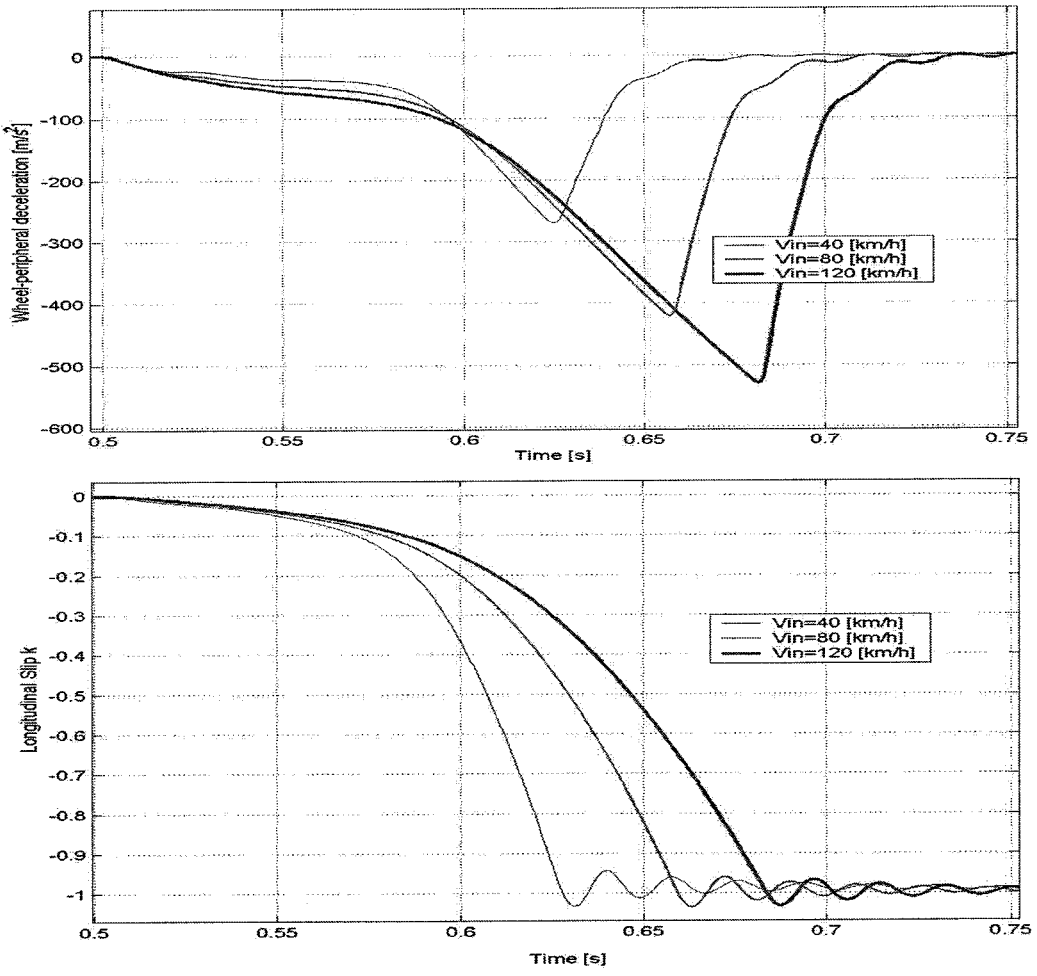

Figure 13.2: *Experiment 2. Wheel-peripheral deceleration $\dot{\Omega}_{per}$ and longitudinal slip κ curves for different initial braking velocities. All other model parameters are fixed. For –20% slip the wheel-peripheral deceleration reaches higher values at high initial velocities.*

13.2.3. Conclusions on Experiment 1 and Experiment 2

Form the experiments we can conclude that a single fixed value of the peripheral wheel deceleration is not suitable criterion to judge whether or not the wheel is about to lock. However, if the wheel peripheral deceleration is combined with the longitudinal slip a more reliable, compound criterion can be established. It is possible to improve reliability

of the deceleration threshold criterion if it is adapted with respect to the initial braking velocity. Than for a given initial velocity, known rate of brake torque increase and known other model parameters a reliable value of the wheel peripheral deceleration threshold can be found.

13.3. Experiment 3

In an attempt to obtain more data on the wheel deceleration dependence on initial velocity the range of V_{in} in Experiment 2 is extended. The other conditions in this Experiment 3 are the same as in Experiment 2. Additional criterion is adopted in this experiment based on the ratio of the wheel angular deceleration $\dot{\Omega}$ and the wheel angular velocity Ω. In this experiment values of the wheel peripheral deceleration, and of the ratio $-\dot{\Omega}/\Omega$ are recorded when the slip thresholds of -10% and -20% are crossed. The results from Experiment 3 are given in Table 13.3 and shown in Figures 13.3, 13.4 and 13.5.

Table 13.3: *Results obtained from Experiment 3*

Data for the -10% slip level. R1=19000 Nm/s			
V_{in} [k/h]	$\dot{\Omega}_{per}$ [m/s^2]	Time [s]	$-\dot{\Omega}/\Omega$ [Hz]
120	-90	0.083	2.8
100	-80	0.081	3.2
80	-60	0.078	3.4
70	-52	0.077	3.5
60	-50	0.075	4.0
40	-40	0.072	4.6
Data for the -20% slip level. R1=19000 Nm/s			
V_{in} [k/h]	$\dot{\Omega}_{per}$ [m/s^2]	Time [s]	$-\dot{\Omega}/\Omega$ [Hz]
120	-175	0.108	6.4
100	-155	0.104	6.7
80	-130	0.100	8.0
70	-120	0.098	8.2
60	-150	0.097	9.0
40	-108	0.091	12.5

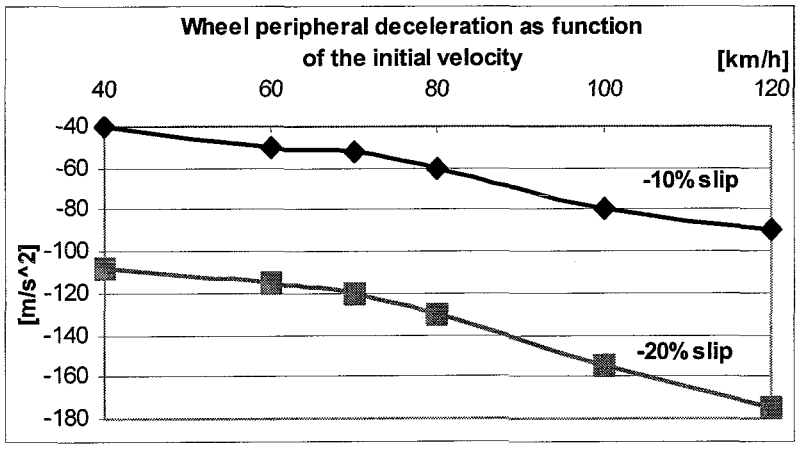

Figure 13.3: *Experiment 3. Wheel peripheral acceleration* $\dot{\Omega}_{per}$ [m/s^2] *for various initial velocities for two slip levels –10% and –20%. R1=19000 Nm/s.*

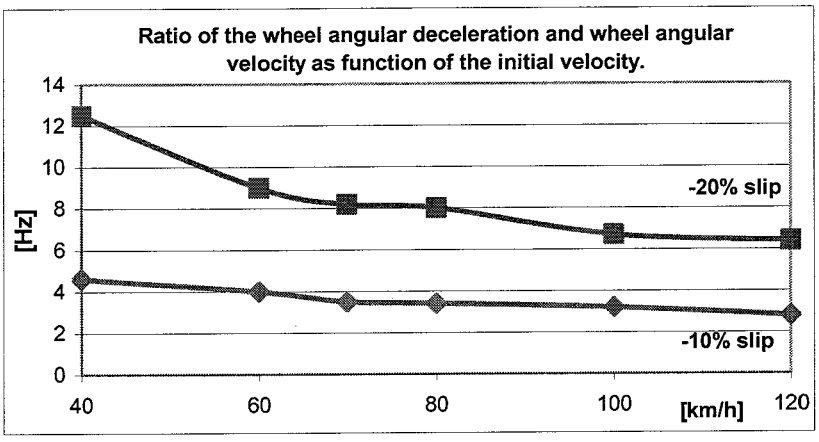

Figure 13.4: *Experiment 3. The ratio $-\dot{\Omega}/\Omega$ at various initial braking velocities for two slip levels -10% and -20%. R1=19000 Nm/s.*

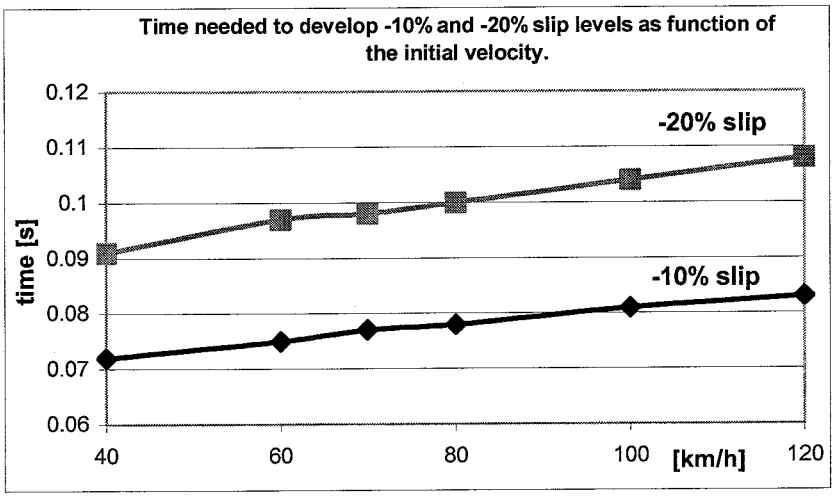

Figure 13.5: *Experiment 3. The time period passed from the instant of brake application to the moment the slip levels -10% and -20% are reached for various initial braking velocity. R1=19000 Nm/s.*

13.3.1. Analysis of the results from Experiment 3

Analysis of these results confirms the conclusions from Experiment 2: that for equal other conditions and fixed model parameters, except for V_{in}, the higher the initial braking velocity, larger the value that the wheel deceleration reaches before the preset slip value is exceeded. The experiment results shown in Figure 13.4 provide evidence that the ratio $-\dot{\Omega}/\Omega$ can be used as wheel lock criterion and is less sensitive to the initial braking velocity than the wheel peripheral deceleration.

13.4. General Conclusions on the Three Experiments

13.4.1. Conclusions on peripheral wheel deceleration threshold (-a)

In conclusion we can state that for high initial velocities the deceleration threshold $-a$ should be set at higher values. In contrast for low initial velocities the $-a$ should be decreased. See Figure 13.3. A fixed value of the $-a$ threshold cannot provide accurate information for optimal braking at various velocities. But if suitable selection of its value is made, it can provide information, though not the optimal one. Reasonable selection for the $-a$ threshold could be a value brained from crossing the –10% slip threshold. The suitable value should be selected in the middle or higher range of the $\dot{\Omega}_{per}$ values. Theoretically, such a selection will be able to provide –10% slip as minimum for high initial braking velocities and slip value exceeding the -10% level, but still below the -20% level for initial velocities from 40 to 120 km/h for high friction road conditions.

13.4.2. Conclusions on the $-\dot{\Omega}/\Omega$ ratio threshold

The results from Experiment 3 reveals that the ratio $-\dot{\Omega}/\Omega$ is a suitable and reliable quantity to be used as a criterion to prevent the wheel locking. See Figure 13.4. It turns out that this criterion is less sensitive to the velocity and to the rate of brake torque increase than the wheel peripheral deceleration. For high initial velocities the $-\dot{\Omega}/\Omega$ threshold should be set at lower values. At low velocities the threshold should attain higher levels. Selection of the proper threshold value should provide slip in the range –10% to –20% for various velocities. Values in the range of 3.5 to 4 [1/sec.] are considered suitable for the data presented in Figure 13.4.

13.4.3. Conclusions on the peripheral wheel acceleration threshold (+*a*)

The value of the positive acceleration threshold $+a$ has to be a fairly small positive number. This threshold is used to mark a positive tendency in the wheel acceleration. The braked wheel stops to decelerate and just starts to speed up after the brake torque reduction. Appropriate threshold values are 2 to 5 m/s^2.

13.4.4. Conclusions on peripheral wheel acceleration threshold (*A*)

The A threshold value should denotes Ω recovery from the predicted lock and a stabile wheel acceleration. The threshold A should be higher than $(+a)$. Selection of too high values for A results in higher recovered wheel speed and lower slip values before the brake torque is increased again. The A threshold dependence on the angular wheel velocity is similar to that of the (–a) threshold. High speeds Ω correspond to high threshold levels. At lower speeds Ω the threshold value should be decreased. Suitable threshold values are 9 to 15 m/s^2

14. Braking Performance Study

14.1. Study the Influence of the Different Wheel Lock Criteria on the Vehicle Braking Performance.

The goal of this simulation study is to compare the vehicle braking performance on flat roads as well as on uneven roads, when various wheel lock criteria are used by the ABS. The study includes test results from the vehicle braking performance without ABS.

By combining output signals from *Signal Processing Block* we can form various sets of inputs to the *Logic Controller Block.* We will explore the braking performance of the vehicle model with four signal sets. These signal-sets differ from one another in the wheel lock criterion signal used to trigger the *Hold Command* input of the *Logic Controller Block.* See Figures 11.25, 11.26.

In all experiments the slip-comparator signal triggers the *Decrease Command* of the *Logic Controller Block.* Due to the implemented logic of operation (described in section 11.4.2.6, see Figure 11.25) the Decrease Command will take effect only after the Hold Command.

14.2. Tire moment $M_{y,r\,corr}$ Criterion Control Braking

To explore the possibilities of improving the vehicle braking performance if additional information on the tire moment $M_{y,r\,corr}$ is utilized the approach of the next section was used. This approach requires that the tire moment $M_{y,r}$ and the normal force $F_{z,c}$ are measured, for instance by a 'smart' tire

Using the derivations in section 5.3.2 where correction of the tire torque $M_{y,r}$ (delivered by the SWIFT model) was made we can conclude that with data for the normal tire load and guess of the friction coefficient we can calculate expected $M_{y,r\ corr}$ and respectively the magnitude of the needed braking torque T_b. We will assume linear vertical tire stiffness $k_{z,tire}$ constant vertical load $F_{z,c}$ and no changing road conditions. On base of the made assumptions we can compute the value of the corrected tire moment.

The actual problem is that $M_{y,r\,corr}$ depends on the normal force and the friction coefficient. On flat road the normal force can be considered as constant. We need estimate of the expected maximum of the corrected tire moment for a given conditions. A reliable estimate of $M_{y,r\ corr}$ is important, because comparing the measured value with the expected maximum, one can control the brake torque T_b to utilize the maximum of the tire-road friction.

On an uneven roads the normal force $F_{z,c}$ is no longer a constant. The variations in $F_{z,c}$ magnitude as well as in the road friction coefficient will interfere the process of reliable estimate calculation of expected $max(M_{y,r\,corr})$.

14.2.1. Braking torque calculation

The torque $r_{load}\,.\,F_{x,c}$ of the longitudinal force $F_{x,c}$ on the rim is called the corrected tire torque $M_{y,r\,corr}$. With $F_{x,c}=\mu_x\,.\,F_{z,c}$ and $r_{load}=r_0-F_{z,c}/k_{z,tire}$ (see Section 5) this result in:

$$M_{y,r\_corr.} = \mu_x \cdot F_{z,c} \cdot \left(r_0 - \frac{F_{z,c}}{k_{z,tire}} \right) \tag{14.1}$$

The maximum value of the $M_{y,r\ corr}$ is expected at the peak of the μ_x. From the properties of the employed tire is known that $\mu_{x\ max} = 1.207$ for a normal load $F_{z,c}$ =3355 N. (see Figures 5.7 and 5.8):

$$\max\left(M_{y,r\_corr.}\right) = \mu_{x\max} \cdot F_{z,c} \cdot \left(r_0 - \frac{F_{z,c}}{k_{z,tire}} \right) \approx 1200 \text{ [Nm]} \tag{14.2}$$

Due to moment contributions by the inertia of the tire belt and the wheel, actual barking torque has to be enlarged. The final magnitude of the nominal brake torque equals the sum of the corrected tire moment (max.) and the torque contributions of the tire-belt and wheel. This equation reads:

$$T_b = \max\left(M_{y,r\_corr.}\right) - I_{belt} \cdot \dot{\Omega} - I_p \cdot \dot{\Omega} \tag{14.3}$$

For $\dot{\Omega}_{per}$ around -10 m/s^2 the value of the nominal brake torque is:

$$T_{b,nom.} = 1217 \text{ [Nm]} \tag{14.4}$$

14.2.2. The Tire-moment-control algorithm

The idea of the algorithm is to maintain the brake torque around the value calculated by Equation (14.4), which value ensures maximum of the corrected tire torque (soon after the brake torque reach a stable value), respectively maximum of the longitudinal force $F_{x,c}$, thus maximum deceleration and minimum stopping distance. In fact during the phase of brake torque buildup the actual value of $\dot{\Omega}_{per}$ is much higher than the early suggested –10 m/s^2. This will require larger T_b in the beginning. To fulfill the requirements in a straightforward way the following approach was taken. The maximum value of the deliverable brake torque $T_{b,max}$ was limited to1300 [Nm], the threshold of the nominal minimum brake torque $T_{b,nom,min}$ was set to 1180 [Nm] and the threshold value of the nominal brake torque $T_{b,nom}$ was set to 1217 [Nm].

The designed algorithm can be described as follow:
Initialy the brake torque T_b increases with rate R1=19000 Nm/s until it reaches $T_{b,max}$. No further increase of the torque is possible and T_b is held at this value. The wheel decelerates and because the applied brake torque is higher than that according Equation (14.4) the maximum of the friction coefficient is exceeded and the wheel tend to lock.
After the slip threshold is exceeded the brake torque is reduced to $T_{b,nom,min}$. If after that, the slip still remains beyond the threshold, T_b is decreased further until the (+***a***) threshold is crossed and the decrease is stopped. The torque reduction will cause the wheel to

accelerate. When one of the thresholds A or +a is crossed, a command is given to increase the torque with modulated rate R1=2533 Nm/s until the maximum $T_{b,nom}$ is reached and the torque is hold. No further action is taken until the slip threshold is crossed again. The algorithm in the form of a flow chart diagram is shown in Figure 14.1.

After a few simulations it appear that the calculated values of the brake torque have to be adjusted. After several iterations the following values of the brake torque were adopted: $T_{b,max}$= 1300 Nm, $T_{b,nom}$ =1275 Nm and $T_{b,nom,min}$ =1200 Nm.

14.3. Braking performance on a flat road and on an uneven road

The performance of the emergency straight-line braking vehicle using different wheel lock criteria is investigated by simulation.
On the flat road the braking performance is studied at three initial velocities: 40, 60, and 80 km/h. The study of the braking performance on uneven road is made at the initial velocity of 80 km/h.

Simulation results for initial velocity 80 km/h on the flat road and the uneven road are shown in section 14.4. For flat road, the simulation results at 40 and 60 km/h are given in **Appendix-F.** The general model parameters and data used in these simulations are given in Table 14.1.

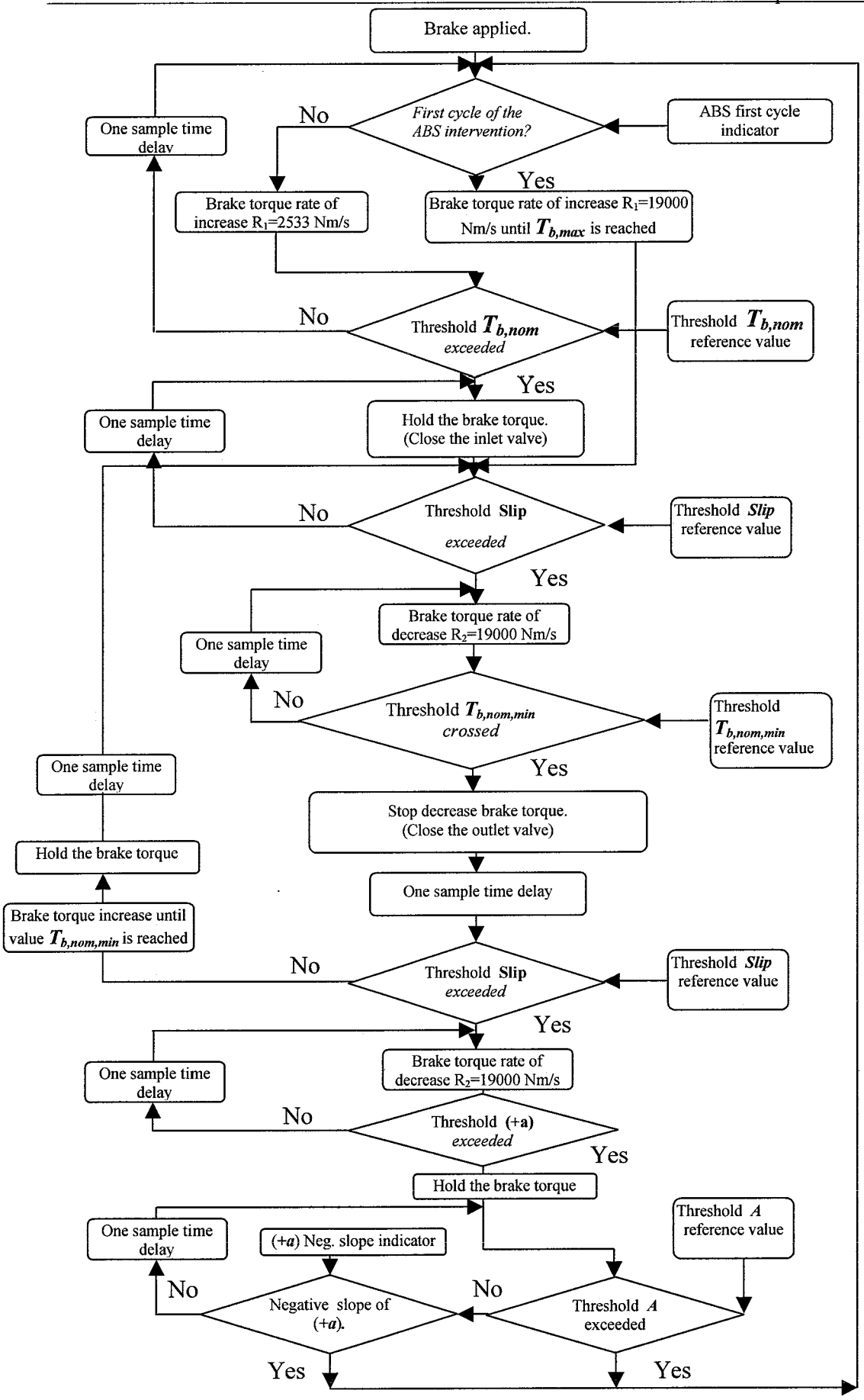

Figure 14.1: *Block diagram of the Tire torque $M_{y,r\,corr}$ criterion control braking.*

Table 14.1: Data used for the tire and quarter vehicle model.

Parameter			Value	Dimension
Vehicle	Quarter of the vehicle mass	m_2	300	kg
	Mass of the axle and components	m_1	35	kg
	Suspension spring stiffness	k_z	20000	N/m
	Suspension damper damping	c_z	2000	Ns/m
	Vertical tire stiffness	$k_{z,tire}$	200000	N/m
	Suspension compliance stiffness	k_x	100000	N/m
	Suspension compliance damping	c_x	2000	Ns/m
Tire	Wheel polar moment of inertia	I_p	1.04	$kg.m^2$
	Tire belt polar moment of inertia	I_{belt}	0.695	$kg.m^2$
	Wheel angular velocity before braking	Ω_0	Variable	rad/s
	Type – 205/60 R15			
	Unloaded radius	r_o	0.3135	m
	Loaded (rolling) radius	r_{load}	0.2968	m
	Effective rolling radius	r,eff	0.3067	m
	Mass of the belt	m_{belt}	7	kg
Road	surface		Asphalt	
	condition		Dry	
	profile		Smoot or Uneven	
Brake	Rate of the brake torque increase	R_1	19000	N.m/s
	Rate of the modulated brake torque increase	R_1	2533	N.m/s
	Rate of the brake torque decrease	R_2	19000	N.m/s

14.4. Simulation Results for initial velocity 80 km/h

A simulation results are presented in form of plots of important vehicle and ABS variables. Statistical data for some of the variables are presented in tables. For each of the employed wheel lock criteria separate table provides the numerical values of the threshold levels that have been used.
For both set of simulations, i.e. simulations for the flat road and for the uneven road, the results are presented in the following sequence:

- Braking without ABS control
- Peripheral wheel acceleration $\dot{\Omega}_{per}$ criteria control braking
- Wheel slip criterion control braking
- Combined slip and wheel peripheral acceleration $\dot{\Omega}_{per}$ criteria control braking
- Wheel $\dot{\Omega}/\Omega$ ratio criterion control braking
- Tire moment $M_{y,r\,corr}$ criterion control braking

At the end comparison between the utilized different wheel lock criteria and the associated stopping distances is given in tables.

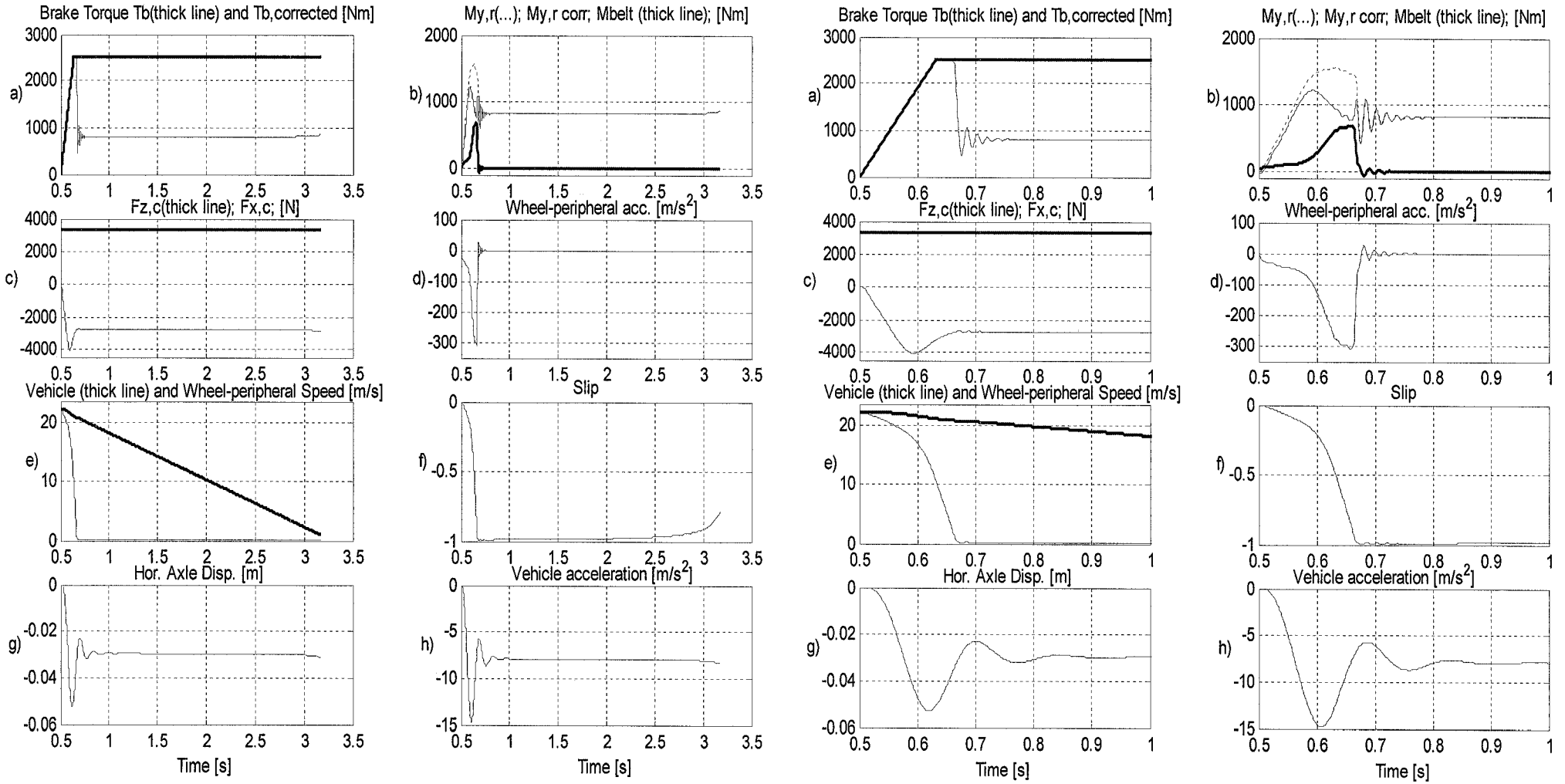

Figure 14.2: *Flat road - Braking maneuver without ABS control, V_{in} 80 km/h. The right-hand side ensemble of plots shows zoom in of the time window 0.5 -1 sec. The instant of the brake maneuver initiation is t_0=0.5 sec. T_b max = 2500 Nm.*

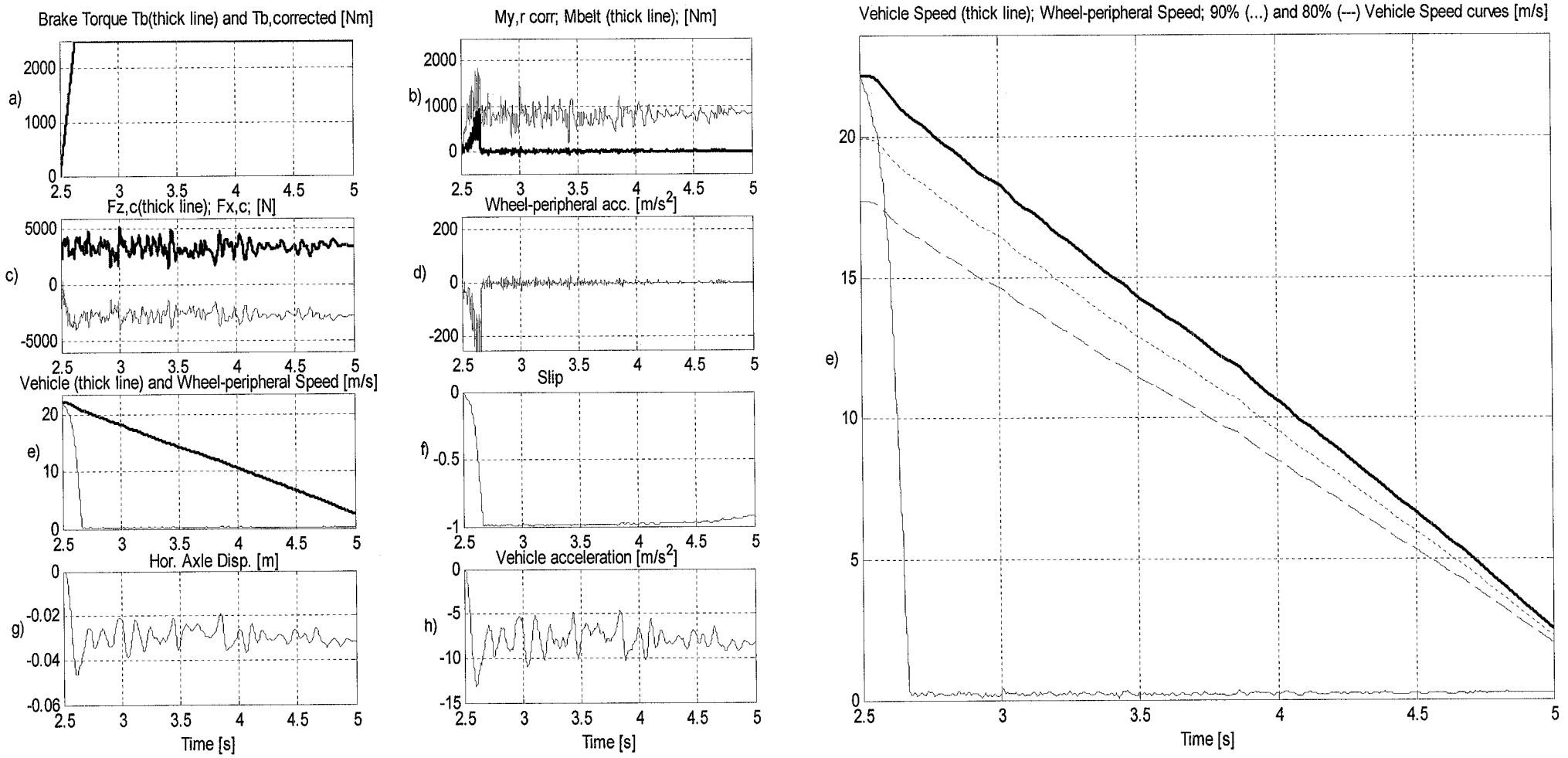

Figure 14.3: *Uneven road - Braking maneuver without ABS control, V_{in} 80 km/h. The right-hand side plot shows zoom in of the sub-graph window e). The instant of the brake maneuver initiation is t_0=2.5 sec. T_b max = 2500 Nm.*

Table 14.2: *Flat road -Braking without ABS control, statistics data, V_{in} 80 km/h*

Parameter	Dimension	Max value	Mean value	Min value	Standard deviation
Vehicle accel.	m/s^2	-14.81	-8.18	-5.69	-5.6927
Slip	-	99.45	93.38	11.69	11.69
$M_{y,r\ corr}$	Nm	1208.9	826.5	414.6	0.4146
$F_{x,c}$	N	-4079.0	-2778.0	-2697.1	-2.6971
$F_{z,c}$	N	3359.1	3356.0	3355.3	3.3553
Stopping distance from 80 km/h to 3.6 km/h [m]		31.17			
Time to reach at velocity 3.6 km/h [s]		2.67			

Table 14.3: *Uneven road - Braking maneuver without ABS control, statistics data, V_{in} 80 km/h.*

Parameter	Dimension	Max value	Mean value	Min value	Standard deviation
Vehicle accel.	m/s^2	-11.04	-7.81	-4.59	1.2365
Slip	-	99.67	97.87	91.65	1.4915
$M_{y,r\ corr}$	Nm	1512.7	802.5	171.3	0.1536
$F_{x,c}$	N	-4065.6	-2694.8	-1308.0	0.4400
$F_{z,c}$	N	5161.9	3325.8	1577.1	0.5683
Stopping distance from 80 km/h to 3.6 km/h [m]		31.27			
Time to reach at velocity 3.6 km/h [s]		2.50			

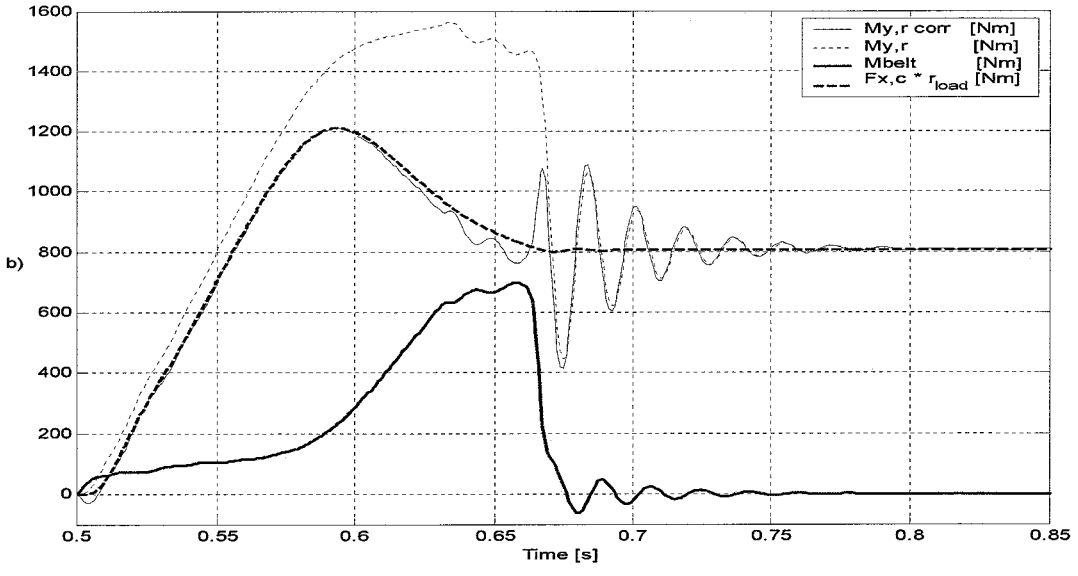

Figure 14.4: *Flat road - Braking maneuver without ABS control, V_{in}=80 km/h. Zoom in of the sub-graph b) of Figure . The graph shows the tire moment $M_{y,r}$ calculated by the SWIFT mode, the corrected tire moment $M_{y,r\ corr}$ – friction component, the tire belt moment M_{belt} –due to belt inertia, and the moment created by the longitudinal force $F_{x,c}$ times loaded tire radius r_{load}.*

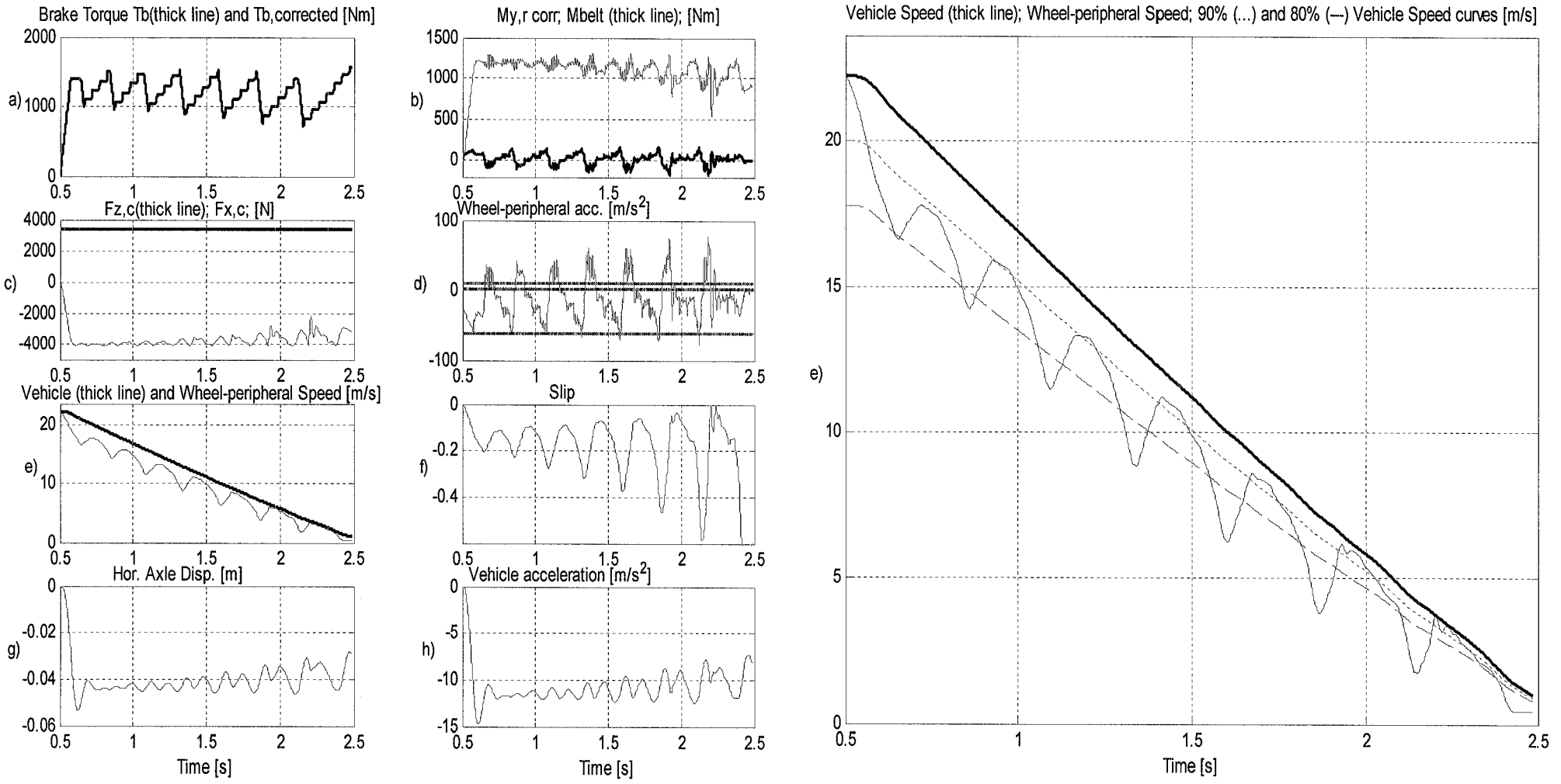

Figure 14.5: *Flat road - Peripheral wheel acceleration criteria control braking, V_{in}=80 km/h.. The right-hand side shows zoom in of the sub-graph e). The instant of the brake maneuver initiation is t_0=0.5 sec. T_b max = 2500 Nm.*

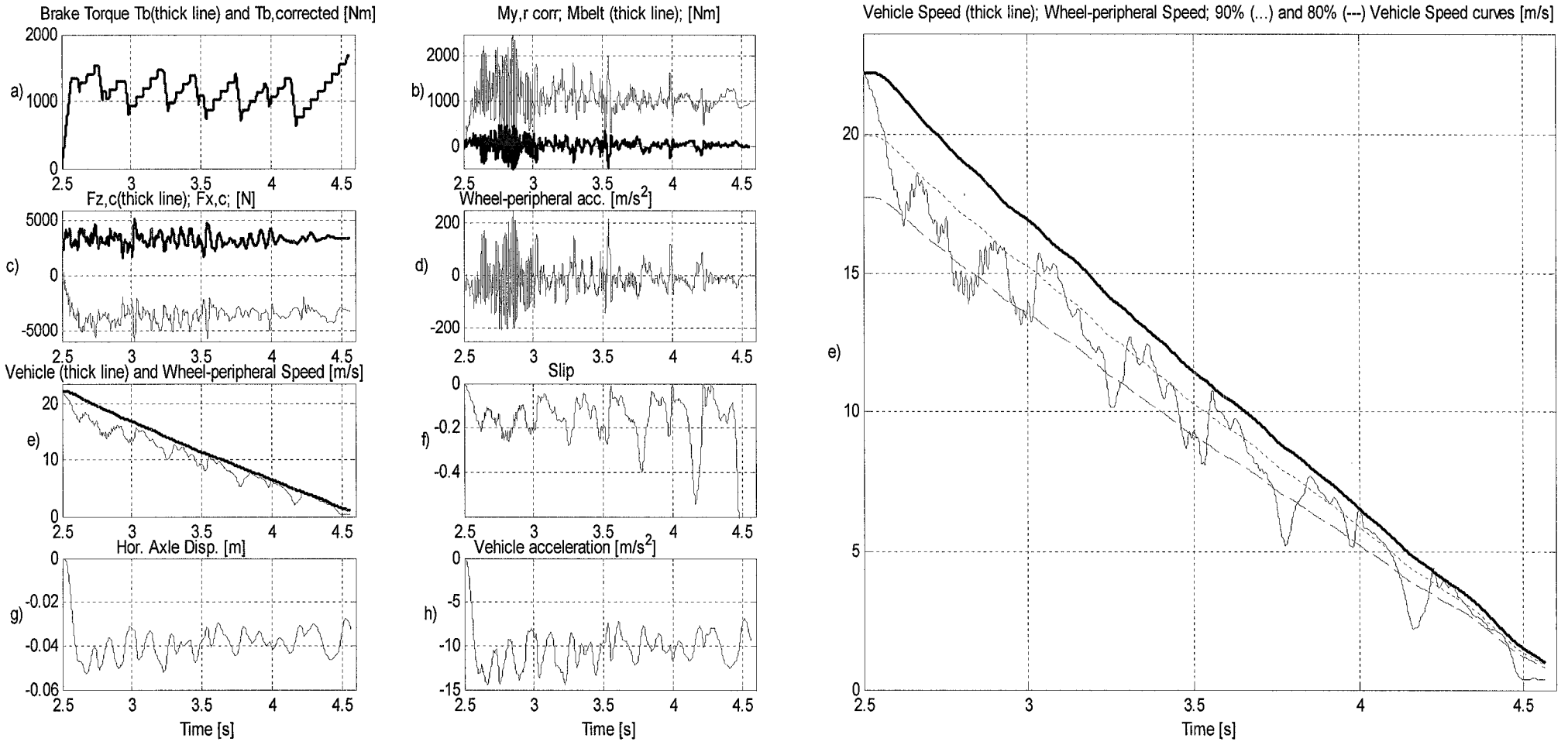

Figure 14.6: *Uneven road - Peripheral wheel acceleration criteria control braking,, V_{in}=80 km/h. The right-hand side plot shows zoom in of the sub-graph e). The instant of the brake maneuver initiation is t_0=2.5 sec. T_b max = 2500 Nm.*

Table 14.4: *Flat road - Peripheral wheel acceleration criteria control braking, statistics data, V_{in}=80 km/h.*

Parameter	Dimension	Max value	Mean value	Min value	Standard deviation
Vehicle accel.	m/s^2	-14.79	-10.97	-7.18	1.2855
Slip	-	70.22	18.62	-0.23	13.6159
$M_{y,r\,corr}$	Nm	1316.4	1112.7	543.5	0.1185
$F_{x,c}$	N	-4082.6	-3736.0	-2133.3	0.3674
$F_{z,c}$	N	3357.5	3356.0	3354.2	0.0004
Stopping distance from 80 km/h to 3.6 km/h [m]		22.78			
Time to reach at velocity 3.6 km/h [s]		1.99			

Table 14.5: *Uneven road - Peripheral wheel acceleration criteria control braking, statistics data, V_{in}=80 km/h.*

Parameter	Dimension	Max value	Mean value	Min value	Standard deviation
Vehicle accel.	m/s^2	-14.47	-10.66	-6.91	1.7917
Slip	-	74.64	16.62	-2.03	12.0453
$M_{y,r\,corr}$	Nm	2561.4	1088.0	-15.8	0.3582
$F_{x,c}$	N	-6113.1	-3661.5	-1846.0	0.6916
$F_{z,c}$	N	5137.2	3327.1	1581.4	0.5379
Stopping distance from 80 km/h to 3.6 km/h [m]		23.63			
Time to reach at velocity 3.6 km/h [s]		2.07			

Table 14.6: *Peripheral wheel acceleration criteria control braking, V_{in}=80 km/h. Employed triggering signals and their threshold values.*

Set -1		
Command	**Triggering signal**	**Threshold value**
Hold	***- a***	-60 m/s^2
Decrease	***> Slip***	-20%
Stop Decrease	***+ a***	4 m/s^2
Increase	***A***	10 m/s^2

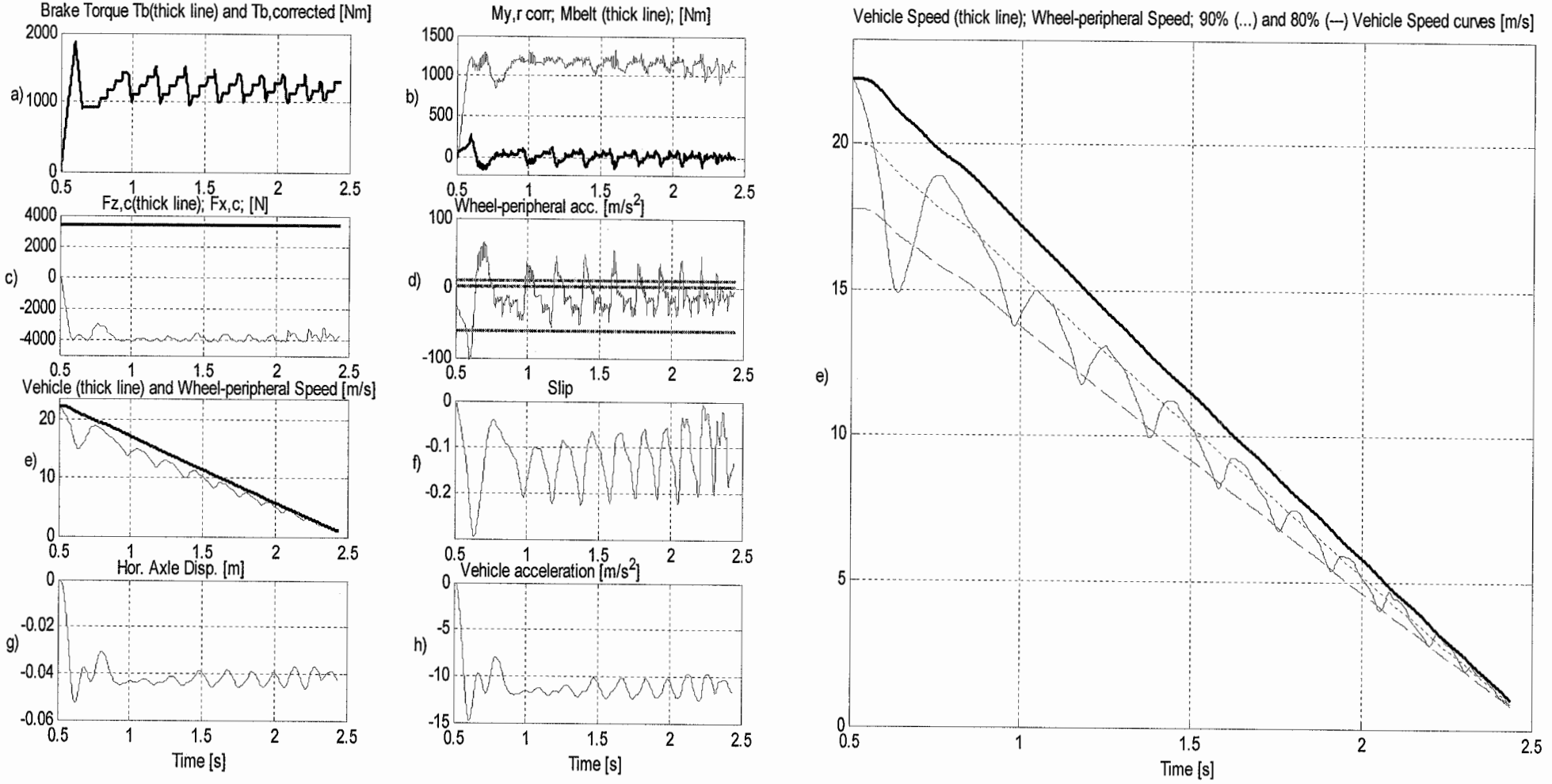

Figure 14.7: Flat road - Wheel slip criteria control braking, V_{in}=80 km/h.. The right-hand side shows zoom in of the sub-graph e). The instant of the brake maneuver initiation is t_0=0.5 sec. T_b max = 2500 Nm.

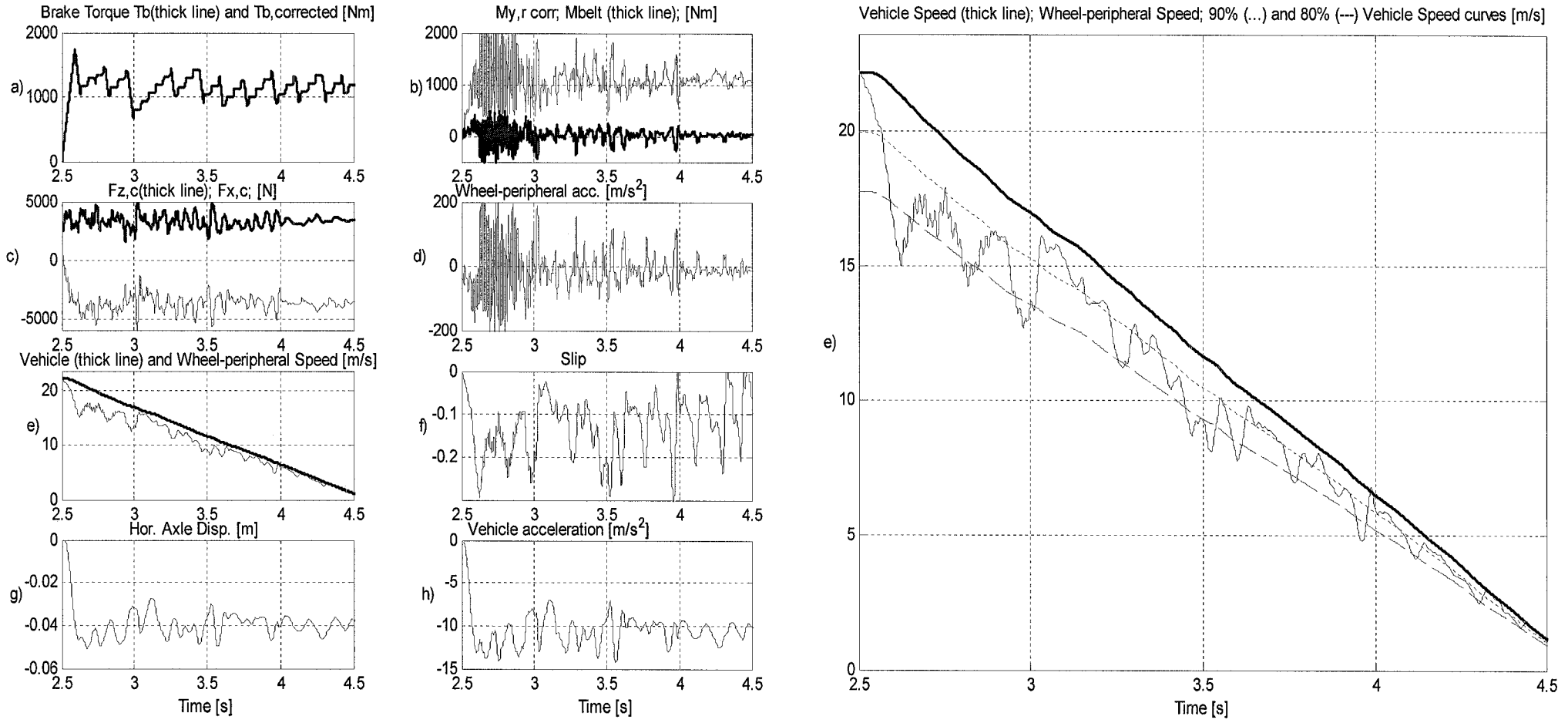

Figure 14.8: *Uneven road - Wheel slip criteria control braking, V_{in}=80 km/h.. The right-hand side shows zoom in of the sub-graph e). The instant of the brake maneuver initiation is t_0=2.5 sec. T_b max = 2500 Nm.*

Table 14.7: *Flat road - Wheel slip criteria control braking, statistics data, V_{in}=80 km/h.*

Parameter	Dimension	Max value	Mean value	Min value	Standard deviation
Vehicle accel.	m/s^2	-14.81	-11.31	-7.90	0.9927
Slip	-	29.40	12.56	0.43	5.8015
$M_{y,r\,corr}$	Nm	1323.9	1146.8	851.0	0.0771
$F_{x,c}$	N	-4080.9	-3849.7	-3000.4	0.2359
$F_{z,c}$	N	3357.4	3356.0	3354.9	0.0004
Stopping distance from 80 km/h to 3.6 km/h [m]		22.96			
Time to reach at velocity 3.6 km/h [s]		1.94			

Table 14.8: *Uneven road - Wheel slip criteria control braking, statistics data, V_{in}=80 km/h.*

Parameter	Dimension	Max value	Mean value	Min value	Standard deviation
Vehicle accel.	m/s^2	-14.37	-10.72	-2.95	1.7597
Slip	-	30.61	13.35	-3.49	6.7784
$M_{y,r\,corr}$	Nm	2640.6	1094.4	41.9	0.3538
$F_{x,c}$	N	-6043.1	-3687.5	-1333.4	0.6824
$F_{z,c}$	N	5135.5	3331.9	1584.1	0.5342
Stopping distance from 80 km/h to 3.6 km/h [m]		23.61			
Time to reach at velocity 3.6 km/h [s]		2.02			

Table 14.9: *Employed Wheel slip criteria control braking, V_{in}=80 km/h. Employed triggering signals and their threshold values.*

Set -2		
Command	**Triggering signal**	**Threshold value**
Hold	***> Slip***	-20%
Decrease	***> Slip***	-20%
Stop Decrease	***+a***	4 m/s^2
Increase	***A***	10 m/s^2

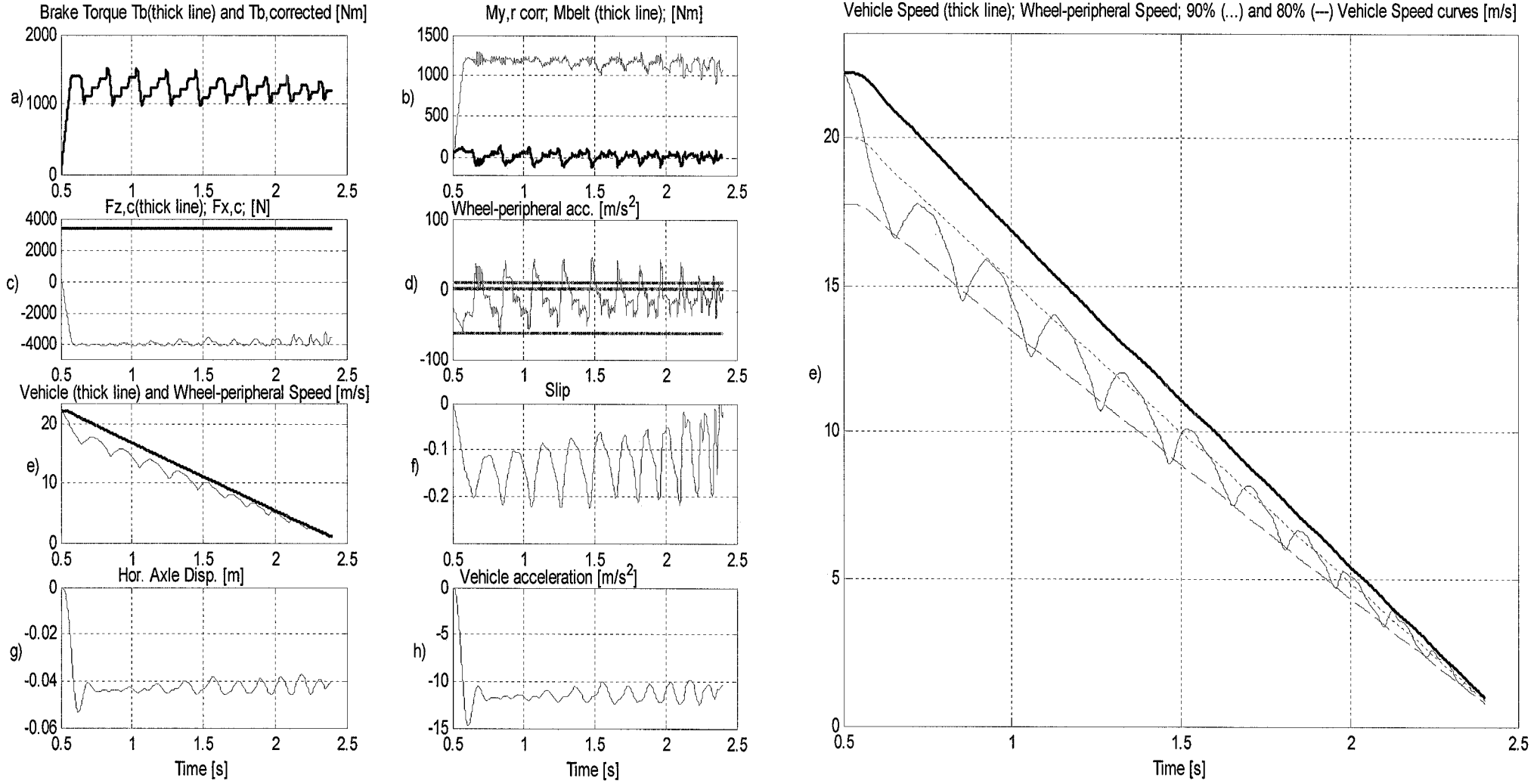

Figure 14.9 : *Flat road - Combined slip and wheel peripheral acceleration criteria control braking, V_{in}=80 km/h.. The right-hand side shows zoom in of the sub-graph e). The instant of the brake maneuver initiation is t_0=0.5 sec. T_b max = 2500 Nm.*

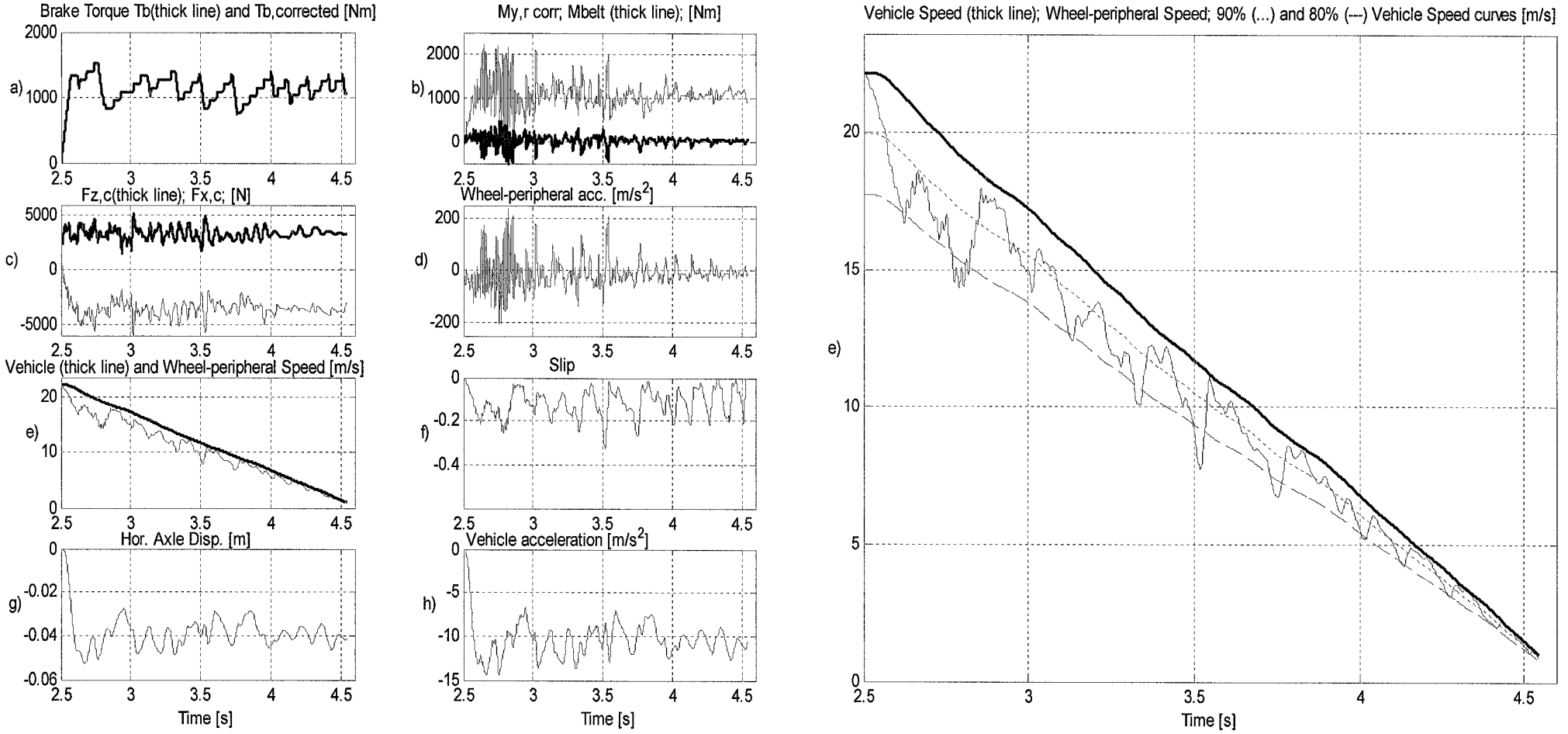

Figure 14.10: *Uneven road - Combined slip and wheel peripheral acceleration criteria control braking, V_{in}=80 km/h.. The right-hand side shows zoom in of the sub-graph e). The instant of the brake maneuver initiation is t_0=2.5 sec. T_b max = 2500 Nm.*

Table 14.10: *Flat road - Combined slip and wheel peripheral acceleration criteria control braking, statistics data, V_{in}=80 km/h.*

Parameter	Dimension	Max value	Mean value	Min value	Standard deviation
Vehicle accel.	m/s^2	14.79	-11.50	-7.83	0.8105
Slip	-	22.30	12.58	-1.99	5.2036
$M_{y,r\,corr}$	Nm	1330.6	1165.0	878.9	0.0620
$F_{x,c}$	N	-4080.6	-3910.8	-3074.9	0.1791
$F_{z,c}$	N	3356.9	3356.0	3354.9	0.0003
Stopping distance from 80 km/h to 3.6 km/h [m]		22.31			
Time to reach at velocity 3.6 km/h [s]		1.9			

Table 14.11: *Uneven road - Combined slip and wheel peripheral acceleration criteria control braking, statistics data, V_{in}=80 km/h.*

Parameter	Dimension	Max value	Mean value	Min value	Standard deviation
Vehicle accel.	m/s^2	-14.47	-10.67	-6.71	1.6745
Slip	-	32.72	12.07	-8.16	6.5124
$M_{y,r\,corr}$	Nm	2245.9	1089.9	65.1	0.3123
$F_{x,c}$	N	-6122.3	-3661.7	-1759.7	0.6710
$F_{z,c}$	N	5143.6	3330.4	1575.7	0.5382
Stopping distance from 80 km/h to 3.6 km/h [m]		23.93			
Time to reach at velocity 3.6 km/h [s]		2.05			

Table 14.12: *Combined slip and wheel peripheral acceleration criteria control braking, threshold values, V_{in}=80 km/h. Employed triggering signals and their threshold values.*

Set -3		
Command	**Triggering signal**	**Threshold value**
Hold	***- a*** and ***> Slip***	-60 m/s^2 and -20%
Decrease	***> Slip***	-20%
Stop Decrease	***+ a***	4 m/s^2
Increase	***A***	10 m/s^2

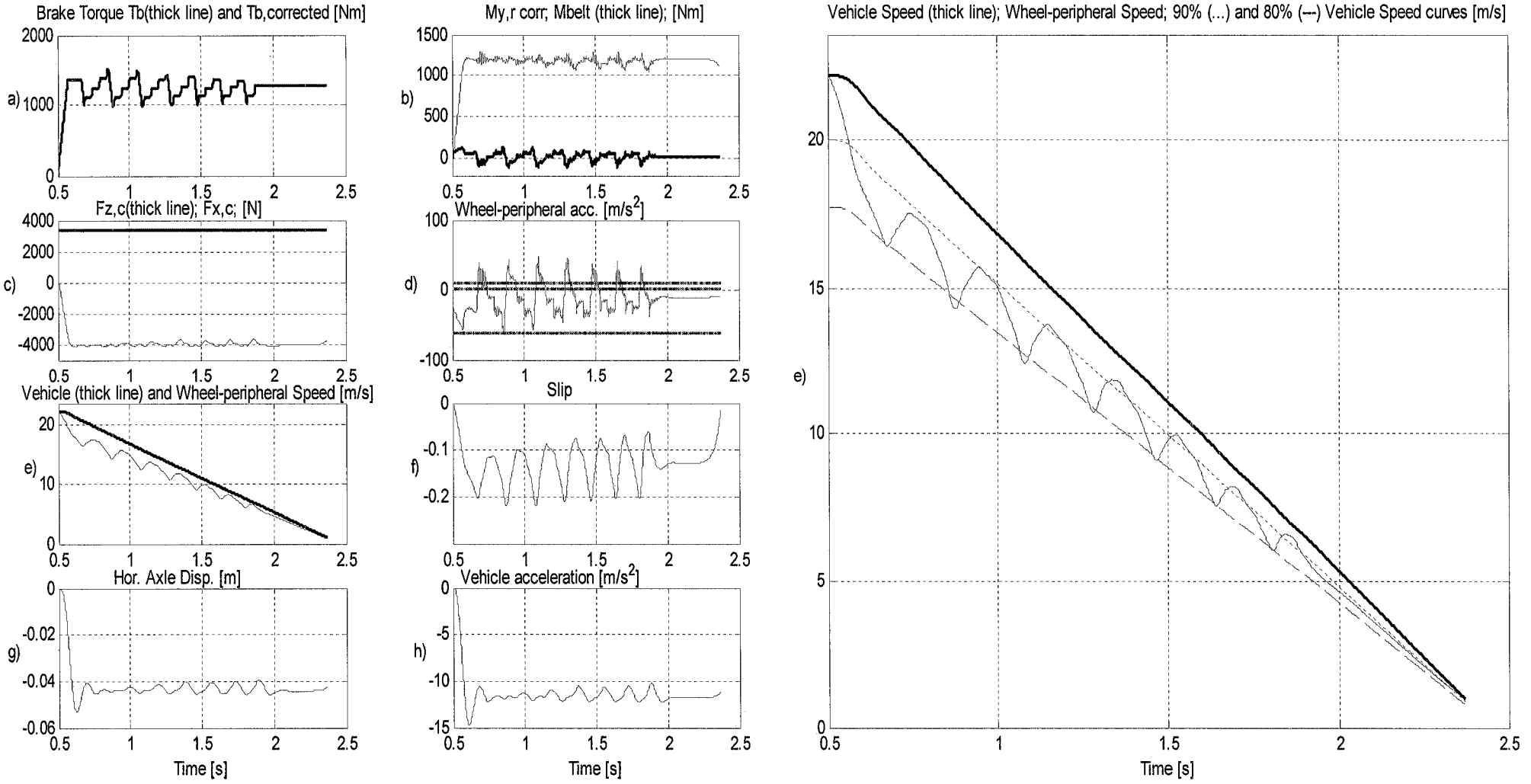

Figure 14.11: *Flat road - Wheel $\dot{\Omega}/\Omega$ ratio criteria control braking, V_{in}=80 km/h.. The right-hand side shows zoom in of the sub-graph e). The instant of the brake maneuver initiation is t_0=0.5 sec. T_b max = 2500 Nm.*

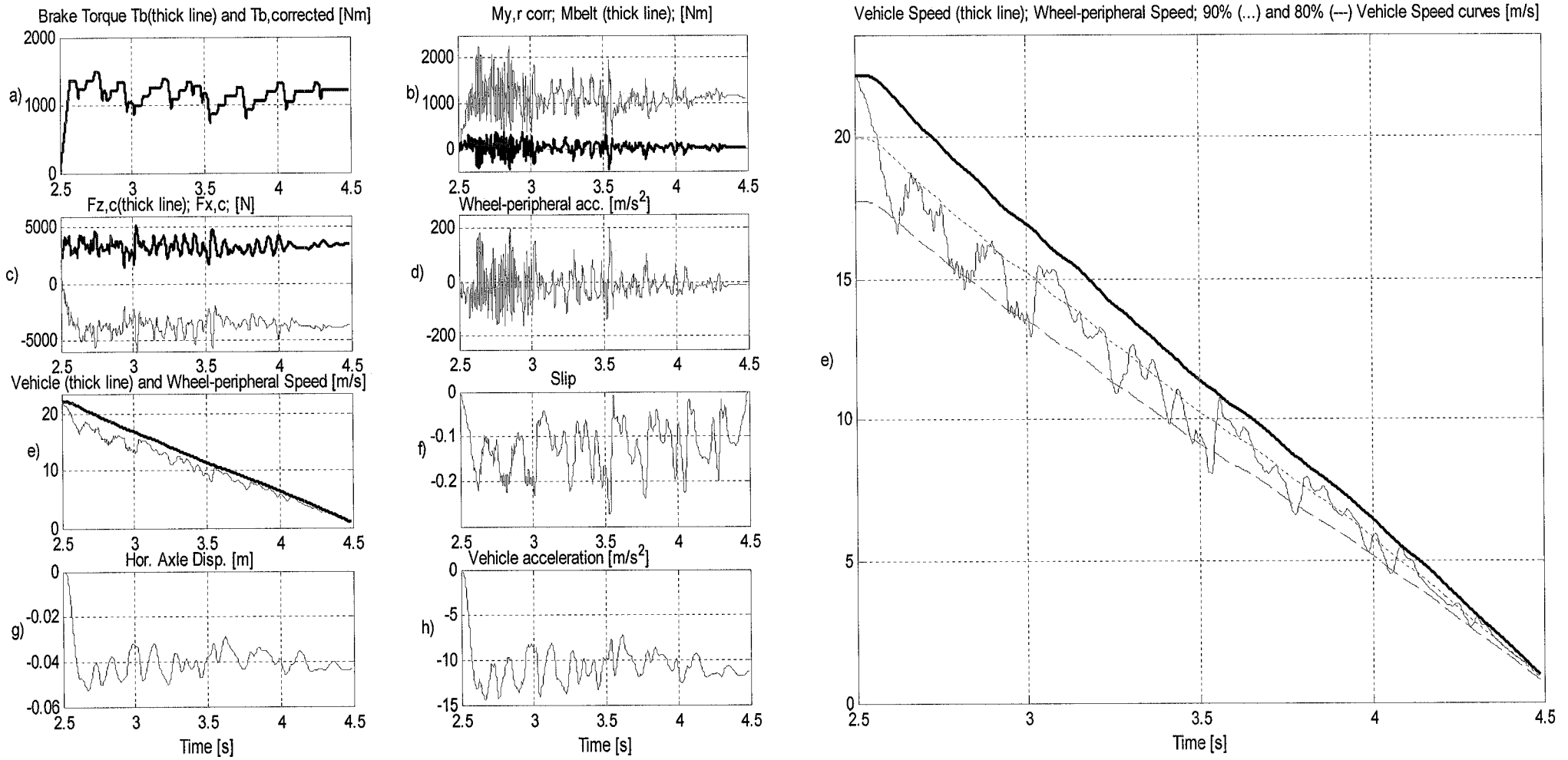

Figure 14.12: *Uneven road - Wheel $\dot{\Omega}/\Omega$ ratio criteria control braking, V_{in}=80 km/h.. The right-hand side shows zoom in of the sub-graph e). The instant of the brake maneuver initiation is t_0=2.5 sec. T_b max = 2500 Nm.*

Table 14.13: *Flat road - Wheel $\dot{\Omega}/\Omega$ ratio criteria control braking, statistics data, V_{in}=80 km/h.*

Parameter	Dimension	Max value	Mean value	Min value	Standard deviation
Vehicle accel.	m/s^2	-14.72	-11.67	-10.05	0.6327
Slip	-	22.01	13.30	1.50	3.9021
$M_{y,r\,corr}$	Nm	1299.6	1184.2	1046.0	0.0392
$F_{x,c}$	N	-4080.5	-3978.0	-3553.9	0.1079
$F_{z,c}$	N	3356.8	3356.0	3355.1	0.0003
Stopping distance from 80 km/h to 3.6 km/h [m]		22.18			
Time to reach at velocity 3.6 km/h [s]		1.87			

Table 14.14: *Uneven road - Wheel $\dot{\Omega}/\Omega$ ratio criteria control braking, statistics data, V_{in}=80 km/h.*

Parameter	Dimension	Max value	Mean value	Min value	Standard deviation
Vehicle accel.	m/s^2	-14.42	-10.89	-3.66	1.7104
Slip	-	27.44	12.72	-0.37	5.3345
$M_{y,r\,corr}$	Nm	2277.4	1111.5	302.4	0.3009
$F_{x,c}$	N	-6157.0	-3738.8	-1467.9	0.6665
$F_{z,c}$	N	5137.9	3327.0	1577.8	0.5463
Stopping distance from 80 km/h to 3.6 km/h [m]		23.31			
Time to reach at velocity 3.6 km/h [s]		1.99			

Table 14.15: *Wheel $\dot{\Omega}/\Omega$ ratio criteria control braking, threshold values, V_{in}=80 km/h. Employed triggering signals and their threshold values.*

Set - 4		
Command	**Triggering signal**	**Threshold value**
Hold	*-Om_dot / Om*	3.5 Hz
Decrease	*> Slip*	-20%
Stop Decrease	*+ a*	4 m/s^2
Increase	*A*	10 m/s^2

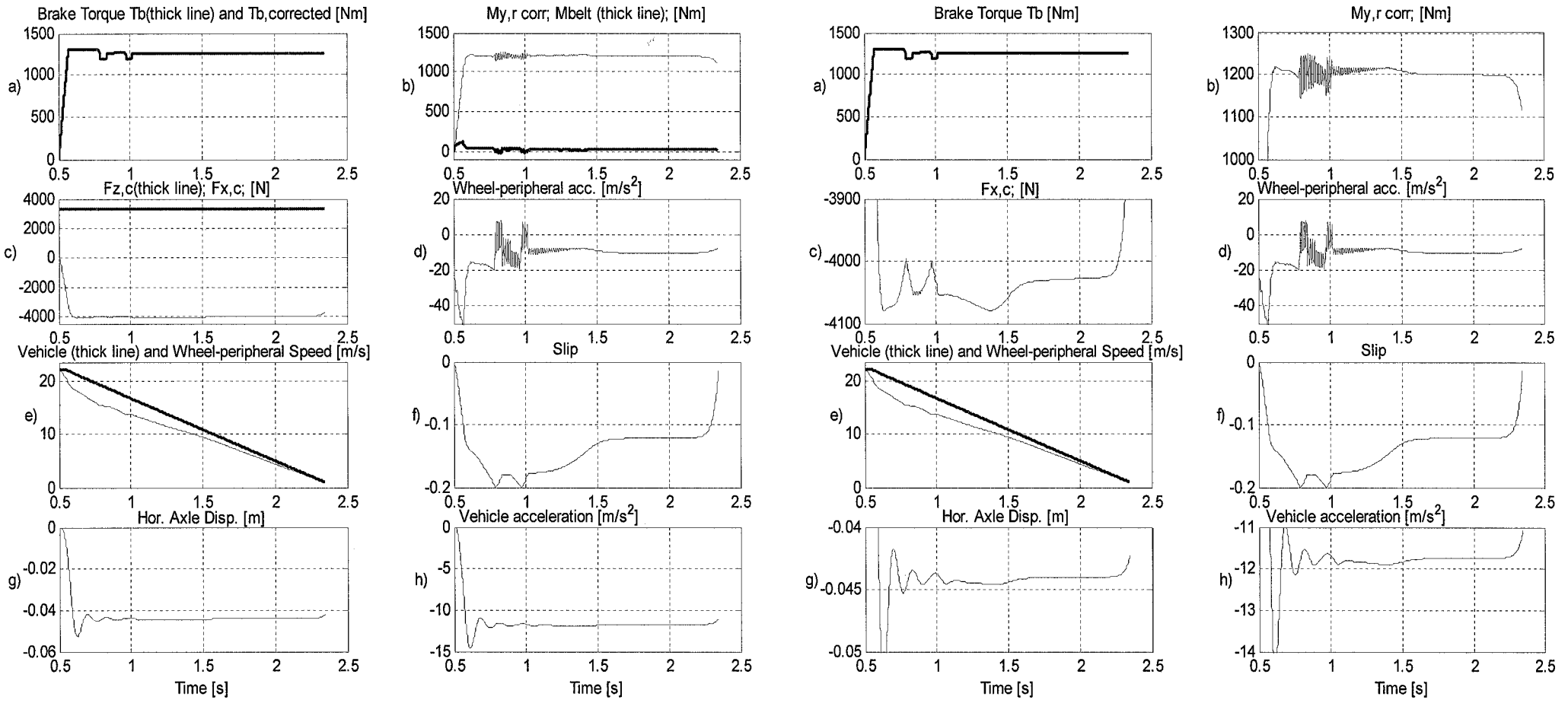

Figure 14.13: *Flat road -Tire moment $M_{y,r\,corr}$ criteria control braking, V_{in}=80 km/h. The right-hand side ensemble of plots offers zoom in of the amplitudes. The instant of the brake maneuver initiation is t_0=0.5 sec. T_b max = 1300 Nm.*

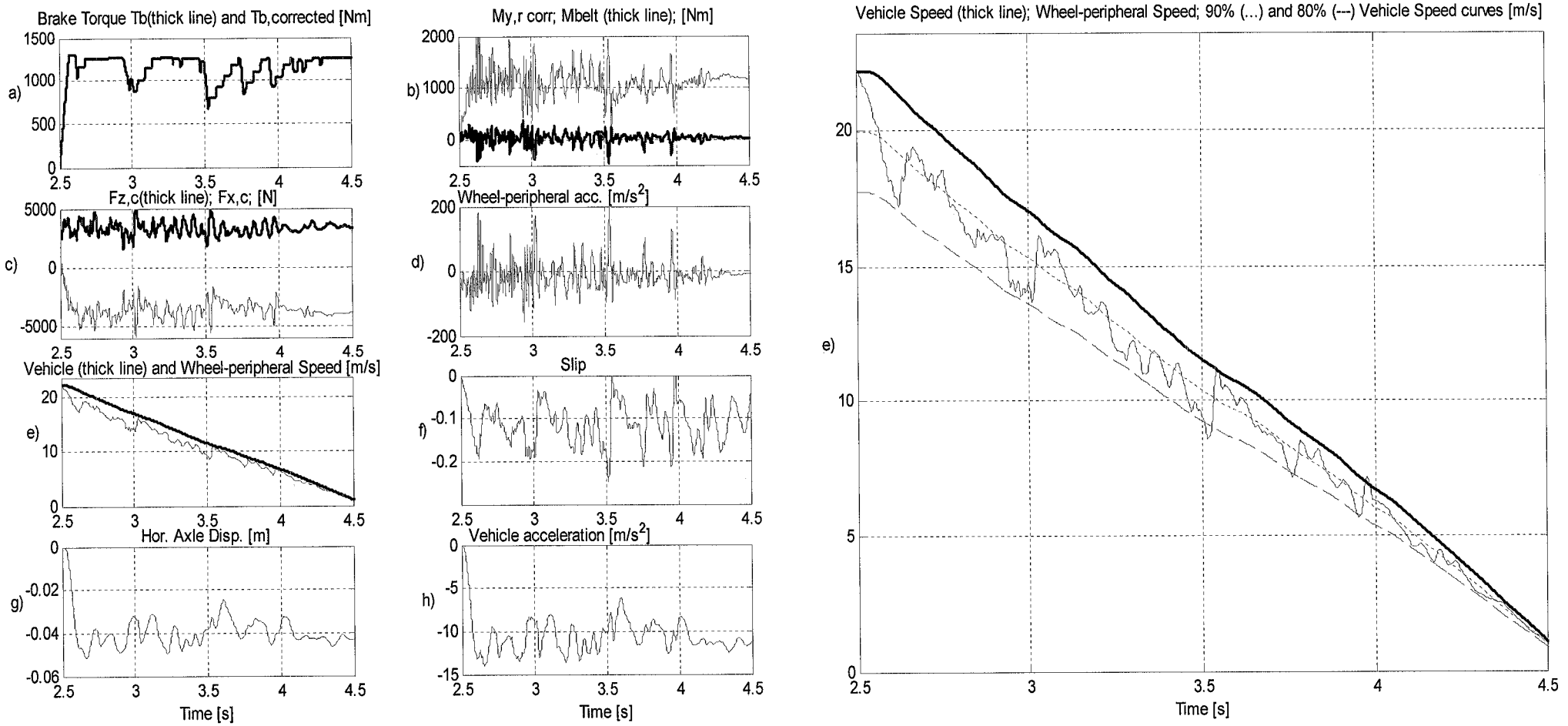

Figure 14.14: *Uneven road -Tire moment $M_{y,r\,corr}$ criteria control braking, V_{in}=80 km/h. The right-hand side plot shows zoom in of the sub-graph window e).. The instant of the brake maneuver initiation is t_0=2.5 sec. T_b max = 1300 Nm.*

Table 14.16: *Flat road - Tire moment $M_{y,r\ corr}$ criteria control braking, statistics data, V_{in}=80 km/h.*

Parameter	Dimension	Max value	Mean value	Min value	Standard deviation
Vehicle accel.	m/s^2	-14.56	-11.83	-9.51	0.4851
Slip	-	20.06	14.47	1.45	3.1098
$M_{y,r\ corr}$	Nm	1250.5	1200.8	1035.2	0.0203
$F_{x,c}$	N	-40794	-4031.6	-3444.6	0.0604
$F_{z,c}$	N	3356.6	3356.0	3355.6	0.0001
Stopping distance from 80 km/h to 3.6 km/h [m]		21.88			
Time to reach at velocity 3.6 km/h [s]		1.85			

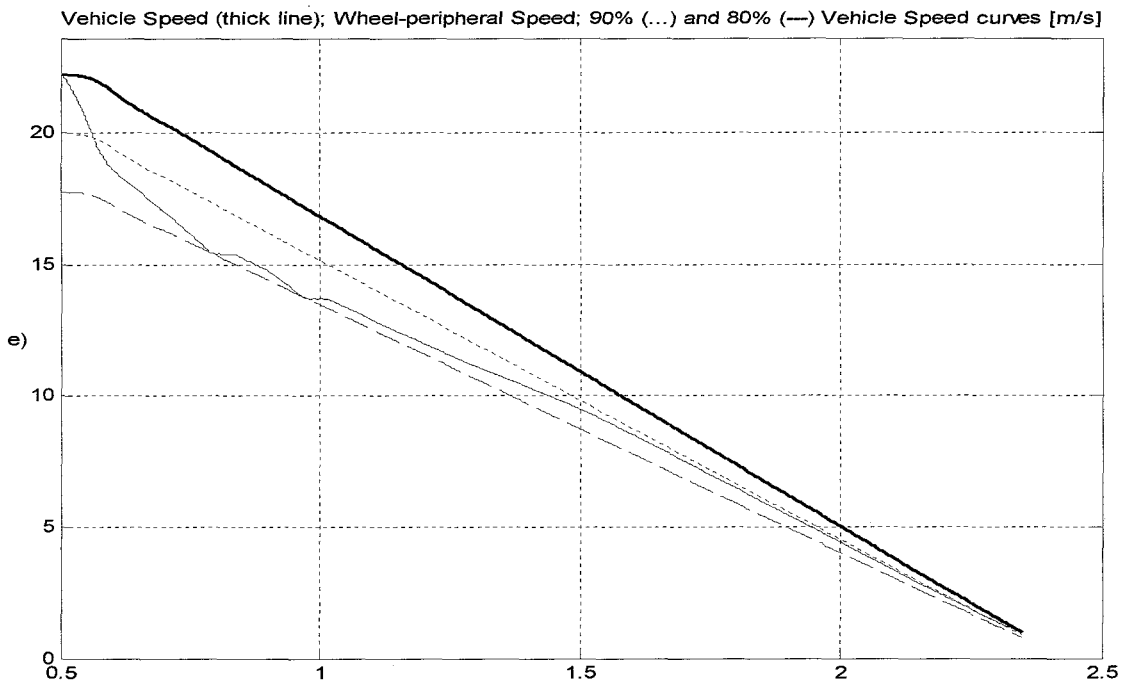

Figure 14.15: *Flat road -Tire moment $M_{y,r\ corr}$ criteria control braking, V_{in}=80 km/h. The graph offers zoom in of the sub-graph e). The instant of the brake maneuver initiation is t_0=0.5 sec. T_b max = 1300 Nm.*

14.4.1. Results summary

The data of the several vehicle variables obtained from the braking performance study on flat and uneven roads are given in Table 14.17 and Table 14.18 respectively. Comparison of the stopping distances on both type roads for V_{in} = 80 km/h is presented in Table 14.19.

Table14.17: *Flat road. Comparison between the simulation results obtained by utilizing different wheel lock criteria. V_{in}=80 km/h, dry asphalt, tire type – 205/60 R15, brake torque rate of increase R1=19000 Nm/s, modulated R1=2533 Nm/s, brake torque rate of decrease R2=19000 Nm/s.*

		ABS - OFF		**ABS - ON**									
		Locked Wheel braking		**Tire moment control braking**		**Wheel Acceleration control braking**		**Slip control braking**		**Slip and wheel acc. control braking**		**Wheel $\dot{\Omega}/\Omega$ ratio control braking**	
Parameter	**Dimension**	Mean value	Standard deviation	Mean value	Standard deviation	Mean value	Standard deviation	Mean value	Standard deviation	Mean value	Standard deviation	Mean value	Standard deviation
Vehicle accel.	**m/s²**	-8.18	5.6927	-11.83	0.4851	-10.97	1.2855	-11.31	0.9927	-11.50	0.8105	-11.67	0.6327
Slip	**%**	93.38	11.6900	14.47	3.1098	18.62	13.6159	12.56	5.8015	12.58	5.2036	13.30	3.9021
$M_{y,r\,corr}$	**Nm**	826.5	0.4146	1200.8	0.0203	1112.7	0.1185	1146.8	0.0771	1165.0	0.0620	1184.2	0.0392
$F_{x,c}$	**N**	-2778.0	2.6971	-4031.6	0.0604	-3736.0	0.3674	-3849.7	0.2359	-3910.8	0.1791	-3978.0	0.1079
$F_{z,c}$	**N**	3356.0	3.3553	3356.0	0.0001	3356.0	0.0004	3356.0	0.0004	3356.0	0.0003	3356.0	0.0003
Stopping distance (from 80 km/h to 3.6 km/h) **[m]**		**31.17**		**21.88**		**22.78**		**22.96**		**22.31**		**22.18**	
Time to reach at velocity of 3.6 km/h **[s]**		**2.67**		**1.85**		**1.99**		**1.94**		**1.90**		**1.87**	

Table 14.18: *Uneven road -Comparison between the simulation results obtained by utilizing different control signal to trigger the brake torque Hold Command.; V_{in}=80 km/h, high friction surface, tire type – 205/60 R15, brake torque rate of increase R1=19000 Nm/s, modulated R1=2533 Nm/s, brake torque rate of decrease R2=19000 Nm/s.*

		ABS - OFF		ABS - ON									
		Locked Wheel braking		Tire moment control braking		Wheel Acceleration control braking		Slip control braking		Slip and wheel acc. control braking		Wheel $\dot{\Omega}/\Omega$ ratio control braking	
Parameter	**Dimension**	Mean value	Standard deviation	Mean value	Standard deviation	Mean value	Standard deviation	Mean value	Standard deviation	Mean value	Standard deviation	Mean value	Standard deviation
Vehicle accel.	**m/s²**	-7.81	1.2365	-10.50	2.0800	-10.66	1.7917	-10.72	1.7597	-10.67	1.6745	-10.89	1.7104
Slip	**%**	97.87	1.4915	11.30	4.7900	16.62	12.0453	13.35	6.7784	12.07	6.5124	12.72	5.3345
$M_{v,r\,corr}$	**Nm**	802.5	0.1536	1076	0.2900	1088.0	0.3582	1094.4	0.3538	1089.9	0.3123	1111.5	0.3009
$F_{x,c}$	**N**	-2694.8	0.4400	-3617	0.8000	-3661.5	0.6916	-3687.5	0.6824	-3661.7	0.6710	-3738.8	0.6665
$F_{z,c}$	**N**	3325.8	0.5683	-	-	3327.1	0.5379	3331.9	0.5342	3330.4	0.5382	3327.0	0.5463
Stopping distance (from 80 km/h to 3.6 km/h) [m]		**31.27**		**23.71**		**23.63**		**23.61**		**23.93**		**23.31**	
Time to reach velocity of 3.6 km/h [s]		**2.50**		**1.99**		**2.07**		**2.02**		**2.05**		**2.01**	

Table 14.19*: Comparison between the stopping distances in meters as function of different wheel lock criteria at initial velocity of 80 km/h. Conditions: dry asphalt, tire type – 205/60 R15, brake torque rate of increase R1=19000 Nm/s, modulated R1=2533 Nm/s, brake torque rate of decrease R2=19000 Nm/s. Computed ideal theoretical braking distance assumes constant vehicle deceleration of 11.84 m/s² (1.207*9.81 m/s²) from the instant of brake application till moment the vehicle reaches 3.6 km/h. If the same deceleration is kept, the vehicle passes only additional 0.04 m until stand still.*

		ABS - OFF	ABS - ON					
		Locked Wheel braking	Theoretical minimum at 1.207*g m/s²	Tire moment control braking	Wheel $\dot{\Omega}_{per}$ control braking	Slip control braking	Slip and wheel $\dot{\Omega}_{per}$ control braking	Wheel $\dot{\Omega}/\Omega$ ratio control braking
Stopping distance (from 80 km/h to 3.6 km/h) [m]	***Flat road***	**31.17**	**20.81**	**21.88**	**22.78**	**22.96**	**22.31**	**22.18**
	Uneven road	**31.27**		**23.71**	**23.63**	**23.61**	**23.93**	**23.31**

15. Conclusions on the results for V_{in} = 80 km/h

15.1. A Flat Road

Analysis of the braking performance of the test vehicle shows that the stopping distance is significantly reduced when an anti-lock barking control is used if compared with the conventional (non ABS control) braking.

Comparing the results obtained by the ABS control braking with different wheel lock criteria (see Table 14.17), can be concluded that the tire torque control braking has the shortest stopping distance. Table 15.1 gives an arrangement of the criteria in increasing stopping distance order.

Table 15.1: *Flat road. Different wheel lock criteria arranged in decreasing performance order for V_{in} =80 km/h.*

Num	Wheel lock criteria	Stopping distance [m]	Difference in the distance with respect to the Theoretical stopping minimum [m]
1	Tire moment $M_{y,r\,corr}$ control braking	21.88	+1.07
2	Wheel $\dot{\Omega}/\Omega$ ratio control braking	22.18	+1.37
3	Slip and wheel acc. control braking	22.31	+1.50
4	Wheel Acceleration control braking	22.78	+1.97
5	Slip control braking	22.96	+2.15

From the examination of Figure 14.5 is evident that though $\dot{\Omega}_{per.}$ is set at fixed level the slip needed to develop that wheel acceleration is growing fast (see Figure 14.5 subplots d and f) at low vehicle velocities. Despite the fact that no correction of the wheel peripheral acceleration is made the achieved stopping distance is two meters longer than the theoretical minimum. It is true that the value of the wheel peripheral deceleration threshold was set with respect to the initial velocity (see Table 14.6 and Table 13.3).

Unexpected, the longest stopping distance is obtained by slip control braking. The explanation of this result is that during the first braking cycle, slip reaches values from -40% initially to -5% thereafter. This large slip deviation from the peak value causes reduction in the magnitude of the longitudinal force $F_{x,c}$ (see Figure 14.7c) which leads to lower deceleration for the first braking cycle, but due to the high vehicle velocity in this period the result is increased stopping distance in total.

Reviewing the simulation results on Figure 14.7 another question arises. Why despite of the slip control, the wheel slip in the first braking cycle reaches high values beyond the threshold level? The comments on the observed result are: due to the high rate of brake torque increase R_1 the T_b is already attained high values when the slip threshold is crossed. Even immediate decrease of the T_b thereafter the threshold crossing the wheel is already at high slip levels. In the consequent braking cycles the increase rate R_1 of T_b is reduced.

15.2. An Uneven Road

Analysis of the braking performance on an uneven road shows that the stopping distance with anti-lock barking control is significantly reduced if compared with the conventional braking.

Comparing the results on uneven road obtained by the ABS control braking when different wheel lock criteria are employed (see Table 14.18), we can conclude that the $\dot{\Omega}/\Omega$ ratio control braking has the shortest stopping distance for the given conditions. Table 15.2 gives the arrangement of the criteria in order of increasing stopping distance. In the table are presented also the difference in the stopping distance with respect to the flat road when the same criterion is used.

Table 15.2: *Uneven road. Different wheel lock criteria sorted in order of the decreasing braking performance for V_{in} =80 km/h.*

Num	Wheel lock criteria	Stopping distance [m]	Difference with respect to the flat road performance [m]
1	Wheel $\dot{\Omega}/\Omega$ ratio control braking	23.31	+1.13
2	Slip control braking	23.61	+0.65
3	Wheel Acceleration control braking	23.63	+0.85
4	Tire moment $M_{y,r\,corr}$ control braking	23.71	+1.83
5	Slip and wheel acc. control braking	23.93	+1.62

The tire moment control braking is at fourth position. The decrease in barking performance compared with the results obtained on a flat road is expected. The deterioration in the performance can be explained with the earlier made assumption (see Section 14.2) for the fixed values of the normal force $F_{z,c}$ and of the loaded radius r_{load}. Road unevenness causes a disturbance of $F_{z,c}$ and r_{load}, and respectively in $M_{y,r\,corr.}$, so the efficiency of the control algorithm is decreased.

It is interesting to analyze the deterioration in the braking performance on an uneven road with respect to that on a flat road, for the same wheel lock criterion. Data of this analyze are provide in the last column of Table 15.2. According to the results, the wheel slip control braking is less sensitive to the road disturbances, second in this performance is the wheel acc. criterion.
Unexpected is the result in the braking performance obtained by the combined wheel slip and acc. criterion. Somehow the deterioration in the stopping distance is almost equal to the sum of the stopping distances of the slip control and the acceleration control used separately.
Earlier was explained why the performance of the tire torque $M_{y,r\,corr.}$ control braking is not satisfactory enough. It appears that this is the criterion on which the uneven road had the greatest impact.

16. Concluding remarks and recommendations

16.1. Concluding remarks

The results of the braking performance study for different wheel lock criteria used by the ABS on a flat road (V_{in}= 40, 60 and 80 km/h) and on an uneven road (V_{in}= 80) are compared in Figure 16.1 and Figure 16.2 respectively.

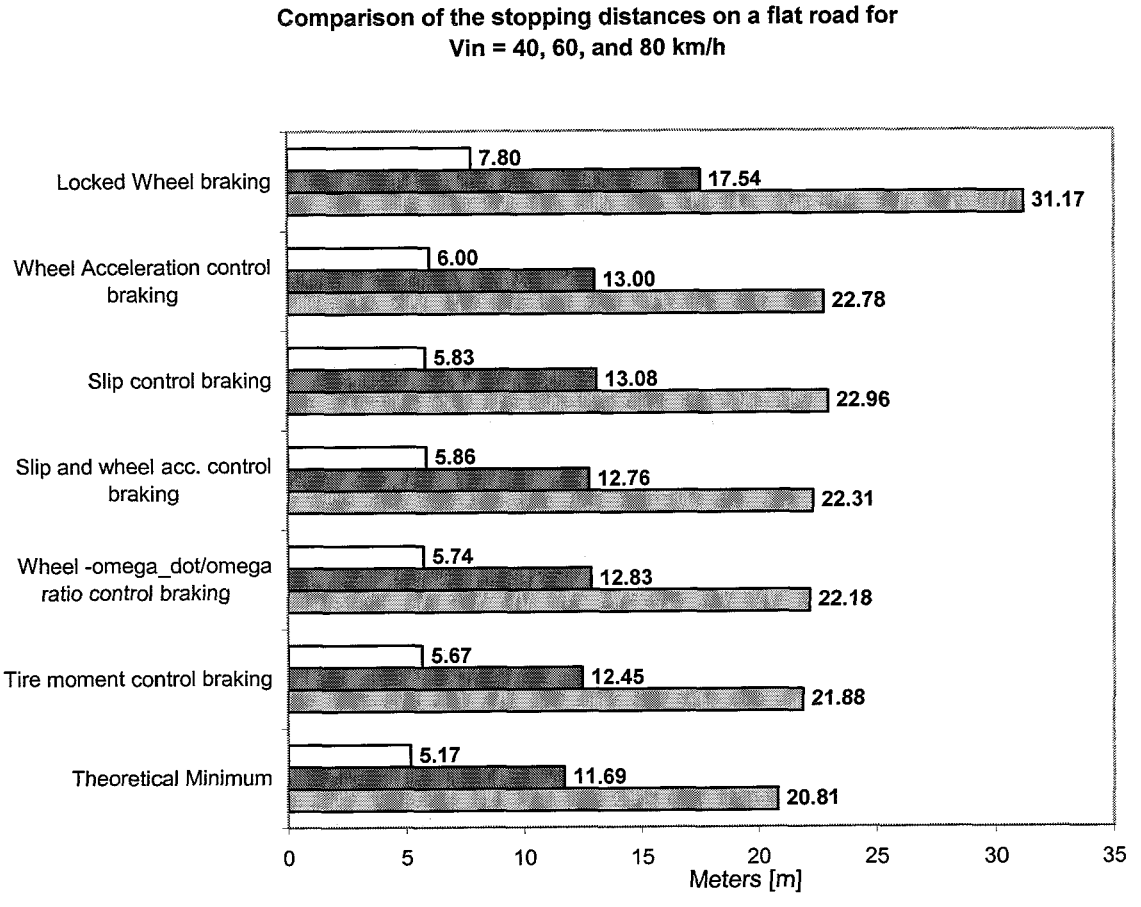

Figure 16.1: *Flat road. Comparison between the results obtained by utilizing different control signals The results are presented in groups of three bars. The top bar corresponds to V_{in}=40 km/h, the middle to 60 km/h and the lower bar to 80 km/k. Conditions: dry asphalt, tire type – 205/60 R15, brake torque rate of increase* R1=19000 Nm/s, modulated R1=2533 Nm/s, brake torque rate of decrease R2=19000 Nm/s.

From the results on a flat road can be concluded that the control algorithm exploiting the tire moment $M_{y,r\,corr}$ to control the brake torque, provides the shortest stopping distance in the studied range of velocities.

On second position is the $\dot{\Omega}/\Omega$ ratio control braking. It appears that even without other correction (except the one for the initial velocity) with respect to the vehicle velocity this criterion is able to obtain satisfactory results. The selection of suitable threshold value with

respect to the initial velocity is made also for the $\dot{\Omega}_{per}$ criterion, but the obtained results are not as good as for $\dot{\Omega}/\Omega$ criterion (see Figures 14.5 and 14.11).

Reviewing the braking performance on an even road (see Figure16.2) the best results are achieved when the ABS uses the $\dot{\Omega}/\Omega$ criterion. Second in this braking performance study is Slip criterion.
It is interesting to point out that, with slip criterion, the deterioration in the stopping distance is the lowest one if compared with the results on a flat road.
In contrary the most significant deterioration in the braking performance is shown by the tire moment $M_{y,r\ corr}$ and the combined slip and wheel peripheral acceleration criteria. The explanation of the tire moment criterion performance is already known, but yet it is not clear why the performance of the combined slip and wheel peripheral acceleration criterion is deteriorated to this extend, and in the same time, if the slip and the wheel peripheral acceleration are used as separate criteria, the performance is better.

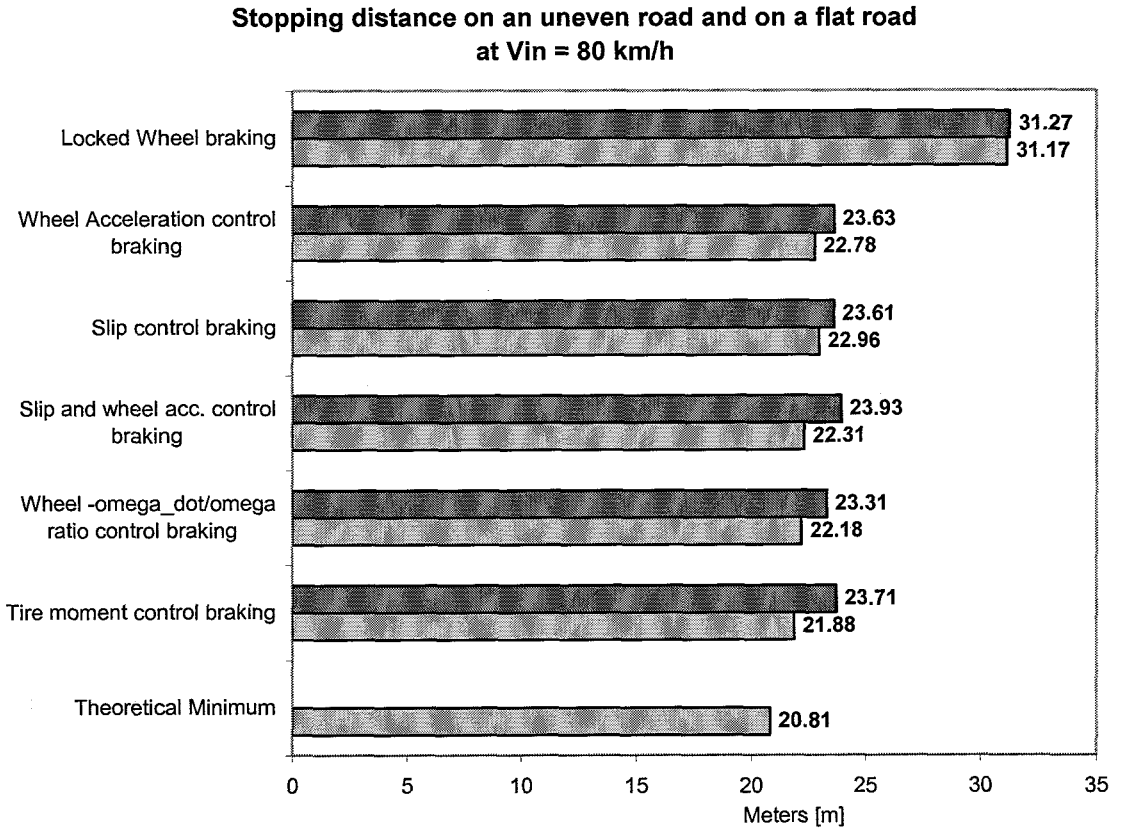

Figure 16.2: *Comparison between the results obtained by utilizing different control signals. The results are presented in groups of two bars. The top bar corresponds to an uneven road, and the lower bar to a flat road. Conditions: V_{in} =80 km/h, dry asphalt, tire type – 205/60 R15, brake torque rate of increase R1=19000 Nm/s, modulated R1=2533 Nm/s, brake torque rate of decrease R2=19000 Nm/s.*

16.2. Recommendations

In order to improve the braking performance further study of the wheel lock criteria and braking algorithms is necessary.

The stopping distance can be further reduced to some extend by introducing dynamic threshold levels instead using fixed values. This is valid for all acceleration thresholds as well as for the ratio $\dot{\Omega}/\Omega$. All of the mentioned variables are velocity dependent to lesser or greater extend, so dynamic correction of the threshold values will contribute to the optimal choice of the variable. One possible way of doing this is the look-up table correction. Of course this approach requires extensive experiments for the data collection, but on this stage it will also contribute to the better understanding of the nonlinear process of braking.

Suggestion for possible approximation in the threshold value estimation of the wheel angular deceleration is presented below. This approximation links the wheel angular deceleration $\dot{\Omega}$ with the following variables: the rate of brake torque change R_1, wheel angular velocity Ω, the normal load of the tire $F_{z,c}$, the loaded tire radios r_{load}, the peak value of the friction coefficient $\mu_{x,p}$ and its corresponding value of the slip κ_p.

$$\dot{\Omega}_p = \frac{\Omega \cdot R_1 \cdot \kappa_p}{\mu_{x,p} \cdot F_{z,c} \cdot r_{load}} \quad [\mathrm{rad/s^2}] \tag{16.1}$$

So Equation (16.1) gives an approximation of the value of the wheel angular deceleration Ω_p at which a maximum of the longitudinal force $F_{x,c}$ *is expected*

Another suggestion is to investigate an algorithm to correct for the brake torque in the current braking cycle on base of its mean value from the previous braking cycle. The idea is suggested after investigation of the brake torque variations in Figures 14.11a, 14.9a, 14.7a and 14.5a. Of course a similar pattern of the T_b is noticed for the initial velocities of 40 km/h and 60 km/h. From the investigated plots, is evident that T_b variations are about the desired value of the braking torque, which value correspond to the maximum of the tire moment $M_{y,r\,corr}$. For some of the criteria T_b converges with the time to a certain value. If the mean value of the brake torque from a previous braking cycle is used as reference for T_b in the current cycle it might help for faster convergence to a desired value.

17. References

[1] I. Besselink, *Vehicle Dynamics*, Lecture Notes, Eindhoven University of Technology, 2003.

[2] T. Birch, (1990), *Automotive Braking Systems*, 2nd edition Harcourt Brace College Publishers, 1995, ISBN 0-03-010657-5

[3] Delft Tyre -*Tyre models user Manuel*, TNO Automotive, Delft, The Netherlands, May 2002.

[4] R. Guntur, *Adaptive Brake Control Systems*, PhD Thesis, Delft University of Technology, The Netherlands, WTND no.70, 1975.

[5] M. Hoffmann, E. Fischer and B. Richter, *The incorporation of tire models into vehicle simulations*,1st international colloquium on Tyre Models for Vehicle Dynamic Analysis, Delft, The Netherlands, October 21-22, 1991,Vehicle System Dynamics, Vol. 21 supplement, 1993,pp. 49-57.

[6] P. van der Jagt, H.B. Pacejka and A.R. Savkoor, *Influence of tyre and suspension dynamics on the braking performance of an anti-lock barking system on un even roads*, Proceeding of 2nd international EAEC Conference on New Developments in Powertrain and Chassis Engineering, IMechE C382/047, Strasburg, France, June 14-16, 1989, pp. 453-460

[7] R. Johansson, A, Rantzer, *Nonlinear and Hybrid Systems in Automotive Control*, Springer, Great Britain 2003, ISBN 1-85233-652-8

[8] R. Jurgen, *Automotive Electronics Handbook*, McGraw-Hill, 1994, ISBN 0-07-033189-8
U. Kiencke, L. Nilsen, *Automotive Control Systems*, SAE, Springer, 2000, ISBN 3-540-66922-1

[9] B.de Kraker, D.van, Campen, *Mechanical vibrations*, Shaker Publishing, The Netherlands, 2001, ISBN 90-423-0165-1

[10] R. Limpert, *Brake Design and Safety*, SAE, 1999, ISBN 1-56091-915-9

[11] W. Matschinsky, *Road Vehicles Suspension*, translation by Alan Baker, Professional Engineering Publishing Limited, Suffolk, United Kingdom, 2000, ISBN 1-86058-303-8.

[12] *MF-Tyre, MF-MCTyre and SWIFT-Tyre-Installation and Users manual for Matlab/Simulink,* TNO Automotive, Delft, The Netherlands, April 2003.

[13] H. B. Pacejka, *Tyre and Vehicle Dynamics*, Butterworth-Heinemann, Oxford, 2002 ISBN 0-7506-5441-5R.

[14] H. Pacejka, I. Besselink, *Magic Formula Tyre Model with Transient Properties*, Vehicle Dynamics supplement Vol. 27, Swets & Zeitlinger Publishers, ISBN 90-256-1488-31997

[15] Robert Bosch GmbH, *Driving-safety systems* 2nd edition, SAE, Imprime en Allemagne,Germany, 1999,
ISBN 0-7680-0511-6

[16] SAE, *Anti-Lock Braking Systems for Passenger Cars and Light Trucks – A Review*, PT-29, Selected papers through 1986, SAE, 1987, ISBN 0-89883-117-2

[17] M. Satoh and S. Shiraishi, *Excess operation of Antilock Brake System on a Rough Road,* Honda R & D Company Ltd., Japan, Paper C18/83 - Braking of Road Vehicles, 1983, pp. 197-205

[18] J.Y. Wong, *Theory of Ground Vehicle*, 3th edition, John Wiley& Sons, 2001, ISBN 0-471-35461-9

[19] P.W. Zegelaar, *The dynamic response of tyres to brake torque variations and road unevenness*, PhD Thesis, Delft University of Technology, The Netherlands, 1998,
ISBN 90-370-0166-1

[20] Parts of the DELFT-TYRE product line: *MF-Tool, MF-MCTool, MF-Tyre, MF-MCTyre & SWIFT-Tyre* developed at TNO Automotive, Delft, The Netherlands.

[21] H.-J. Unrau, J. Zamow
TYDEX-Format, *Description and Reference Manual, Release 1.1*, Initiated by the International Tire Working Group, July 1995.

[22] A. Riedel, *Standard Tire Interface-STI, Release 1.2,* Initiated by the Tire Workgroup, June 1995.

Appendix – A

Axis Systems

A.1. W-Axis System

SWIFT-Tyre [1] conforms to the ***TYDEX STI*** conventions described in the ***TYDEX-Format*** [2] and the *Standard Tire Interface* [2]. Two **TYDEX** coordinate systems with ISO orientation are particularly important. The *C*- and *W*-axis systems are shown in Figure A.1.

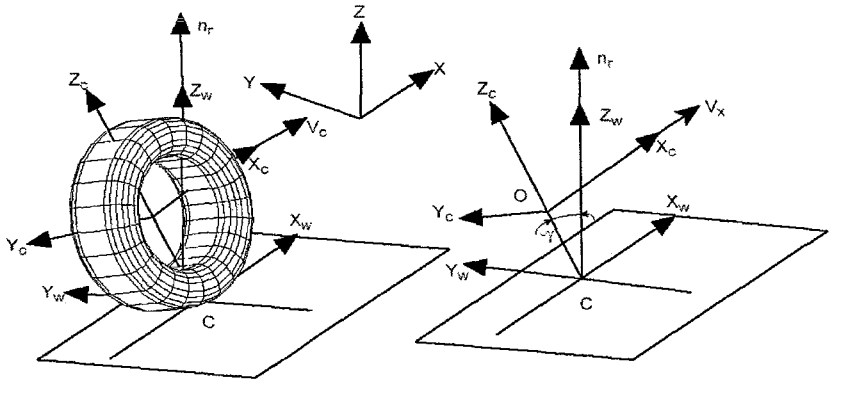

Figure A.1: *TYDEX C- and W-Axis systems used in SWIFT-Tyre, according to TYDEX*

The *c*-axis system is fixed to the wheel carrier with the longitudinal x_c-axis parallel to the road and in the wheel plane (x_c-z_c-plane). The origin O of the *c*-axis system is the wheel center. The origin of the W-axis system is the road contact-point ***c,*** i.e. the intersection of the wheel plane, the plane through the wheel spindle and the road tangent plane. The orientation of the W-axis system agrees to ISO. The forces and torques calculated by ***SWIFT-Tyre***, which depend on the vertical wheel load F_z along the z_w-axis and the slip quantities, are related to the W-axis system. The x_w-y_w-plane is the tangent plane of the road in the contact point *c*. The camber angle is defined as the inclination angle between the wheel plane and the normal n_r to the x_w-y_w- plane.

A.2.The Contact-Point c and the Normal Load

The tire is assumed to have only a single contact point *C* with the road. Furthermore, for calculating the motion of the tire relative to the road, the road is approximated by its tangent plane at the point below the wheel center (see Figure A.2). The tangent plane is an accurate approximation of the road, as long as the road radius of curvature is not too small (that is, not smaller than 2 meters).
The tire-road contact forces mainly depend on the tire mechanical properties (that is, stiffness and damping), the road condition (that is, the friction coefficient between tire and road, the road structure), and the motion of the tire relative to the road (that is, the amount and direction of slip).
Major forces and moments on a vehicle arise from the contact of the tires with the road. The vertical loads transfer the weight of the vehicle to the road. Due to the compliance of the tires, a vehicle is cushioned against disturbances by small road irregularities. The traction and braking forces arise from the longitudinal tire forces. Lateral forces are required to control the direction of travel of the vehicle. Proper description of the dynamic

behavior of a vehicle requires an accurate model of the tire-road contact forces and moments under various conditions.

Table A.1: *General Definitions*

Term	*Definition*
Inertial coordinate system	Inertial space according to ISO
Road tangent plane	Tangent plane to the road in *c*
Wheel center O	Center of the wheel
C axis system	Coordinate system fixed to the wheel carrier at the Wheel center orientation according ISO.
Wheel plane	The plane, formed by the wheel when it is considered a rigid disc with zero thickness.
Contact point *c*	Contact point between tire and road, defined as the intersection of the wheel plane and the projection of the wheel axis onto the road plane.
W-axis system	Coordinate system at the tire contact point *c*, orientation according ISO.

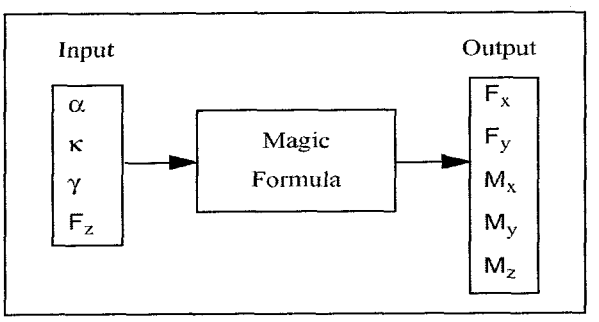

Figure A.2: *Input and output variables of the magic formula tire model. The model outputs forces and moments for both the contact point* **c** *and the wheel center.*

Figure 3.3 presents the input and output vectors. In this diagram the tire is assumed to be uniform and to move over a flat road surface. The input vector results from motions of the wheel relative to the road.
The forces and moments are output quantities of the tire model. They are assumed to act on a rigid disc with the inertial properties of the undeflected tire. The forces may differ from the corresponding forces acting on the road due to the vibrations of the tire relative to the wheel rim. Braking and traction torques are considered as acting on the rotating disc. For more detailed explanation on the SWIFT model refer to [ ] and Section 5.

Table A.2: *Input and output variables of the magic formula tire in plain model in the contact point* ***c.***

Input Variables		**Output Variables (in contact point *c*)**	
Longitudinal slip κ	[-]	Longitudinal force $F_{x,c}$	[N]
Slip angle $\alpha = 0$	[rad]	Lateral force $F_{y,c}$	[N]
Camber angle $\gamma = 0$	[rad]	Overturning couple $M_{x,c}$	[Nm]
Normal wheel load $F_{z,c}$	[N]	Rolling resistance torque $M_{y,c} = 0$	[Nm]
		Aligning torque $M_{z,c}$	[Nm]
Basic Tire Parameters			
Nominal (rated) load F_{z0}		[N]	
Unloaded tire radius r_0		[m]	
Tire belt mass m_{belt}		[kg]	

A.3. Units

Next to the convention to the **TYDEX** W-axis system, all units of the parameters and variables in ***SWIFT-Tyre*** are SI units.

Appendix – B

SWIFT-Tyre with Standard Tyre Interface

Calculates tire forces and moments in the wheel carrier using SWIFT [3,20,21,22].

B.1. Inputs:

- **road:** In SWIFT-Tyre, the road profile must be given in an ASCII file when the check box 'Effective inputs' is selected. In the road property file the road height is specified as a function of traveled distance. The left and right track data may be different; the appropriate track data is selected depending on the role of the tire in the model. SWIFT uses a zero-order sample and hold when evaluating the road profile. For accuracy reason it is important that the sample points coincide with the data provided by the user, otherwise interpolated data will be used. So one should use road data with a fixed sample interval and specify this value for ROAD_INCREMENT in the [MODEL] section of the tire property file. Typically, the road sample interval should be in the range of 0.1-0.2 meters or larger
- **dis:** a vector with the x, y and z-coordinate of the wheel carrier in the global axis system.

- **tramat:** a vector with nine components to specify the transformation from wheel carrier axis system to the global axis system. Tramat (1..3) gives the matrix representation in the global frame of the unit vector along the local x-axis of carrier position. The same applies to tramat(4..6) being the local y-axis and to tramat(7..9) for local z-axis.

- **angtwc** (1): rotation angle of the wheel with respect to the wheel carrier about the wheel spin axis. vel (3): a vector with three components: the global velocity of the wheel center expressed in the wheel carrier local frame.

- **omega :** three components of the global angular velocity of the wheel centre expressed in the wheel carrier local frame (x, y and z component).

- **omegar:** a vector of the relative angular velocity of the wheel with respect to the wheel carrier about the wheel spin axis.

B.2. Outputs:

- **force:** the three components (in the wheel carrier frame) of the force, exerted by the tire on the rim at the wheel center.

- **torque:** matrix containing moments applied by the tyre onto the rim at the centre of the wheel, expressed in the carrier axis system. Torque as three components representing the moments in the x, y and z direction

- **varinf:** array containing 40 extra output variables on tyre behavior. The digit in brackets denotes the number of the parameter column in the *varinf* matrix

Most important ones:

- varinf(1): slip angle
- varinf(2): longitudinal slip
- varinf(3): camber angle
- varinf(4..9): Fx, Fy, Fz, Mx, My, Mz at the tyre contact point
- varinf(10): tyre deflection
- varinf(11): deflection velocity, normal to the ground
- varinf(12): effective rolling radius
- varinf(13..15): x, y, z coordinate of the contact point center
- varinf(16..18): x, y, z component of the normal to the road
- varinf(19): longitudinal relaxation length
- varinf(24): longitudinal slip velocity Vsx
- varinf(26): wheel forward velocity Vx

The complete definition of the *varinf* -array is presented in the Table B.1

Table B.1: *Definition of VARINF -array*

Num.	Description	Num.	Description
1	Slip angle (steady state definition)	21	Friction coefficient x
2	Longitudinal slip (steady state definition)	22	Friction coefficient y
3	Camber angle	23	Not used
4	Longitudinal force Fx in contact point	24	Longitudinal slip velocity Vsx
5	Lateral force Fy in contact point	25	Lateral slip velocity Vsy
6	Vertical force Fz in contact point	26	Wheel forward velocity Vx
7	Overturning moment Mx in contact point	27	Derivative of longitudinal deformation du/dt
8	Rolling resistance moment My in contact point	28	Derivative of lateral deformation dv/dt
9	Self aligning moment Mz in contact point	29	Longitudinal slip (used in Magic Formula evaluation)
10	Radial deflection	30	Slip angle (used in Magic Formula evaluation)
11	Deflection velocity (normal to ground)	31	Pneumatic trail
12	Effective rolling radius	32	Residual moment Mz
13	x-coordinate contact point position (global frame)	33	Moment arm of Fx
14	y-coordinate contact point position (global frame)	34	Gyroscopic moment Mz
15	z-coordinate contact point position (global frame)	35	Braking induced plysteer force
16	x-component of the normal to the road (global frame)	36	Distance traveled
17	y-component of the normal to the road (global frame)	37	Effective plane height
18	z-component of the normal to the road (global frame)	38	Effective plane angle
19	Longitudinal relaxation length	39	Effective plane curvature
20	Lateral relaxation length	40	Contact length

B.3. Parameters:

Tyre ID is an integer value identifying the tyre block. This number will be printed when messages related to the tyre block are printed. Please take care that the numbers within 1 model are unique. In case effective inputs is used the following applies: Odd tyre id's will use the left track data in the data file while even tyre id's will use the right track data from the given data file.

Use mode defines the operating mode of the tyre block. See Table 3 of section 2.5.1.

Table B.3: *Definition of USE_MODE*

operating mode	SWIFT
vertical spring only	20
longitudinal only (Fx ,My)	21
lateral only (Fy, Mx, Mz)	22
uncombined (Fx, Fy, Mx, My, Mz)	23
combined (Fx, Fy, Mx, My, Mz)	24 (default)
mirroring of lateral characteristics	Multiply USE_MODE with -1
swift statics	add 100 to positive USE_MODE or negate USE_MODE and subtract 100

- ***Tyre property file*** is the file name of the tyre property file (absolute or relative to current working directory)
- ***Road*** enables to choose road input via file (Data file (effective inputs)) or as flat road (external inputs (smooth road).).
- ***Road data file*** contains the file location (absolute or relative to current working directory)

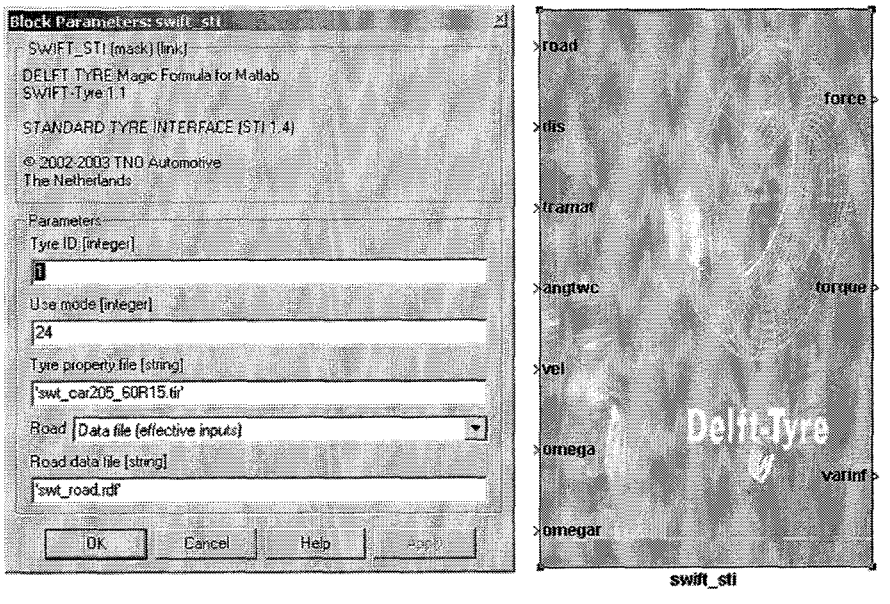

Figure B.1: *View of the* ***Block Parameters*** *of the SWIFT - STI*

B.4. General notes:

- All calculations are made using SI-units (m, rad, N, kg, s)
- The ISO sign convention is adopted for the definitions of slip and tire forces

Appendix – C

Printout of an example script file for model initial conditions setting.

```
m2 = 300;        % Quarter of the vehicle body mass - [kg].
m1= 35;          % Mass of the axle, rim, brakes ... and all associated parts [kg]
Ip = 0.95;       % Polar moment of inertia of the rotating parts [kg*m^2]
cz = 2000;       % Suspension damping in vertical direction [N*s/m]
kz = 20000;      % Suspension stiffness in vertical direction [N/m]
cx = 2000;       % Suspension damping in horizontal direction [N*s/m]
kx = 100000;     % Suspension stiffness in horizontal direction [N/m]
Vin = 80/3.6;    % Initial vehicle velocity [m/s]
r_eff = 0.3056;  % Effective rolling radius of the loaded tire [m]
ro = 0.3135;     % Unloaded radius of the tire [m]
Om_in = Vin/r_eff;  % Initial angular tire velocity [rad/s]
Z10 = ro - 9.81*(m1+m2+mb)/200000;  % Initial Z-position of the axle global
coordinates[m]
Z20 = (Z10+(-9.81*m2/kz));  % Initial Z-displacement of the vehicle body [m]
X10 = 0;         % Initial X-displacement of the axle [m]
X20 = 0;         % Initial X-displacement of the vehicle body [m]
```

Appendix – D

D.1. The Magic Formula model

The Magic Formula is the essence of an empirical tire model. Such models are based on the mathematical representation of measured tire data, rather than modeling the tire structure itself. Empirical tire models are usually used in full vehicle simulations. The tire forms only a part of the entire simulation model and the computational load of that part in the model should be fairly low. The development of the Magic Formula started in the mid-eighties. The first version developed by Edbert Bakker and professor Pacejka. Since then several versions have been developed. All versions show the same basic form for the pure slip characteristics: a sine of an arctangent. The Magic Formula for longitudinal slip reads:

$$F_x = D \cdot \sin\left[C \cdot \arctan\left\{B(\kappa + S_h) + E(\arctan(B(\kappa + S_h)) - B(\kappa + S_h))\right\}\right] + S_V$$

Where F_x stands for the longitudinal force and κ denotes the longitudinal slip. The coefficients *B, C, D* and *E* together with the offsets S_h and S_V characterize the shape of the slip characteristics. Each coefficient represents a specific aspect of the slip characteristic: the shape factor C influences the overall shape of the characteristic, the peak factor *D* influences the maximum value of the haracteristic, the curvature factor *E* influences the characteristic around the peak value, and the slip stiffness *K (= BCD)* influences the slip stiffness at low values of slip. The coefficients of the Magic Formula depend on the vertical load. Dimensionless parameters *p* are introduced to describe this influence:

shape factor $C = p_{C1} \cdot \lambda_C$ (D1)

peak factor $D + \mu \cdot F_Z$ (D2)

friction coefficient $\mu = (p_{D1} + p_{D2} \cdot df_Z) \cdot \lambda_\mu$ (D3)

curvature factor $E = (p_{E1} + p_{E2} \cdot df_Z + p_{E3} \cdot df_Z^2) \cdot \{1 - p_{E4} \operatorname{sgn}(\kappa + S_h)\} \cdot \lambda_E$ (D4)

slip stiffness $K = F_Z \cdot (p_{K1} + p_{K2} \cdot df_Z) \cdot \exp(-p_{K3} \cdot df) \cdot \lambda_K$ (D5)

stiffness factor $B = \dfrac{K}{C \cdot D}$

horizontal shift $S_h = (p_{h1} + p_{h2} \cdot df_Z) \cdot \lambda_h$

vertical shift $S_V = F_Z \cdot (p_{V1} + p_{V2} \cdot df_Z) \cdot \lambda_V \cdot \lambda_\mu$

The relative offset df_z of the vertical load is introduced in Equations (D1):

$$df_Z = (F_Z - F_{Z0}) / F_{Z0} \quad \text{(D6)}$$

Furthermore, this equation introduces six scaling factors λ_C, λ_μ, λ_E, λ_K, λ_h, λ_V, to scale the formula without changing the parameter values. In this way the influence of several important factors can be investigated easily.
In the most recent version of Magic Formula [14] all coefficients and parameters have subscripts to discriminate between the characteristics of longitudinal force,

lateral force or self-aligning torque. In this thesis only the longitudinal tire behavior is considered and no subscripts are used to designate other characteristics

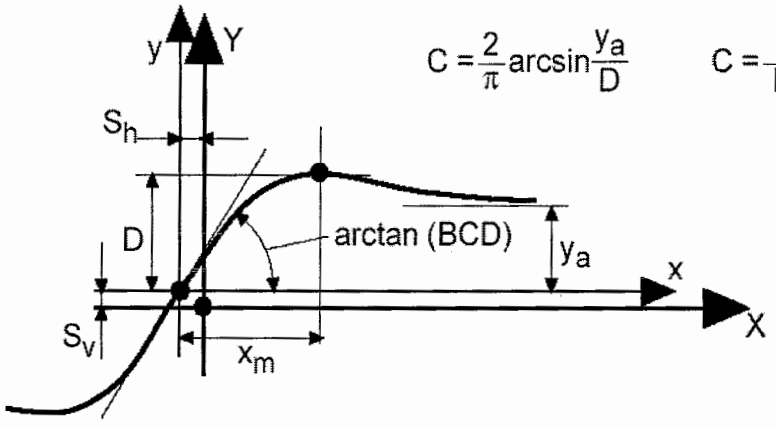

$$C = \frac{2}{\pi}\arcsin\frac{y_a}{D} \qquad C = \frac{Bx_m - \tan(\pi/2C)}{Bx_m - \arctan(Bx_m)} \quad (C>1)$$

The main advantage and disadvantage of the Magic Formula model: it gives an accurate representation of measured data but needs the values of certain parameters.

Appendix – E

E.1 Generator development

The *Generator* is synthesized for this application. The main elements are two timers (see Figure E.1). The *Timer R1* defines the time TO when the valve is open and the *Timer R2* forms the time TC when the valve is closed. To reduce the rate of torque increase the time TO is shorter than the time TC. The both timer starts simultaneously by active signal "1"applied at the *Generator* input *In*. The *Time elapse* output changes from zero to one (boolean values) when the preset time elapses. The inlet valve closes when "1" applied to its input.

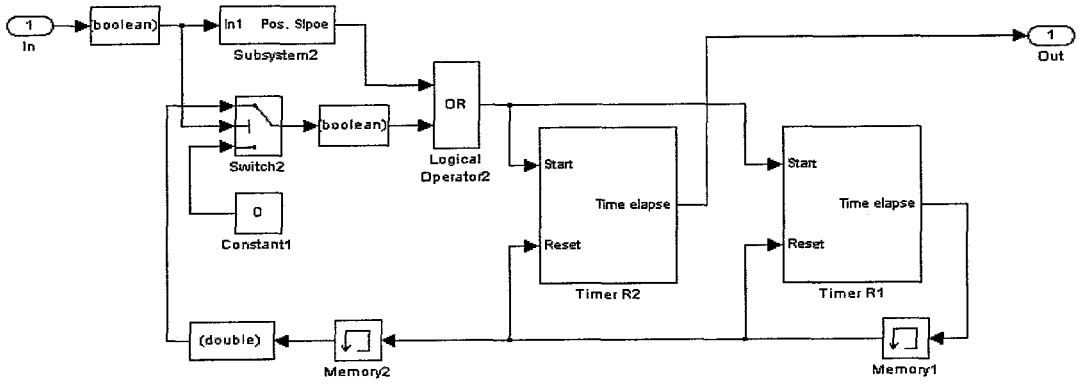

Figure E.1: *Layout of the Generator controlling the inlet valve to produce step brake torque increase*

Until the active signal is available at the *In* input the *Switch 2* closes the loop: *Time elapse* output of *Timer R1*, memory elements one and two, through the *OR* logical operator, to the *Start* inputs of the timers. This loop configuration allows the *Timer 2* output *Time elapse* to self-reset and restarts the timers again each time after the TC time elapse. The generation stops if the active signal at the *In* input changes to zero, than the *Switch 2* breaks the loop and applies zero to the *OR logical operator*. Description of the developed Timer block is given in the next paragraph.

E.2 Timer development

The requirements to of the desired Timer are specified in Table 4

Table E.1: *Timer requirements.*

	Name	Description
Input	1. Start	Pulse which starts the timer
	2. Reset	Pulse which resets the timer
	3. Set time period	Possibility to set a time period. Timer starts and after the preset time period the timer will produce a signal through the time elapse output.
Output	2. Set Time	Outputs the value of the set time period.
	3.Time elapse	Generates a high signal after the set time period expires.

The core of the developed timer consists of the *Integrator*. The input of the integrator is connected to the output of the condition *Switch 2*. See Figure E.2. Until the signal level at the *Switch 2* conditional input is lower than 1 the integrator input is connected to the zero

value of *Constant 1* block and the output of the integrator is zero. The conditional input of the *Switch 2* through the *Switch 1* is connected to the Q output of the input flip-flop.
With this configuration the active signal at the *Start* input will cause switching of the *Switch 2* and interconnection of the *Integrator* input to the value of the *Constant 2* block. By integrating the value of one the integrator output grows progressively in time. The growth of the integrator output is compared with the preset value *TON* (the value of the *Set Time period,* see Table E.1).
When the integrator output value equals the TON value (compared by *Relational Operator*), active signal is applied to the conditional input of the *Switch 1*. This will reconfigure the switches and as a consequence the input of the integrator reconnects to the zero value of the *Constant 1*. The integrator's output value stops to grow and keeps the reached value. To reset the integrator, an active signal has to be applied at the *Reset* input. The S-R Flip-Flop is added to make the timer more stable and to reduce the quality requirements to the staring impulse.

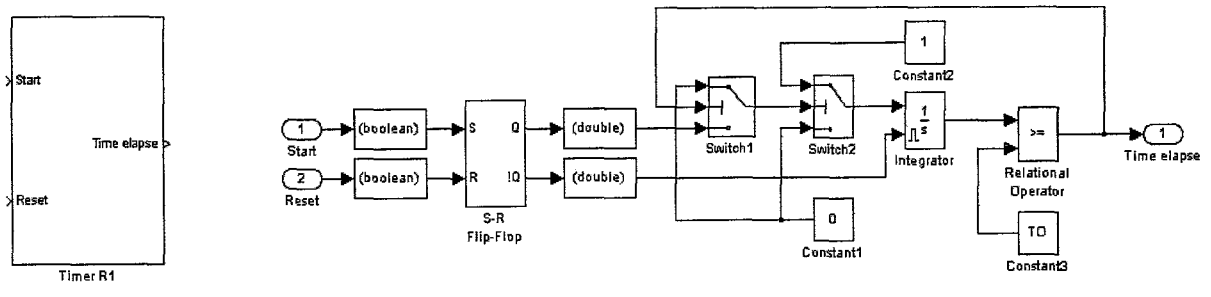

Figure E.2: *View of the Timer block and its layout.*
The developed timer block meets all the requirements posed in Table E.1.

E.2 Slope detector development

The *Slope detector* principle of operation can be described as follow. We will follow the explanation of the positive slope detection. The *Memory* block outputs the value of the input variable with delay one integration step (of the simulation). The *XOR* logical operator outputs "1" only if the two input signals differ to one another.

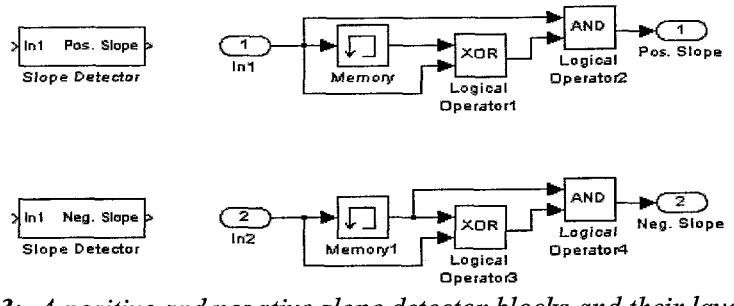

Figure E.3: *A positive and negative slope detector blocks and their layout.*

If the boolean input signal changes from zero to one and holds the one value, due to the delay (introduced by the *Memory* block) the memory input has value 1 and its output has still value 0. The two input signal of the *XOR* are different and the *XOR* outputs "1". Now the logical operator *AND* is supplied with "1" at both of its inputs and changes its output from zero to one. At the next step of integration the memory output and input are both with value 1, now the *XOR* input signals are identical and its output changes to zero. The *AND* output switches from 1 to 0 duo to the *XOR* output change. The result is pulse generated by the positive slope. The pulse-wide is one integration step.

Appendix – F

F.1. Simulation Results on Flat Road for initial velocity V_{in}=40 km/h and V_{in}=60 km/h

A simulation results are presented in form of plots of important vehicle and ABS variables. Statistical data for some of the variables are presented in tables. For each of the employed wheel lock criteria separate table provides the numerical values of the threshold levels that have been used.
For both set of simulations for initial velocities 40 km/h and 60 km/h on a flat road the results are presented in the following sequence:

- Braking without ABS control
- Peripheral wheel acceleration $\dot{\Omega}_{per}$ criteria control braking
- Wheel slip criterion control braking
- Combined slip and wheel peripheral acceleration $\dot{\Omega}_{per}$ criteria control braking
- Wheel $\dot{\Omega}/\Omega$ ratio criterion control braking
- Tire moment $M_{y,r\,corr}$ criterion control braking

At the end comparison between the utilized different wheel lock criteria and the associated stopping distances is given in tables.

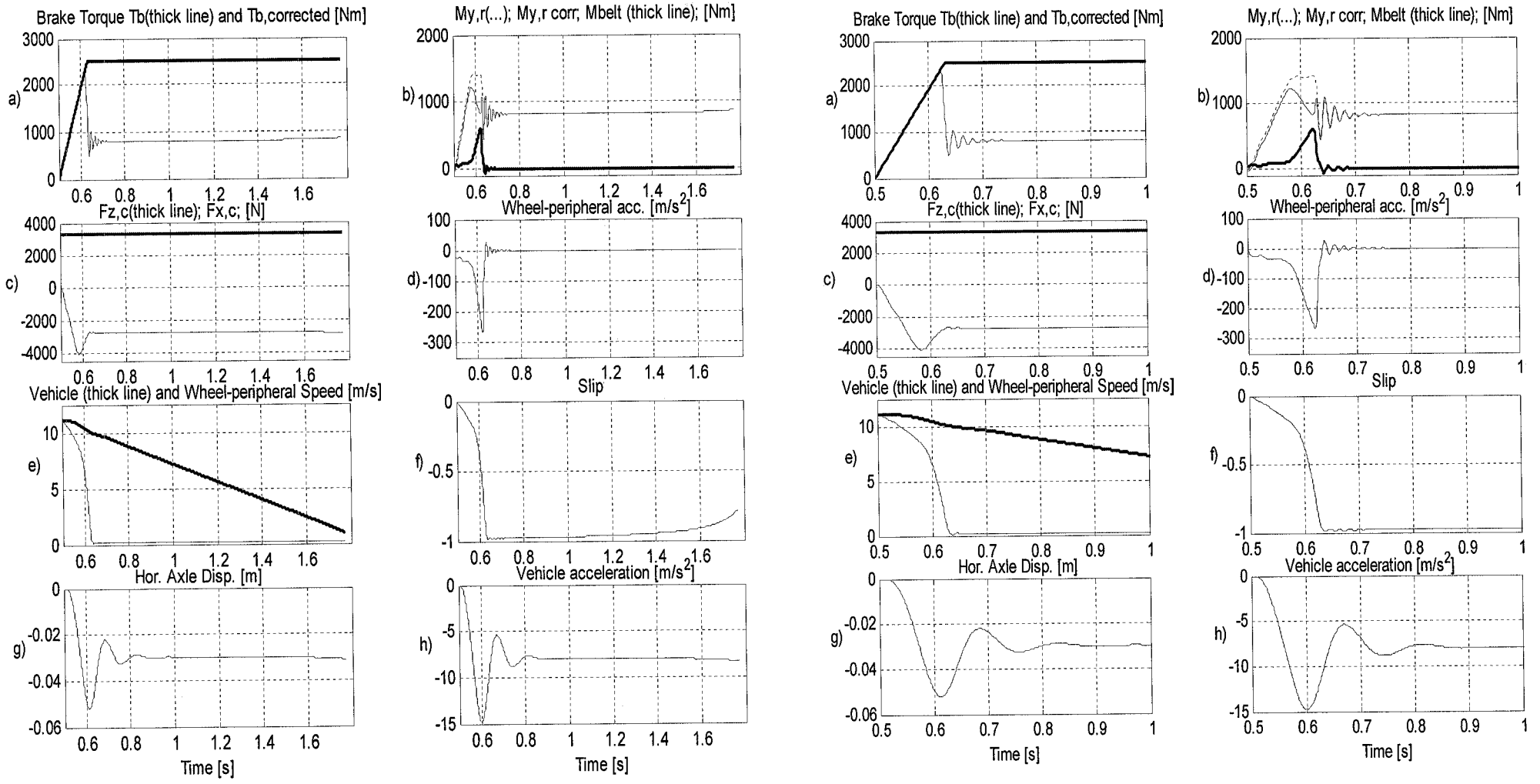

Figure F.2: *Flat road - Braking maneuver without ABS control, V_{in}=40 km/h. The right-hand side ensemble of plots shows zoom in of the time window 0.5 -1 sec. The instant of the brake maneuver initiation is t_0=0.5 sec. T_b max = 2500 Nm*

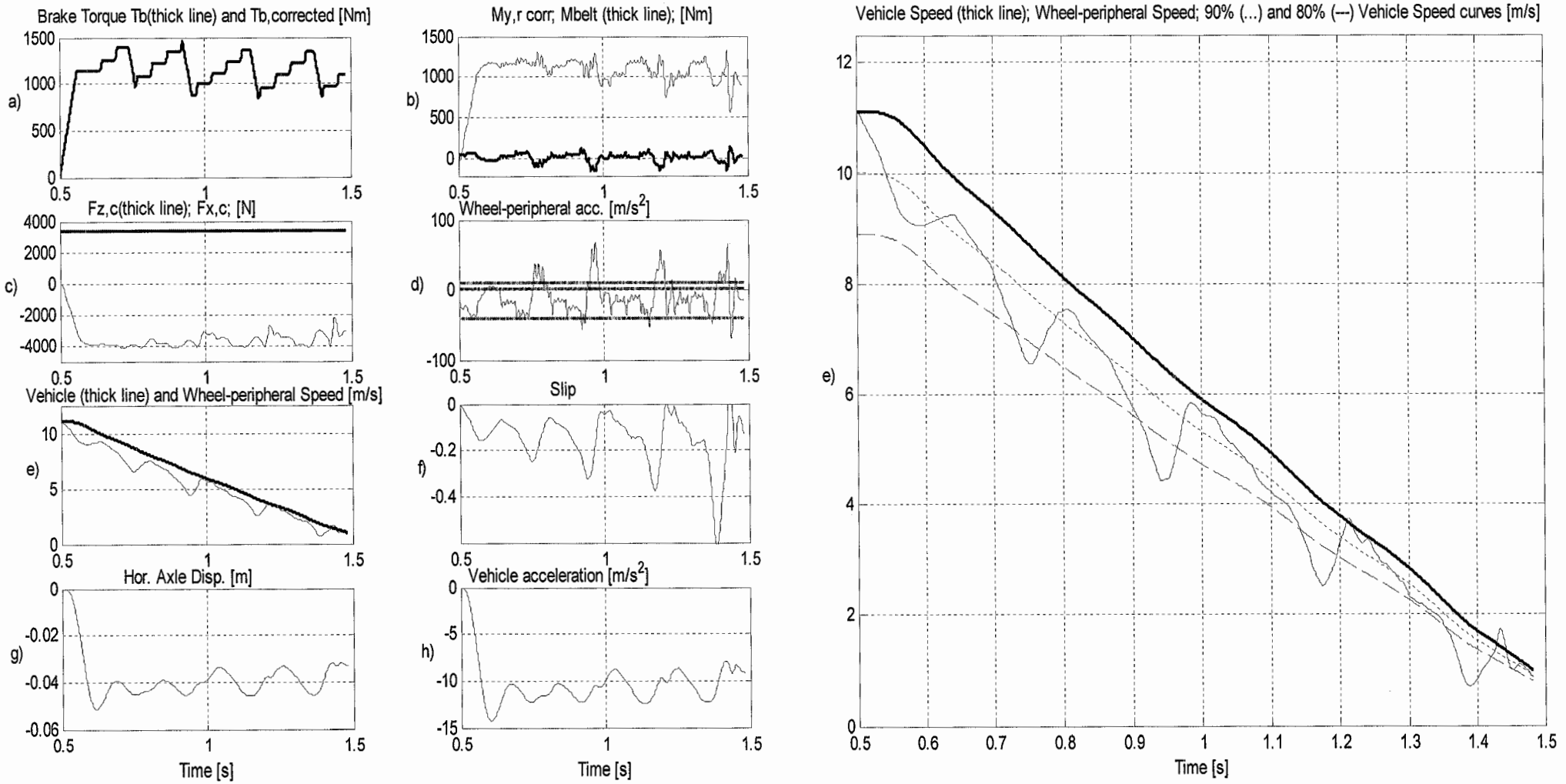

Figure F.2: *Flat road - Peripheral wheel acceleration criteria control braking, V_{in}=40 km/h.. The right-hand side shows zoom in of the sub-graph e). The instant of the brake maneuver initiation is t_0=0.5 sec. T_b max = 2500 Nm.*

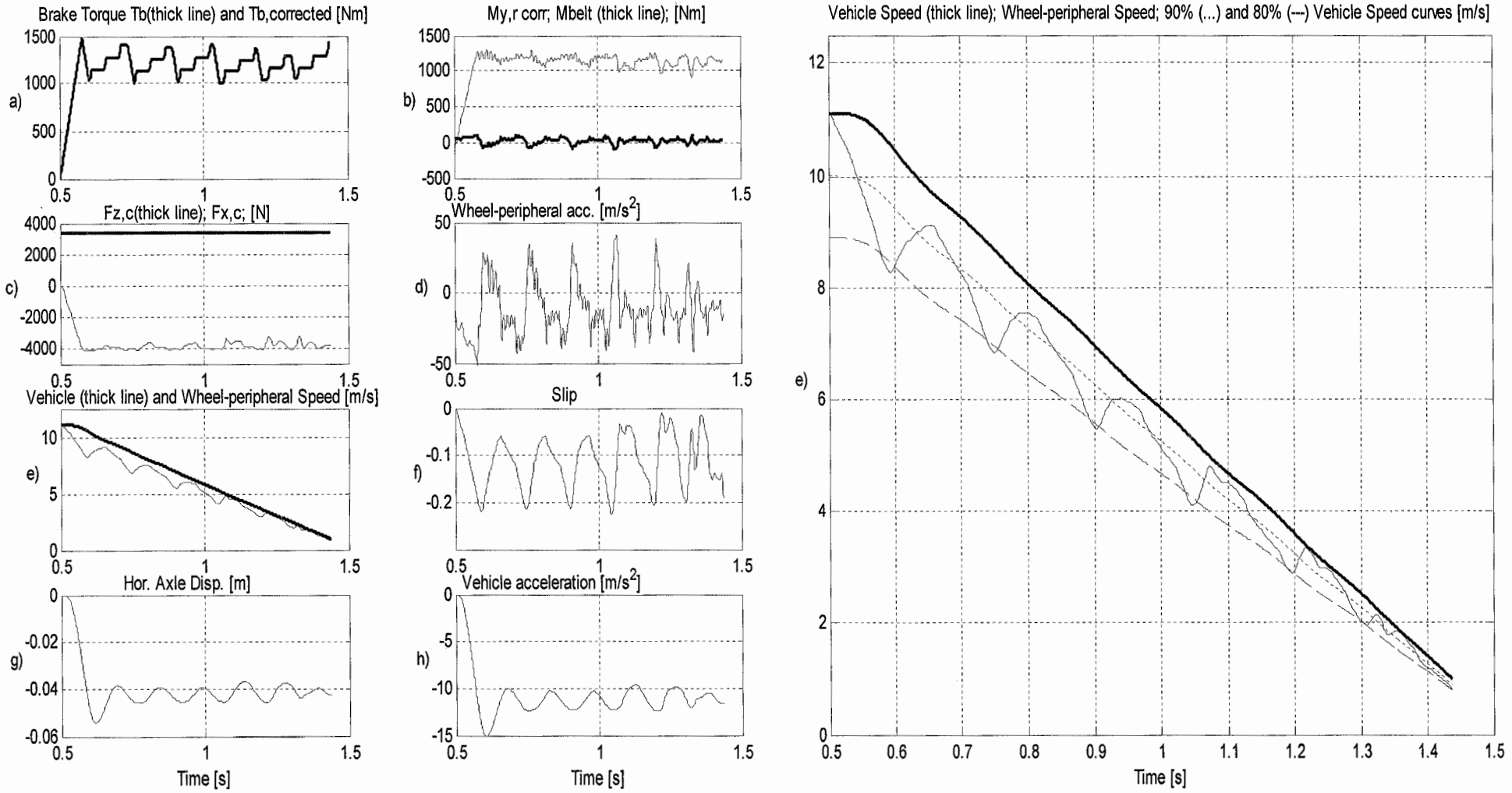

Figure F.3: *Flat road - Wheel slip criteria control braking, V_{in}=40 km/h.. The right-hand side shows zoom in of the sub-graph e). The instant of the brake maneuver initiation is t_0=0.5 sec. T_b max = 2500 Nm.*

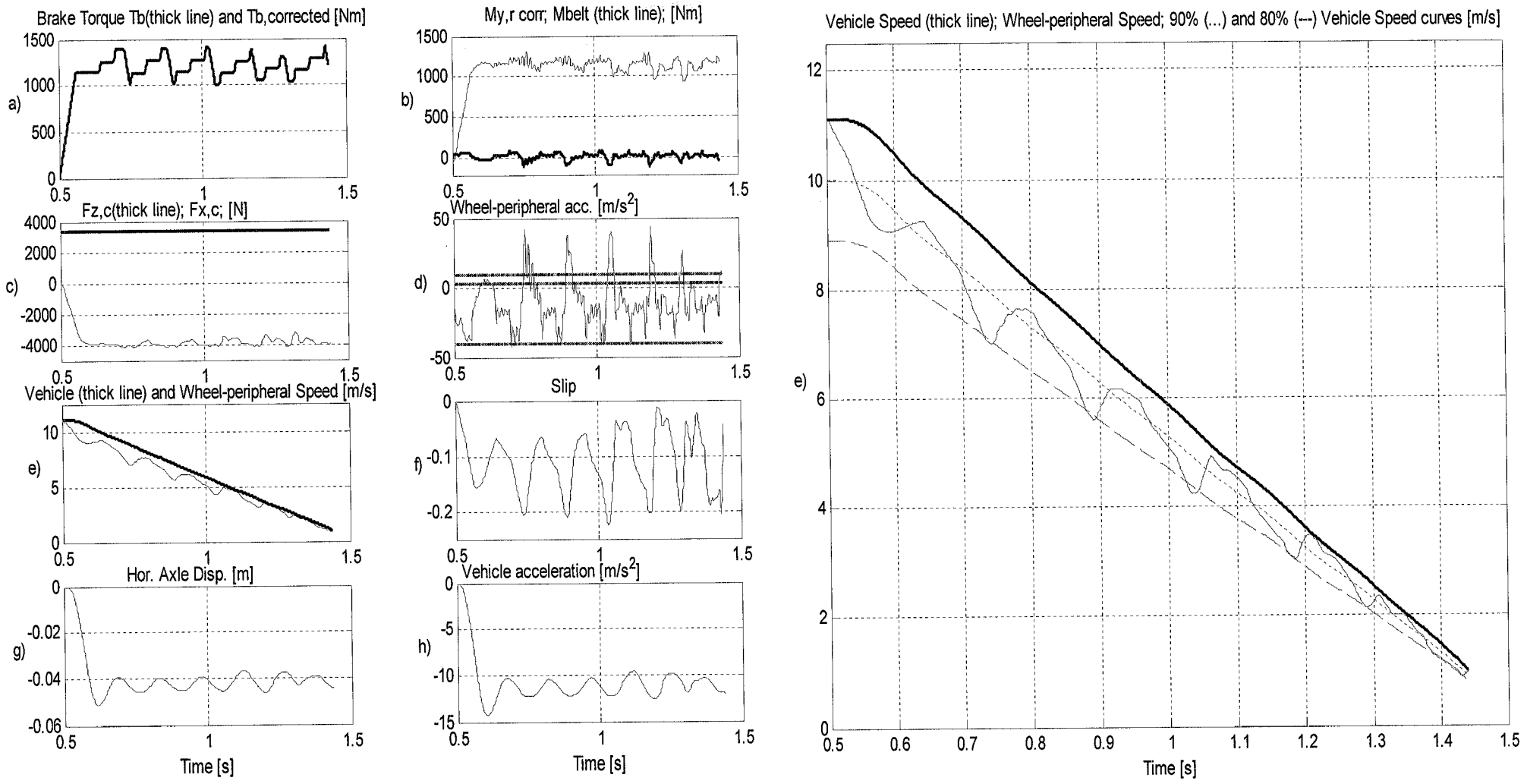

Figure F.4: *Flat road - Combined slip and wheel peripheral acceleration criteria control braking, V_{in}=40 km/h.. The right-hand side shows zoom in of the sub-graph e). The instant of the brake maneuver initiation is t_0=0.5 sec. T_b max = 2500 Nm*

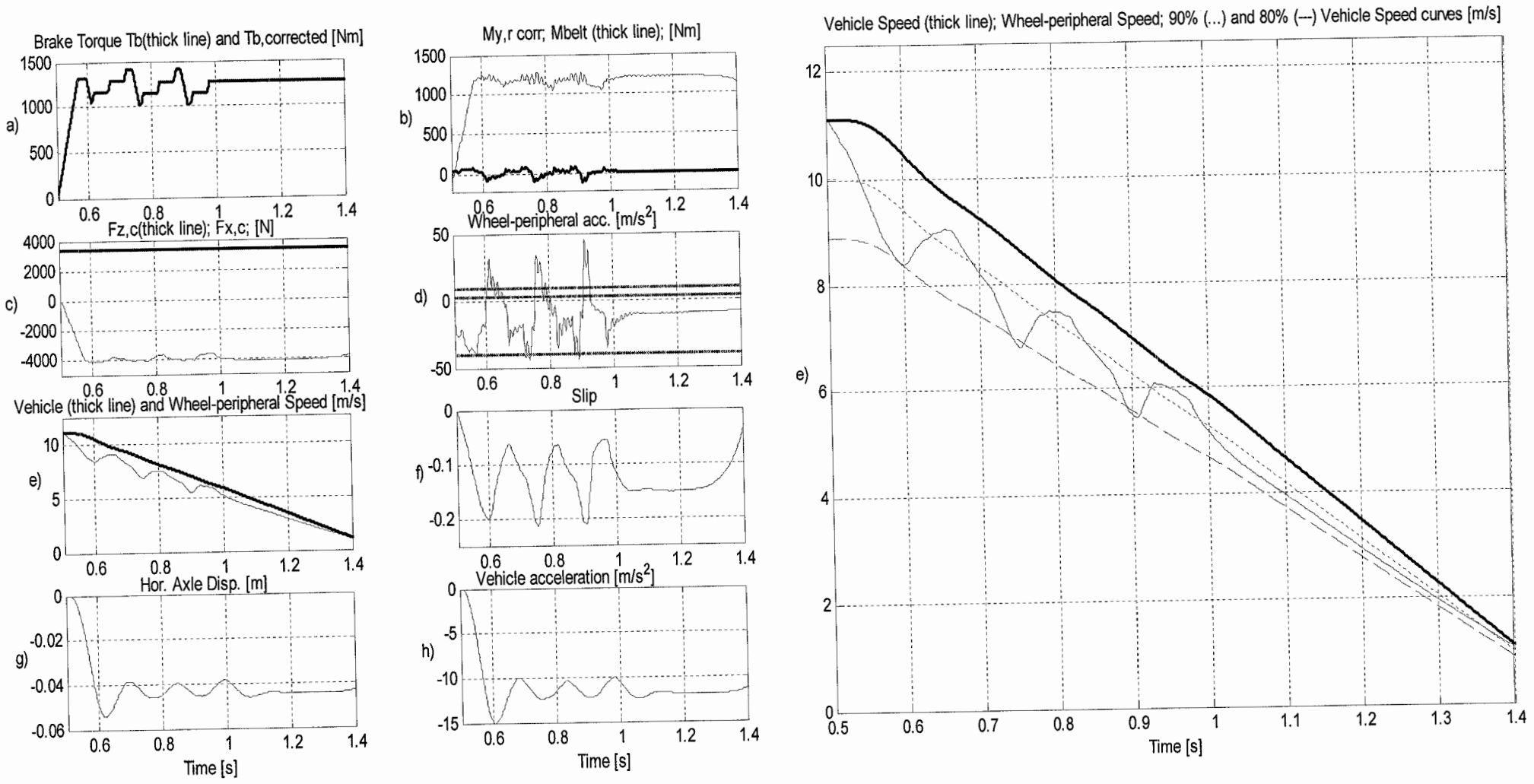

Figure F.5: *Flat road - Wheel $\dot{\Omega}/\Omega$ ratio criteria control braking, V_{in}=40 km/h.. The right-hand side shows zoom in of the sub-graph e). The instant of the brake maneuver initiation is t_0=0.5 sec. T_b max = 2500 Nm.*

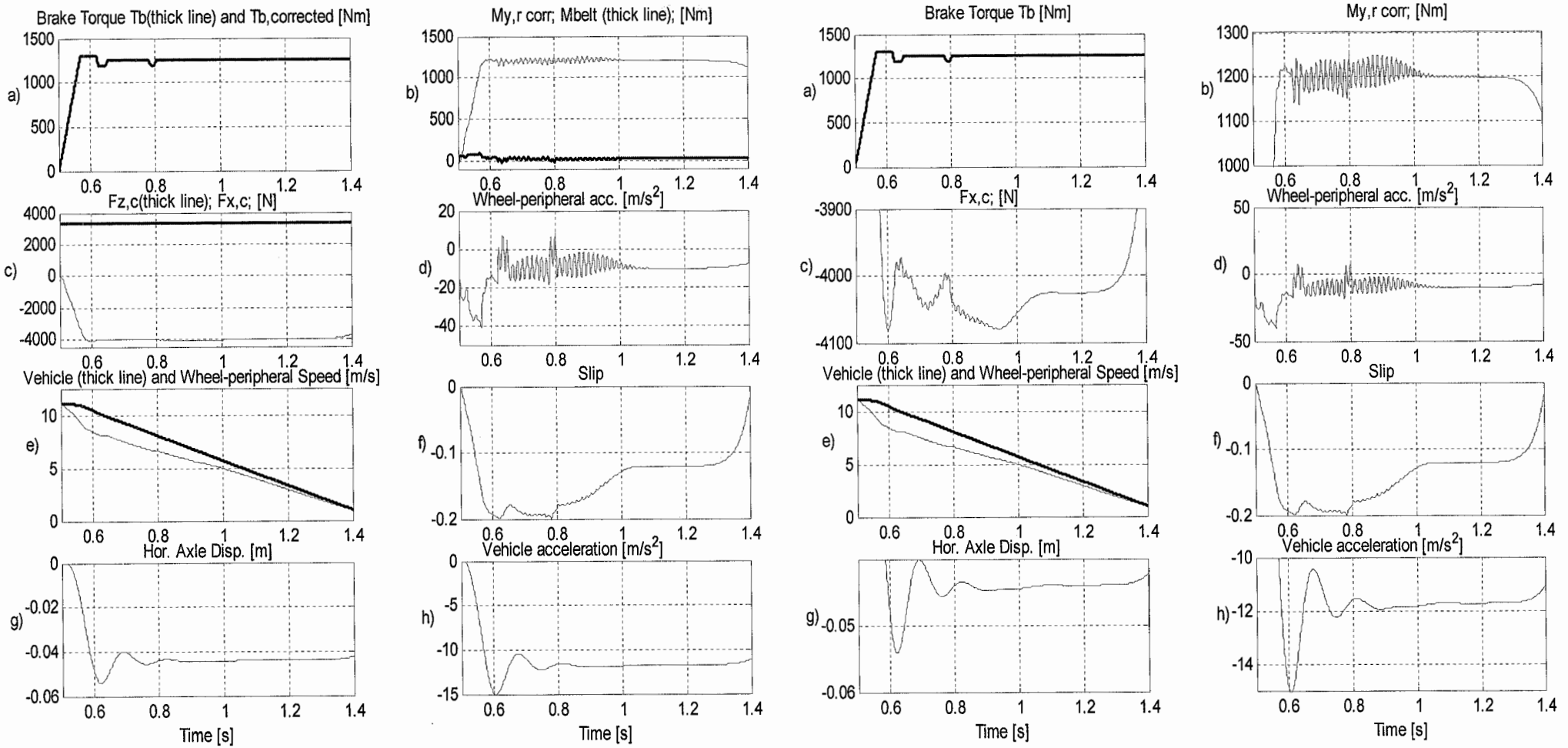

Figure F.6: *Flat road -Tire moment $M_{y,r\,corr}$ criteria control braking, V_{in}=40 km/h. The right-hand side ensemble of plots offers zoom in of the amplitudes. The instant of the brake maneuver initiation is t_0=0.5 sec. T_b max = 1300 Nm*

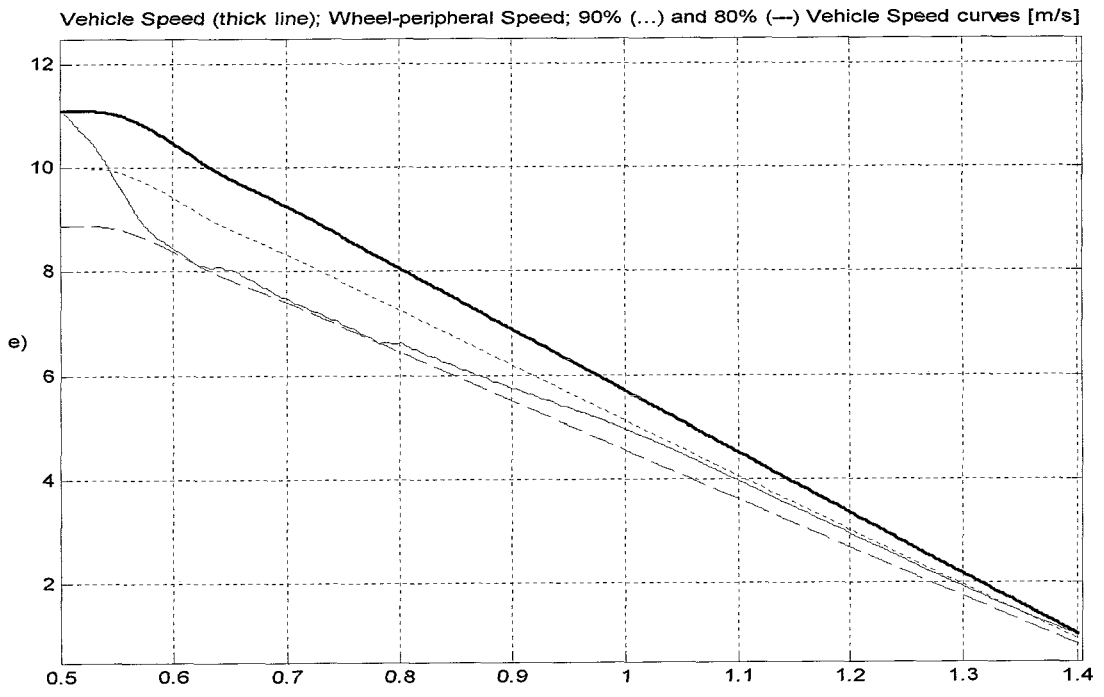

Figure F.7: *Flat road -Tire moment $M_{y,r\,corr}$ criteria control braking, V_{in}=40 km/h. The plot shows zoom in of the Figure 14.6 sub-graph window e). The instant of the brake maneuver initiation is t_0=0.5 sec. T_b max = 1300 Nm.*

Table F.1: *Flat road -Braking without ABS control, statistics data, V_{in}=40 km/h*

Parameter	Dimension	Max value	Mean value	Min value	Standard deviation
Vehicle accel.	m/s^2	-14.82	-8.39	-5.3571	1.6064
Slip	-	98.77	90.06	17.0	17.0168
$M_{y,r}$ corr	Nm	1218.2	838.6	451.4	0.0869
$F_{x,c}$	N	-4080.5	-2817.0	-2690.1	0.2707
$F_{z,c}$	N	3359.1	3356.0	3354.8	0.0004
Stopping distance from 40 km/h to 3.6 km/h [m]		7.80			
Time to reach at velocity 3.6 km/h [s]		1.27			

Table F.2: *Flat road - Peripheral wheel acceleration criteria control braking, statistics data, V_{in}=40 km/h.*

Parameter	Dimension	Max value	Mean value	Min value	Standard deviation
Vehicle accel.	m/s^2	-14.27	-10.72	-7.98	1.3829
Slip	-	61.39	14.73	-22.84	12.1362
$M_{y,r}$ corr	Nm	1328.1	1089.7	566.6	0.1289
$F_{x,c}$	N	-4082.1	-3660.3	-2196.3	0.3857
$F_{z,c}$	N	3357.1	3356.0	3354.5	0.0005
Stopping distance from 40 km/h to 3.6 km/h [m]		6.00			
Time to reach at velocity 3.6 km/h [s]		0.98			

Table F.3: *Peripheral wheel acceleration criteria control braking, V_{in}=40 km/h. Employed triggering signals and their threshold values.*

Set -1		
Command	**Triggering signal**	**Threshold value**
Hold	***- a***	-40 m/s^2
Decrease	***> Slip***	-20%
Stop Decrease	***+ a***	4 m/s^2
Increase	***A***	10 m/s^2

Table F.4: *Flat road - Wheel slip criteria control braking, statistics data, V_{in}=40 km/h.*

Parameter	**Dimension**	**Max value**	**Mean value**	**Min value**	**Standard deviation**
Vehicle accel.	m/s^2	-15.13	-11.46	-9.60	1.0981
Slip	-	22.63	11.55	1.02	5.7120
$M_{y,r\,corr}$	Nm	1300.9	1149.6	909.9	0.0701
$F_{x,c}$	N	-4080.6	-3860.7	-3250.5	0.2041
$F_{z,c}$	N	3357.1	33561	3354.9	0.0004
Stopping distance from 40 km/h to 3.6 km/h [m]		5.83			
Time to reach at velocity 3.6 km/h [s]		0.94			

Table F.5: *Employed Wheel slip criteria control braking, V_{in}=40 km/h. Employed triggering signals and their threshold values.*

Set -2		
Command	**Triggering signal**	**Threshold value**
Hold	***> Slip***	-20%
Decrease	***> Slip***	-20%
Stop Decrease	***+a***	4 m/s^2
Increase	***A***	10 m/s^2

Table F.6: *Flat road - Combined slip and wheel peripheral acceleration criteria control braking, statistics data, V_{in}=40 km/h.*

Parameter	**Dimension**	**Max value**	**Mean value**	**Min value**	**Standard deviation**
Vehicle accel.	m/s^2	-14.27	-11.3863	-9.6060	0.9416
Slip	-	22.53	11.59	1.09	5.5060
$M_{y,r\,corr}$	Nm	1311.6	1148.7	918.4	0.0709
$F_{x,c}$	N	-4080.3	-3853.6	-3169.1	0.2046
$F_{z,c}$	N	3357.0	3356.1	3354.9	0.0004
Stopping distance from 40 km/h to 3.6 km/h [m]		5.86			
Time to reach at velocity 3.6 km/h [s]		0.94			

Table F.7: *Combined slip and wheel peripheral acceleration criteria control braking, threshold values, V_{in}=40 km/h. Employed triggering signals and their threshold values.*

Set -3		
Command	**Triggering signal**	**Threshold value**
Hold	***- a*** and ***> Slip***	-40 m/s^2 and -20%
Decrease	***> Slip***	-20%
Stop Decrease	***+ a***	4 m/s^2
Increase	***A***	10 m/s^2

Table F.8: *Flat road - Wheel $\dot{\Omega}/\Omega$ ratio criteria control braking, statistics data, V_{in}=40 km/h.*

Parameter	Dimension	Max value	Mean value	Min value	Standard deviation
Vehicle accel.	m/s^2	-15.09	-11.62	-5.20	1.3208
Slip	-	21.48	13.11	1.43	4.2037
$M_{y,r\,corr}$	Nm	1283.0	1175.0	0724.6	0.0725
$F_{x,c}$	N	-4080.8	-3943.9	-2462.4	0.2264
$F_{z,c}$	N	3357.2	3356.1	3355.0	0.0003
Stopping distance from 40 km/h to 3.6 km/h [m]		5.74			
Time to reach at velocity 3.6 km/h [s]		0.91			

Table F.9: *Wheel $\dot{\Omega}/\Omega$ ratio criteria control braking, threshold values, V_{in}=40 km/h. Employed triggering signals and their threshold values.*

Set - 4		
Command	**Triggering signal**	**Threshold value**
Hold	*-Om_dot / Om*	4.5 Hz
Decrease	*> Slip*	-20%
Stop Decrease	*+ a*	4 m/s^2
Increase	*A*	10 m/s^2

Table F.10: *Flat road - Optimal criteria control braking, statistics data, V_{in}=40 km/h.*

Parameter	Dimension	Max value	Mean value	Min value	Standard deviation
Vehicle accel.	m/s^2	-15.0618	-11.6823	-4.9438	1.3040
Slip	-	20.0382	14.7547	1.4482	3.7775
$M_{y,r\,corr}$	Nm	1.2508	1.1828	0.6987	0.0724
$F_{x,c}$	N	-4.0800	-3.9708	-2.3877	0.2326
$F_{z,c}$	N	3.3567	3.3561	3.3557	0.0002
Stopping distance from 40 km/h to 3.6 km/h [m]		5.67			
Time to reach at velocity 3.6 km/h [s]		0.90			

Table F.11: *Comparison between the simulation results obtained by utilizing different control signal to trigger the brake torque Hold Command. V_{in}=40 km/h, dry asphalt, tire type – 205/60 R15, brake torque rate of increase R1=19000 Nm/s, modulated R1=2533 Nm/s, brake torque rate of decrease R2=19000 Nm/s.*

		ABS - OFF		**ABS – ON**									
		Locked Wheel braking		**Tire moment $M_{y,r\ corr}$**		**Wheel Acceleration control braking**		**Slip control braking**		**Slip and wheel acc. control braking**		**Wheel $\dot{\Omega}/\Omega$ ratio control braking**	
Parameter	**Dimension**	Mean value	Standard deviation	Mean value	Standard deviation	Mean value	Standard deviation	Mean value	Standard deviation	Mean value	Standard deviation	Mean value	Standard deviation
Vehicle accel.	**m/s²**	-8.39	1.6064	-11.68	1.3040	-10.72	1.3829	-11.46	1.0981	-11.39	0.9416	-11.62	1.3208
Slip	**%**	90.06	17.0168	14.7547	3.7775	14.73	12.1362	11.55	5.7120	11.59	5.5060	13.11	4.2037
$M_{y,r}$ corr	**Nm**	838.6	0.0869	1182.8	0.0724	1089.7	0.1289	1149.6	0.0701	1148.7	0.0709	1175.0	0.0725
$F_{x,c}$	**N**	-2817.0	0.2707	-3970.8	0.2326	-3660.3	0.3857	-3860.7	0.2041	-3853.6	0.2046	-3943.9	0.2264
$F_{z,c}$	**N**	3356.0	0.0004	3356.1	0.0002	3356.0	0.0005	33561.0	0.0004	3356.1	0.0004	3356.1	0.0003
Stopping distance from 40 km/h to 3.6 km/h **[m]**		**7.80**		**5.67**		**6.00**		**5.83**		**5.86**		**5.74**	
Time to reach at velocity 3.6 km/h **[s]**		**1.27**		**0.90**		**0.98**		**0.94**		**0.94**		**0.91**	

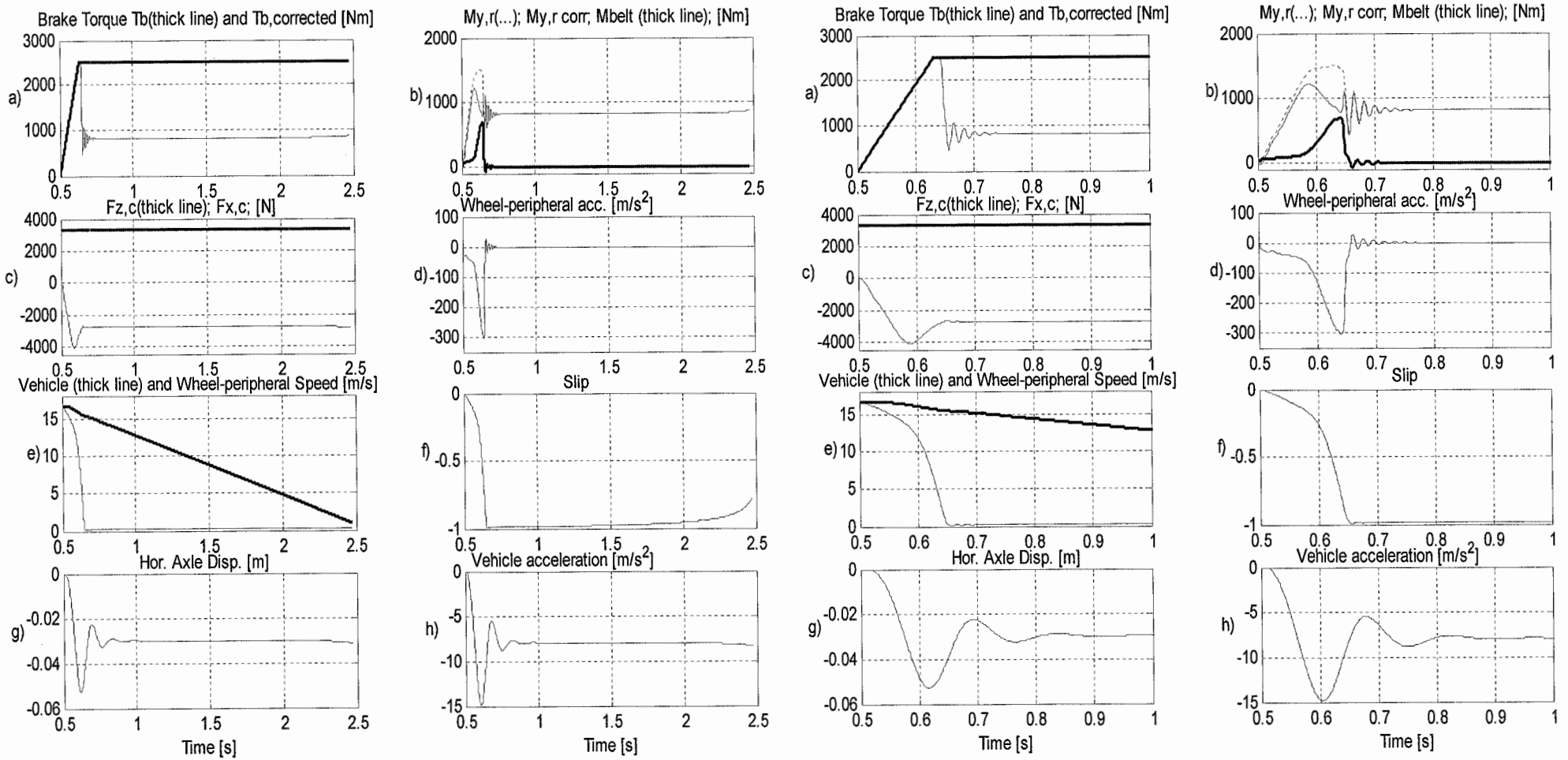

Figure F.8: *Flat road - Braking maneuver without ABS control, V_{in} 60 km/h. The right-hand side ensemble of plots shows zoom in of the time window 0.5 -1 sec. The instant of the brake maneuver initiation is t_0=0.5 sec. T_b max = 2500 Nm.*

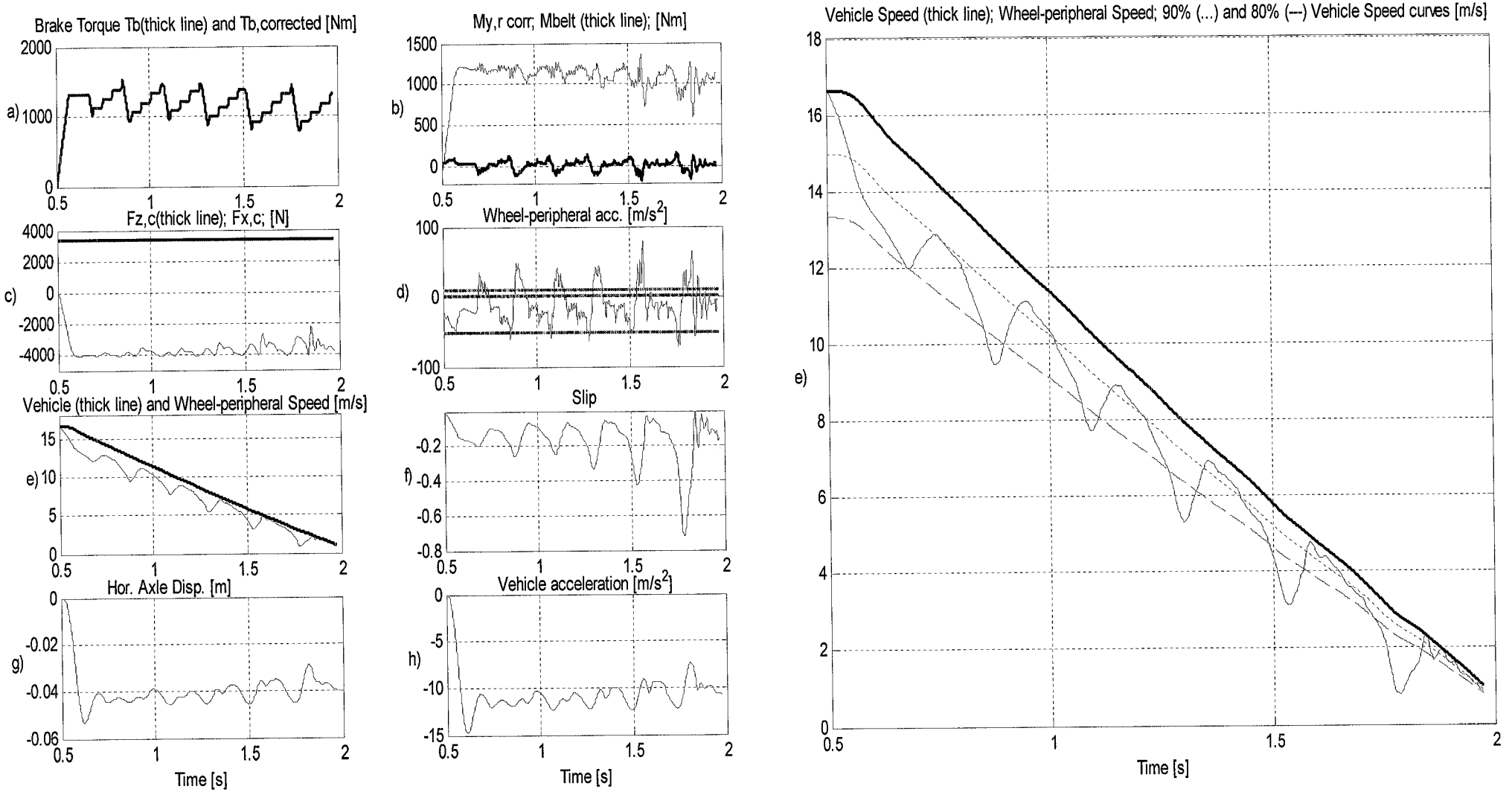

Figure F.9: *Flat road - Peripheral wheel acceleration criteria control braking, V_{in}=60 km/h.. The right-hand side shows zoom in of the sub-graph e). The instant of the brake maneuver initiation is t_0=0.5 sec. T_b max = 2500 Nm.*

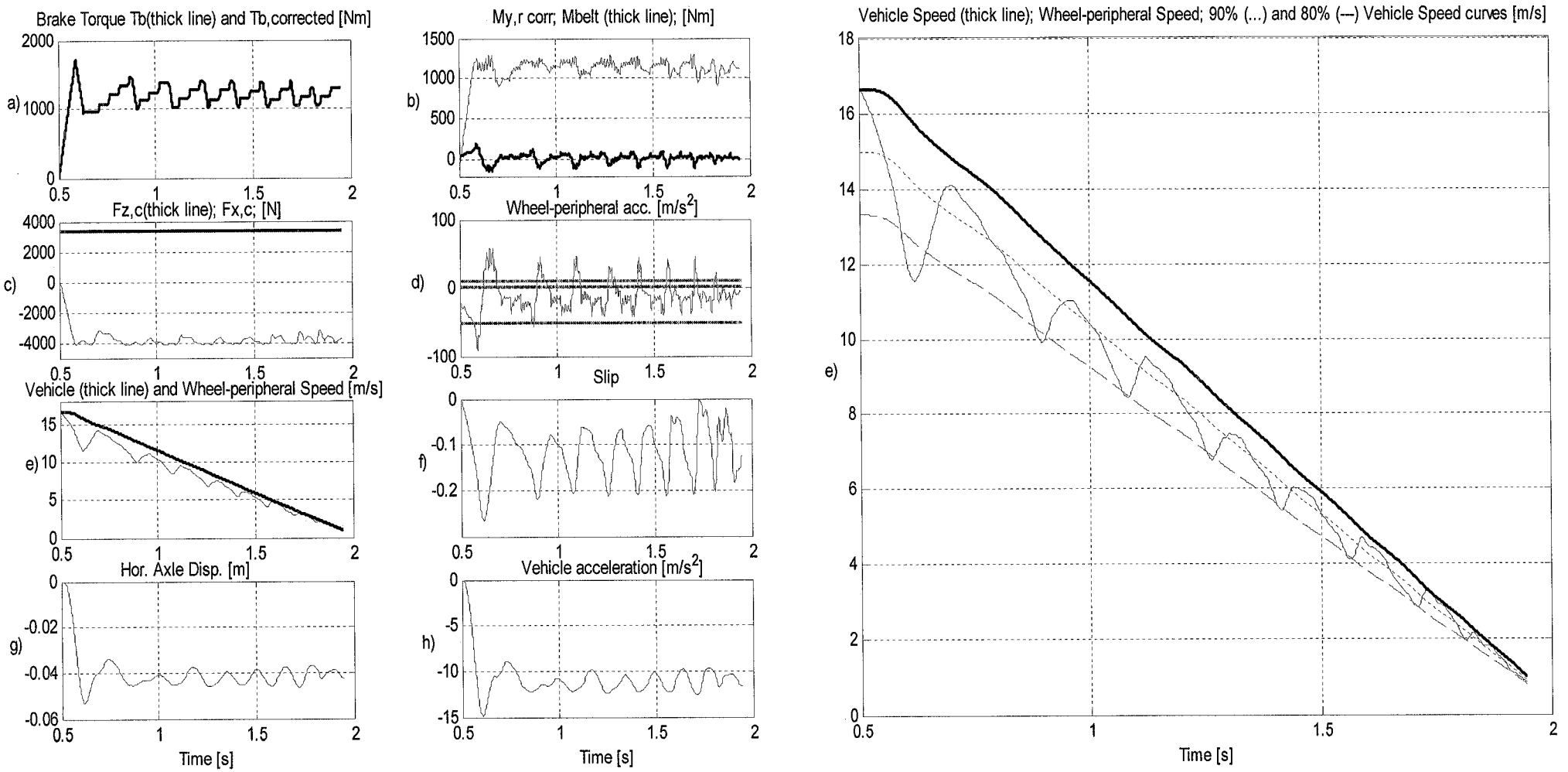

Figure F.10: *Flat road - Wheel slip criteria control braking, V_{in}=60 km/h.. The right-hand side shows zoom in of the sub-graph e). The instant of the brake maneuver initiation is t_0=0.5 sec. T_b max = 2500 Nm*

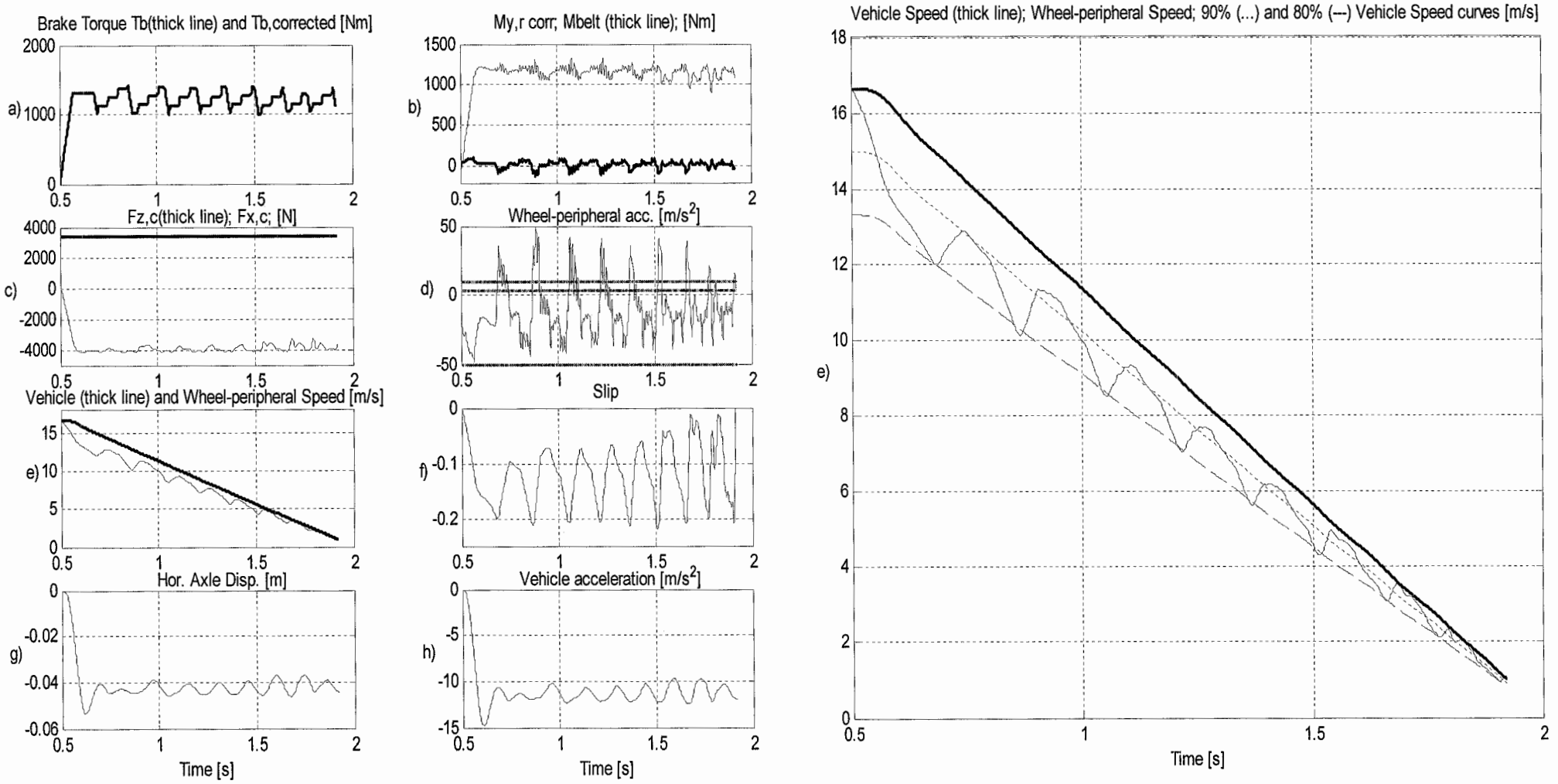

Figure F.11: *Flat road - Combined slip and wheel peripheral acceleration criteria control braking, V_{in}=60 km/h.. The right-hand side shows zoom in of the sub-graph e). The instant of the brake maneuver initiation is t_0=0.5 sec. T_b max = 2500 Nm.*

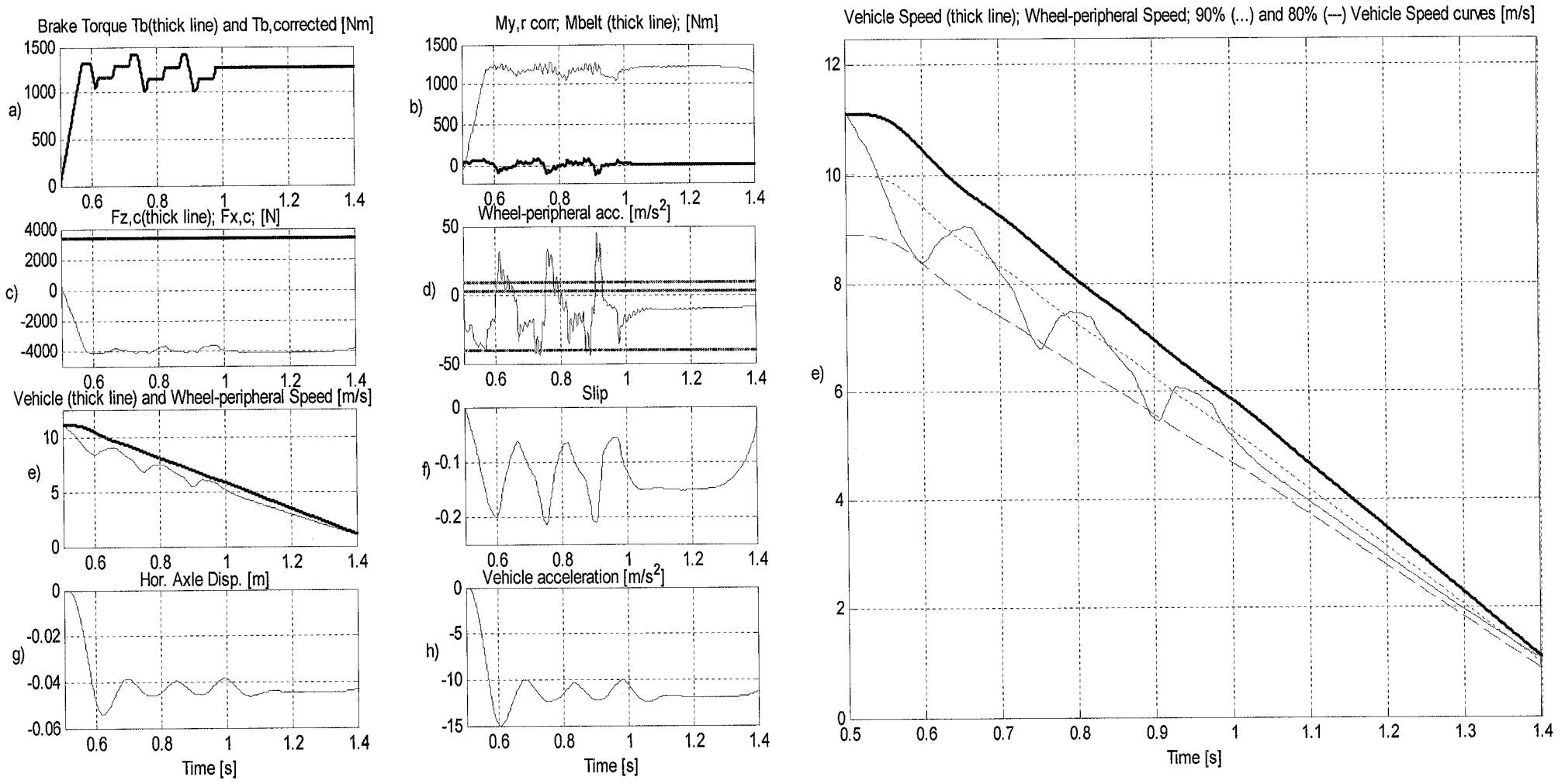

Figure F.12: *Flat road - Wheel $\dot{\Omega}/\Omega$ ratio criteria control braking, V_{in}=60 km/h.. The right-hand side shows zoom in of the sub-graph e). The instant of the brake maneuver initiation is t_0=0.5 sec. T_b max = 2500 Nm.*

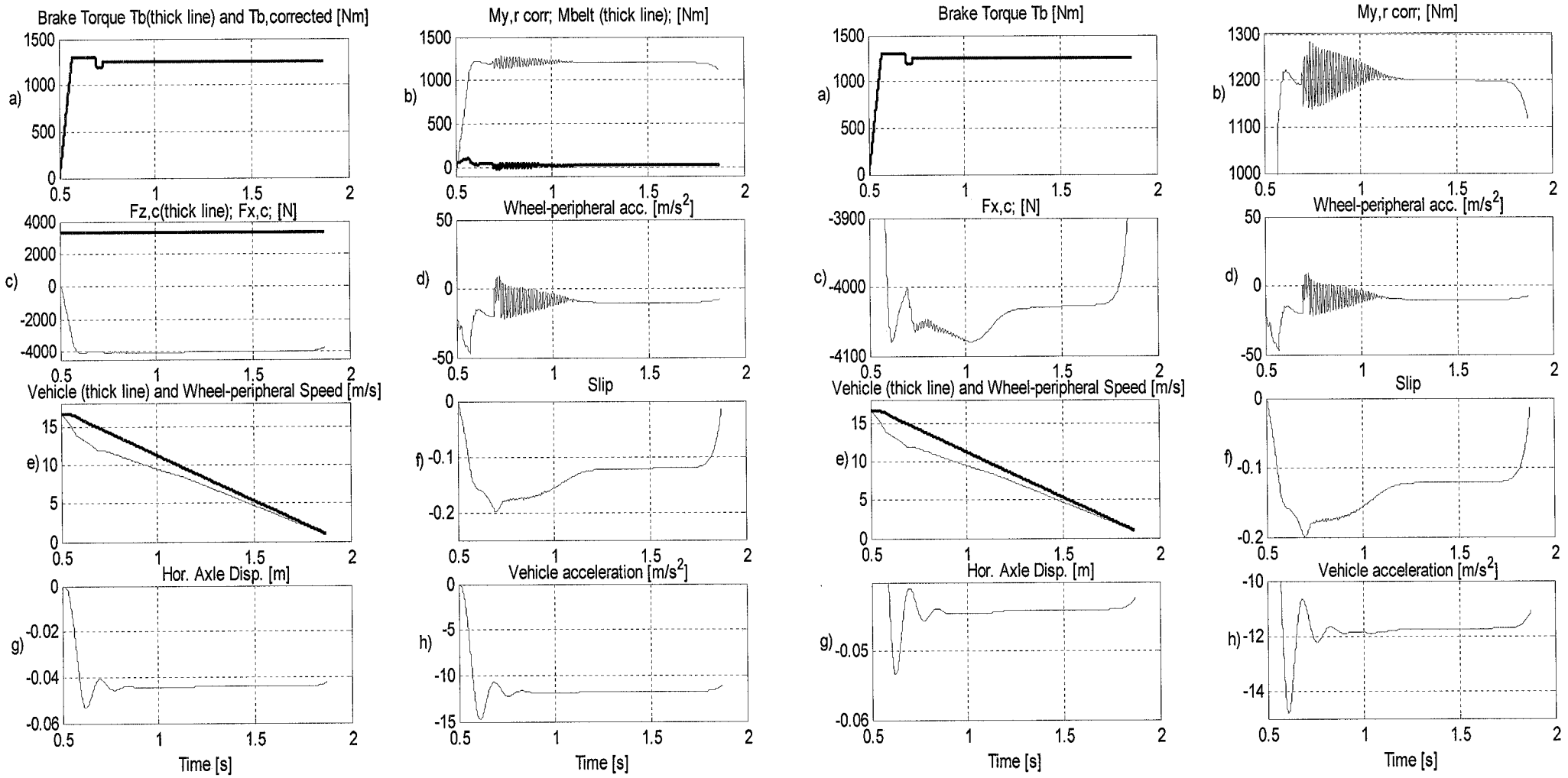

Figure F.13: *Flat road -Tire moment $M_{y,r\,corr}$ criteria control braking, V_{in}=60 km/h. The right-hand side ensemble of plots offers zoom in of the amplitudes. The instant of the brake maneuver initiation is t_0=0.5 sec. T_b max = 1300 Nm.*

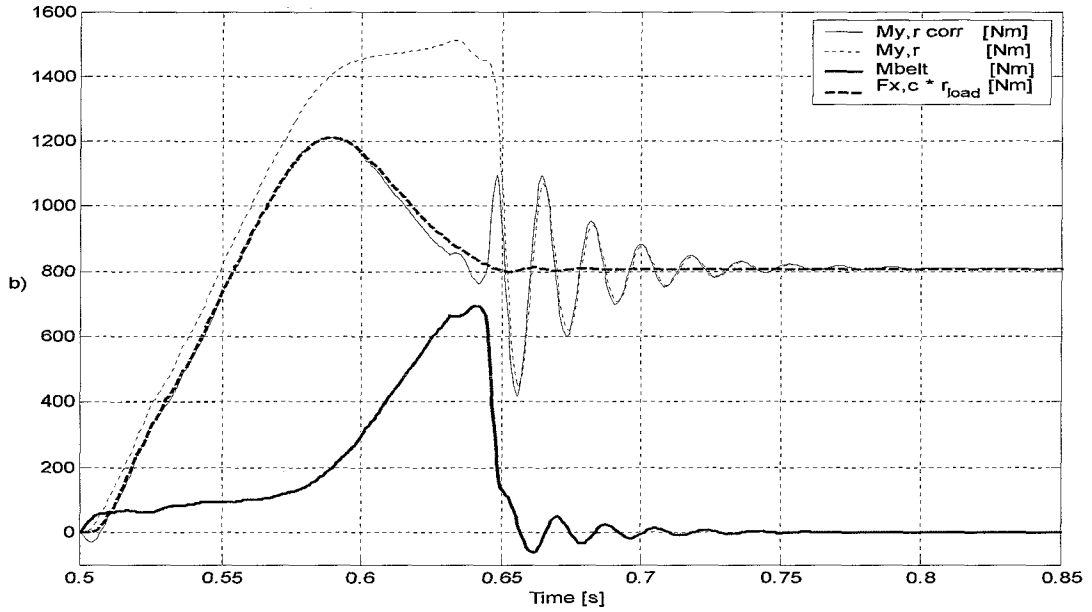

Figure F.14: *Flat road - Braking maneuver without ABS control, V_{in}=60 km/h. Zoom in of the sub-graph b) of Figure14.1. The graph shows the tire moment $M_{y,r}$ calculated by the SWIFT mode, the corrected tire moment $M_{y,r\ corr}$ – friction component, the tire belt moment M_{belt} –due to belt inertia, and the moment created by the longitudinal force $F_{x,c}$ times loaded tire radius r_{load}.*

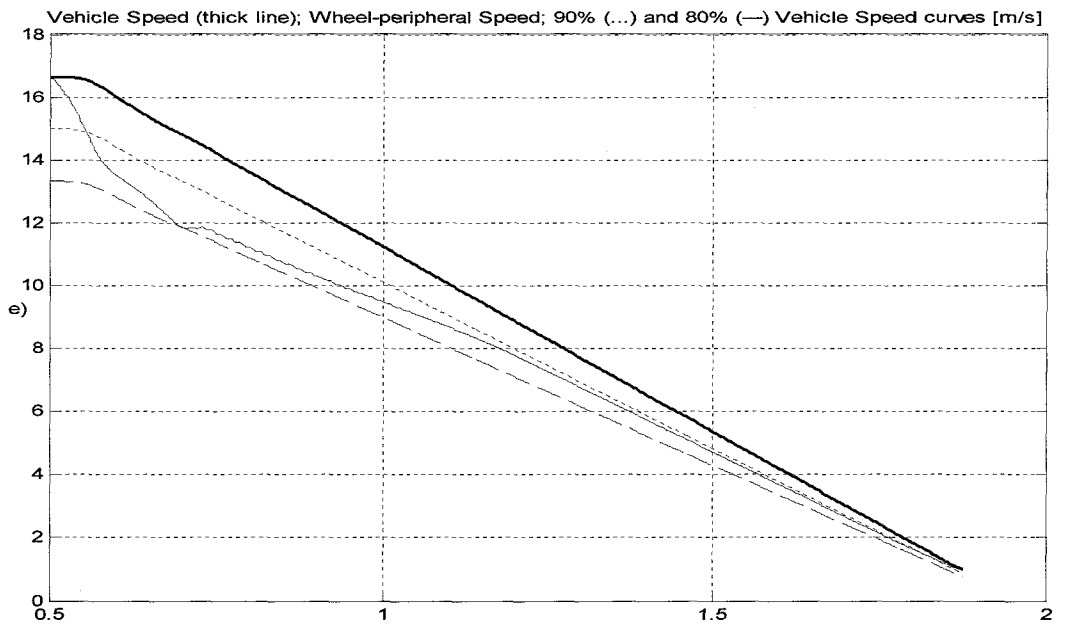

Figure F.15: *Flat road -Tire moment $M_{y,r\ corr}$ criteria control braking, V_{in}=60 km/h. The plot shows zoom in of the Figure 14.6 sub-graph window e). The instant of the brake maneuver initiation is t_0=0.5 sec. T_b max = 1300 Nm.*

Table F.12: *Flat road -Braking without ABS control, statistics data, V_{in} 60 km/h*

Parameter	Dimension	Max value	Mean value	Min value	Standard deviation
Vehicle accel.	m/s^2	-14.85	-8.25	-5.43	1.3431
Slip	-	99.25	92.18	13.64	16.1356
$M_{y,r}$ *corr*	Nm	1209.3	0830.6	0413.6	0.0764
$F_{x,c}$	N	-4079.3	-2791.9	-2693.7	0.2433
$F_{z,c}$	N	3359.4	3356.0	3355.1	0.0003
Stopping distance from 60 km/h to 3.6 km/h [m]		17.54			
Time to reach at velocity 3.6 km/h [s]		1.97			

Table F.13: *Flat road - Peripheral wheel acceleration criteria control braking, statistics data, V_{in}=60 km/h.*

Parameter	Dimension	Max value	Mean value	Min value	Standard deviation
Vehicle accel.	m/s^2	-14.8258	-10.96	-7.3259	1.1761
Slip	-	71.97	16.62	-1.14	11.894
$M_{y,r}$ corr	Nm	1369.8	1113.7	588.2	0.1160
$F_{x,c}$	N	-4082.4	-3735.4	-2244.7	0.3529
$F_{z,c}$	N	3357.1	3356.0	3354.7	0.0004
Stopping distance from 60 km/h to 3.6 km/h [m]		13.00			
Time to reach at velocity 3.6 km/h [s]		1.47			

Table F.14: *Peripheral wheel acceleration criteria control braking, V_{in}=60 km/h. Employed triggering signals and their threshold values.*

Set -1		
Command	**Triggering signal**	**Threshold value**
Hold	***- a***	-50 m/s^2
Decrease	***> Slip***	-20%
Stop Decrease	***+ a***	4 m/s^2
Increase	***A***	10 m/s^2

Table F.15: *Flat road - Wheel slip criteria control braking, statistics data, V_{in}=60 km/h.*

Parameter	Dimension	Max value	Mean value	Min value	Standard deviation
Vehicle accel.	m/s^2	-14.88	-11.30	-8.87	1.0199
Slip	-	26.67	11.95	0.15	5.7484
$M_{y,r\,corr}$	Nm	1302.8	1140.3	899.4	0.0790
$F_{x,c}$	N	-4080.8	-3828.8	-3112.9	0.2366
$F_{z,c}$	N	3357.5	3356.0	3354.7	0.0004
Stopping distance from 60 km/h to 3.6 km/h [m]		13.08			
Time to reach at velocity 3.6 km/h [s]		1.45			

Table F.16: *Employed Wheel slip criteria control braking, V_{in}=60 km/h. Employed triggering signals and their threshold values.*

Set -2		
Command	**Triggering signal**	**Threshold value**
Hold	> ***Slip***	-20%
Decrease	> ***Slip***	-20%
Stop Decrease	+***a***	4 m/s^2
Increase	***A***	10 m/s^2

Table F.17: *Flat road - Combined slip and wheel peripheral acceleration criteria control braking, statistics data, V_{in}=60 km/h.*

Parameter	Dimension	Max value	Mean value	Min value	Standard deviation
Vehicle accel.	m/s^2	-14.83	-11.49	-9.70	0.8730
Slip	-	22.01	12.25	-8.367	5.3930
$M_{y,r\ corr}$	Nm	1332.0	1159.6	907.7	0.0637
$F_{x,c}$	N	-4080.5	-3893.4	-3244.8	0.1836
$F_{z,c}$	N	3357.2	3356.0	3354.6	0.0004
Stopping distance from 60 km/h to 3.6 km/h [m]		12.76			
Time to reach at velocity 3.6 km/h [s]		1.42			

Table F.18: *Combined slip and wheel peripheral acceleration criteria control braking, threshold values, V_{in}=60 km/h. Employed triggering signals and their threshold values.*

Set -3		
Command	**Triggering signal**	**Threshold value**
Hold	- ***a*** and > ***Slip***	-50 m/s^2 and -20%
Decrease	> ***Slip***	-20%
Stop Decrease	+ ***a***	4 m/s^2
Increase	***A***	10 m/s^2

Table F.19: *Flat road - Wheel $\dot{\Omega}/\Omega$ ratio criteria control braking, statistics data, V_{in}=60 km/h.*

Parameter	Dimension	Max value	Mean value	Min value	Standard deviation
Vehicle accel.	m/s^2	-14.93	-11.48	-9.71	0.8796
Slip	-	23.29	12.48	0.74	5.1129
$M_{y,r\ corr}$	Nm	1327.9	1160.9	971.5	0.0559
$F_{x,c}$	N	-4080.9	-3896.9	-3383.1	0.1596
$F_{z,c}$	N	3357.0	3356.1	3354.8	0.0004
Stopping distance from 60 km/h to 3.6 km/h [m]		12.83			
Time to reach at velocity 3.6 km/h [s]		1.42			

Table F.20: *Wheel $\dot{\Omega}/\Omega$ ratio criteria control braking, threshold values, V_{in}=60 km/h. Employed triggering signals and their threshold values.*

Set - 4		
Command	**Triggering signal**	**Threshold value**
Hold	*-Om_dot / Om*	4.5 Hz
Decrease	*> Slip*	-20%
Stop Decrease	*+ a*	4 m/s^2
Increase	*A*	10 m/s^2

Table F.21: *Flat road - Optimal criteria control braking, statistics data, V_{in}=60 km/h.*

Parameter	**Dimension**	**Max value**	**Mean value**	**Min value**	**Standard deviation**
Vehicle accel.	m/s^2	-14.81	-11.85	-9.66	0.6148
Slip	-	20.08	13.84	1.45	2.9803
$M_{y,r\ corr}$	Nm	1283.0	1199.6	1046.2	0.0256
$F_{x,c}$	N	-40795	-40281	-3512.1	0.0613
$F_{z,c}$	N	3356.6	3356.1	3355.9	0.0002
Stopping distance from 60 km/h to 3.6 km/h [m]		12.45			
Time to reach at velocity 3.6 km/h [s]		1.34			

Table F.22: *Comparison between the simulation results obtained by utilizing different control signal to trigger the brake torque Hold Command.* V_{in}*=60 km/h, dry asphalt, tire type – 205/60 R15, brake torque rate of increase* R1=19000 Nm/s, modulated R1=2533 Nm/s, brake torque rate of decrease R2=19000 Nm/s.

		ABS - OFF		**ABS - ON**									
		Locked Wheel braking		**Tire moment** $M_{y,r\,corr}$		**Wheel Acceleration control braking**		**Slip control braking**		**Slip and wheel acc. control braking**		**Wheel $\dot{\Omega}/\Omega$ ratio control braking**	
Parameter	**Dimension**	Mean value	Standard deviation	Mean value	Standard deviation	Mean value	Standard deviation	Mean value	Standard deviation	Mean value	Standard deviation	Mean value	Standard deviation
Vehicle accel.	**m/s²**	-8.25	1.3431	-11.85	0.6148	-10.96	1.1761	-11.29	1.0199	-11.49	0.8730	-11.48	0.8796
Slip	**%**	92.18	16.1356	13.84	2.9803	16.62	11.8937	11.9517	5.7484	12.25	5.3930	12.48	5.1129
$M_{y,r}$ corr	**Nm**	0830.6	0.0764	1199.6	0.0256	1113.7	0.1160	1.1403	0.0790	1159.6	0.0637	1160.9	0.0559
$F_{x,c}$	**N**	-2791.9	0.2433	-4028.1	0.0613	-3735.4	0.3529	-3828.8	0.2366	-3893.4	0.1836	-3896.9	0.1596
$F_{z,c}$	**N**	3356.0	0.0003	3356.1	0.0002	3356.0	0.0004	3356.0	0.0004	3356.0	0.0004	3356.1	0.0004
Stopping distance from 60 km/h to 3.6 km/h **[m]**		**17.54**		**12.45**		**13.00**		**13.08**		**12.76**		**12.83**	
Time to reach at velocity 3.6 km/h **[s]**		**1.97**		**1.34**		**1.47**		**1.45**		**1.42**		**1.42**	

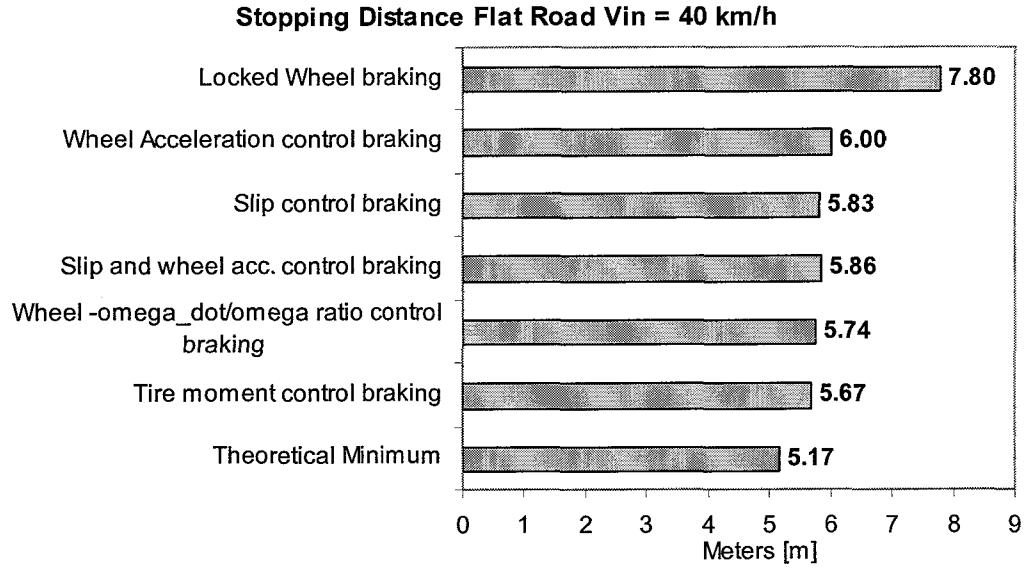

Figure F.23: *Comparison of the results obtained by utilizing different control criteria for V_{in}=40 km/h, dry asphalt, tire type – 205/60 R15, brake torque rate of increase* R1=19000 Nm/s, modulated R1=2533 Nm/s, brake torque rate of decrease R2=19000 Nm/s.

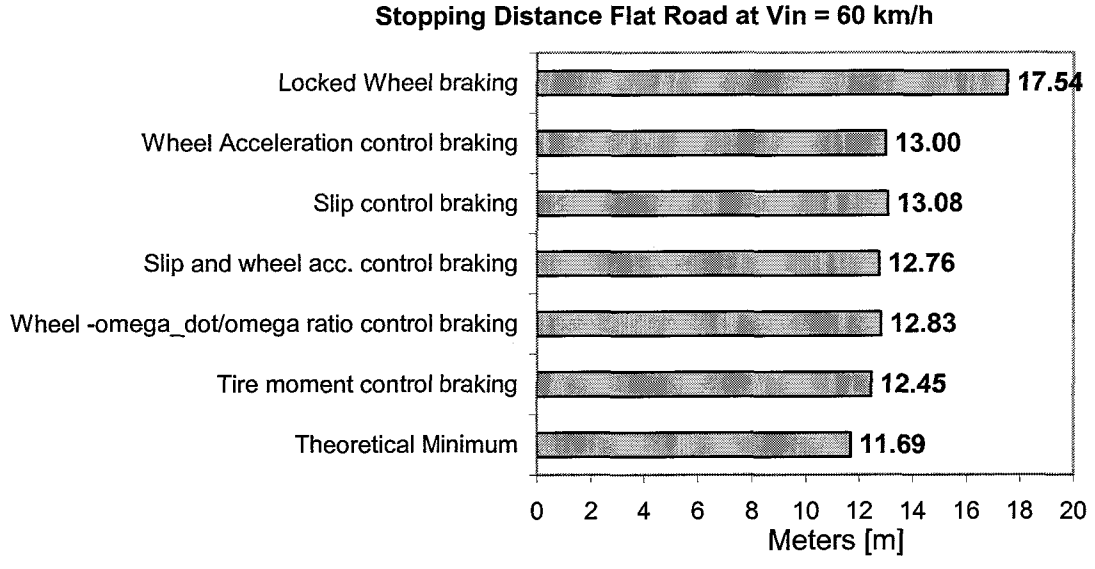

Figure F.24: *Comparison of the results obtained by utilizing different control criteria for V_{in}=60 km/h, dry asphalt, tire type – 205/60 R15, brake torque rate of increase* R1=19000 Nm/s, modulated R1=2533 Nm/s, brake torque rate of decrease R2=19000 Nm/s.